OPTICAL AND ELECTRICAL CHARACTERISTICS OF VERTICAL-CAVITY SURFACE-EMITTING LASERS FOR FREE SPACE OPTICAL COMMUNICATIONS

Salam Nazhan Ahmed AL Zaidi

A thesis submitted in partial fulfilment of the requirements of the

University of Northumbria at Newcastle for the degree of

Doctor of Philosophy

Research undertaken in the Faculty of

Engineering and Environment

Northumbria University, Newcastle upon Tyne

February 2016

Declaration

This work contained in this dissertation has not been accepted in substance for any degree, and it has not been submitted for any candidate for a degree at another university.

Apart from collaboration work mentioned in this thesis, the work is entirely the candidate's own work.

I declare that the word count of this thesis is 42,272 words

Salam Nazhan Ahmed AL Zaidi

February 2016

Signed……. (Candidate)

Date ……..

Acknowledgements

I would like to sincerely thank my supervisor Prof. Ghassemlooy for his guidance and encouragement; his support and consideration during the study time are especially appreciated.

I am grateful to my supervisor Prof. Busawon for his advice, comments and help.

I would like to thank the Department of Physics and Electrical Engineering and Northumbria University for providing a creative environment and supporting all my research activities.

I gratefully acknowledge my sponsors, Ministry of Higher Education and Scientific Research (MOHESR) and Diyala University, Iraq for financial support my research study.

I thank Shuiying Xiang for her cooperation work in part of the simulation results and for sharing her knowledge in this field of expertise with me.

I hereby would like to express my heartfelt thanks to my family for their continued support, special thanks for my wife who has always stood by me providing a source of unending support.

Finally, during my study with the Optical Communications Research Group, NCRLab, I met many inspiring colleagues who became my friends. For this I am especially grateful.

Among my colleagues, I thank in particular Mojtaba for his generous help in some devices matters.

Abstract

Among the number of optical sources, vertical-cavity surface-emitting lasers (VCSELs) are relatively recent type of semiconductor laser devices, which are attractive for a number of applications particularly for free space optical (FSO) communication systems. In such systems reliable optical devices with lower power consumption and low cost are among the key requirements. VCSELs typically operate with unstable output polarization modes, and there is a need to improve their output power regarding to the polarization instability, particularly when introducing the optical feedback (OF).

This thesis investigate a number of key properties of VCSEL including the polarization instability, hysteresis loop (HL), relative intensity noise (RIN) and how to control the polarization switching (PS). The investigations are based on the analytical studies and extensive experimental work. PS properties of VCSEL are investigated by introducing variable polarization optical feedback (VPOF) with the modulation frequency and modulation depth. The dependency conditions for the HL, RIN and PS are determined with VPOF. Under OF, the threshold current (I_{th}) of VCSEL is reduced by 11.5% and the PS, which is demonstrated theoretically and experimentally, is completely suppressed. The PS positions are depending on the polarization angle of OF, OF levels and the bias current. The PS disappeared with the modulation depth of 78.66%, whereas it is entirely vanished with the modulation frequency of 200 MHz. The hysteresis width of the VCSEL polarization modes is reduced by increasing the feedback level. The minimum RIN value of -156 dB/Hz is achieved at a zero degree of the polarization angle for the dominant polarization mode of VCSEL under VPOF.

For the first time, a novel technique based on employing orthogonal polarization OF is proposed to supressed the nonlinearity associated with the modulated VCSEL, where the second, third, and fourth harmonics are completely suppressed to the noise floor. Finally, optimal operating conditions for a high-quality polarization-resolved chaos synchronization of the polarization modes of VCSEL with VPOF are experimentally and theoretically studied. A perfect value of 99% of the correlation dynamics for the chaotic synchronization of the polarization modes of VCSEL is found with a zero time delay over a wide range of polarization angle.

Finally, Simulink and Origin software version 6.1 are used in this work to simulate and plot the results. The simulation results are agreed with the experimental results, which show that the chaotic synchronization dynamic of the polarization modes can be achieved by VPOF.

List of Acronyms

APD	Avalanche photo diode
CA	Configuration A
CB	Configuration B
CM	Current modulation
DBR	Distributed Bragg reflector
EELs	Edge emitting lasers
FSO	Free space optics
GaInAsP	Gallium indium arsenide phosphide
HD	Harmonics distortion
HL	Hysteresis loop
HWP	Half wave plate
ICs	Integrated circuits
InP	Indium phosphide
ISO	Optical isolator
LD	Laser diode
L-I	Light-current
MOCVD	Metal-organic-chemical-vapor-deposition
NDF	Neutral density filter
OB	Optical bi-stability
OOF	Orthogonal optical feedback
OF	Optical feedback
OWC	Optical wireless communications
PBS	Polarization beam splitter
PD	Photodetectors
PEX	Polarization extinction ratio
POF	Parallel optical feedback
PS	Polarization switching

QKD	Quantum key distribution
QWP	Quarter wave plate
RIN	Relative intensity noise
ROF	Relaxation oscillation frequency
RPOF	Rotated polarization optical feedback
RPPOF	Rotating polarization-preserved optical feedback
Rx	Receiver
SFM	Spin-flip model
SLD	Semiconductor laser diode
SNR	Signal to noise ratio
TE	Transverse electric
TM	Transverse magnetic
Tx	Transmitter
XP	X-polarization
YP	Y-polarization
VCSEL	Vertical-cavity surface-emitting laser
VPOF	Variable-polarization optical feedback

List of Symbols

Parameter	Descriptions	Units
$\propto$	Line-width enhancement factor	
a_m	Mirror loss	m^{-1}
a_i	Photon losses	m^{-1}
β_{sp}	Strength of the spontaneous emission	(s^{-1})
Γ	Confinement factor	
$\gamma_{x,y}$	Inverse of photon lifetime for XP &YP mode	(s^{-1})
Δf	Frequency detuning of XP and YP modes	(Hz)
E_{in}	Optical energy inside the cavity	(J)
E_x & E_y	Varying amplitudes of XP & YP mode, respectively	(v/m)
ϵ	Gain saturation coefficient	(m^{-1})
$\xi_{x,y}$	Independent Gaussian white noise	(W/Hz)
η_d	Differential quantum efficiency	
η_i	Injection efficiency	
θ_p	Polarization angle	(Degree)
I	Current density	(mA)
I_b	Bias current	(mA)
I_{dc}	DC bias current	(mA)
I_m	Modulating current	(mA)
k	Feedback strength	(s^{-1})
$k_{x,y}$	Polarization feedback coefficient for XP and YP modes	(s^{-1})

I_{th}	Threshold current	(mA)
λ	Wavelength of laser	(nm)
N	Carrier decay	(m^{-3})
N_o	Carrier density at transparency	(m^{-3})
n_o	Reflective index	(s)
t	Time	(s)
$1/\tau$	Inverse of carrier life time	(s^{-1})
τ_c	Carrier lifetime	(s)
τ_x	Feedback delay for XP mode	(s)
τ_y	Feedback delay for YP mode	(s)
v_g	Grope velocity	(m/s)
$\emptyset$	Phase coefficient	(m/s)
ω	Angular frequency	(Hz)
V	Active volume	(m^3)
V_c	Cavity volume	(m^3)
f_m	Modulation frequency	(Hz)
G_o	Difference between XP and YP gain coefficients	(m^3/s)
L_{ext}	External cavity length	(m)
R	Mean mirror reflectivity	
R_m	External reflectivity	
R_o	Facet reflectivity	
G	Gain coefficient	(m^3/s)

G_y	Gain coefficient for YP mode	(m^3/s)
L_{in}	Internal cavity length	(m)
L	Laser cavity length	(m)
g_o	Linear gain coefficient	(m^3/s)
f_m	Modulation frequency	(Hz)
hv	Photon energy	(J)
R_{sp}	Spontaneous recombination rate	(s^{-1})
q	Unit charge	(C/m)
C	Velocity of light in vacuum	(m/S)

Contents

List of Figures

List of Tables

Chapter 1

Introduction

1.1 Background

Free space optics (FSO) or outdoor optical wireless, is concerned with the transmission of information through the atmosphere from one point to another by using visual or laser beam to get optical communications. A significant progress has been made since 1960s in FSO with the discovery of optical sources, particularly laser sources. Since then, the FSO has become one of the important fields in communications and has attracted a large number of researchers at a global level. The FSO first stated in the military application for covert communication because of inherent security compared with the radio frequency based technologies [1]. FSO technologies have a number of attractive features such as narrow optical beam width, thus avoiding potential interfere with the other beam, low costs system requirements, no fibre optic cables to lay (so no need for expensive rooftop connections equipment), very large bandwidth, excellent frequency re-use capabilities and compatibility with the exiting optical fibre communication networks [2, 3].

In vast majority of the semiconductor laser diode (SLD) applications, such as communication systems employing a high pump source and on optical fibre, the edge emitting lasers (EELs) are the dominant source and are widely used. However, EELs are too costly requiring optical fibre coupling, which results in additional power loss. Therefore, attention has been focused on VCSEL devices with potentially low

manufacturing cost for various applications including optical communication systems. VCSEL is a semiconductor laser, which has a resonant cavity that is vertically formed with the surfaces of the epitaxial layers. The lasing of VCSELs was first demonstrated in 1979 where a gallium indium arsenide phosphide grown on an indium phosphide GaInAsP/InP material was used for the active region, the emitted light had a wavelength of 1300nm. VCSEL devices with optical and electrical properties offer a number of advantages such as a low threshold current, which enables these devices to be directly modulated at high frequencies, small beam divergence that allows good coupling efficiency with the optical fibre, symmetrical output beam profile, small switching transients, circular light-output mode, high packaging density, and very low power consumption compared to the conventional edge-emitting semiconductor laser devices [4]. VCSELs are the key and dominant source in local area networks thanks to their advantages such as wafer scale testing and ease of fabrication [5].

The VCSELs at 850 nm wavelength have been widely used in optical interconnections [6], in local area networks [7] due to their lower-power consumption, higher data rate and low manufacturing cost [8].VCSELs have also been adopted in chaos based optical wireless communications (OWC) thanks to their unpredictable behaviours under the strong optical feedback (OF) regime [9, 10].

In the past few years, the chaotic dynamics of VCSELs with OF has been the subject of great interest for researchers theoretically and experimentally [11, 12], particularly, for secure optical communications. Recently, chaotic synchronization of the orthogonal polarization modes of VCSEL has received wide attention over previously available technology as a means of offering a secure communications [13, 14]. In this context, chaos-based optical communications using laser polarization modes intensity have attracted intensive research interest due to its encryption capabilities [15]. The

information signal is used intensity modulate the VCSEL, which is set to operate in the chaotic oscillation of the polarization mode, and can be retrieved at the receiver upon synchronization with an identical VCSEL [11, 16]. VCSELs have also played an important role in deployment and optimization of high-speed short-range communication links, thanks to their attractive feature [8].

However, VCSEL present a number of problems, including the polarization instability also known as polarization switching (PS). Another drawback is that VCSELs have low power emission compared with EELs. This is because of high reflectivity of the distributed Bragg reflector (DBR) mirror which led to low quantum efficiency [17]. PS can occur at different conditions, such as free running VCSEL operation by either increasing the injection current or changing of the temperature of the laser cavity [18]. PS of VCSELs can also happen by the external parturition, such as an optical feedback [19] and an optical injection [20]. On the other hand, VCSELs usually emit a multi transverse mode especially at high level of injection current due to spatial hole-burning and carrier diffusion effects as a result of large transverse dimensions (~10 μm radius). These drawbacks significantly affect the device performance, and therefore need to be improved. VCSELs are very sensitive to the effects of OF because of their high gain and a very short cavity length (few μm) [21].

External OF, on the other hand, can be used for controlling instability associated with VCSELs thus improving the performance in form of reduced threshold current, as a result of reduced losses inside the laser cavity, and intensity noise [22, 23]. Threshold current reduction of the semiconductor laser is a typical feature of optical feedback [21, 24]. For semiconductor laser diodes a maximum threshold current reduction of 11.5% has been achieved with a short external cavity length (7.5 cm) of the OF [25]. While a maximum threshold reduction of 5.6% has been reported for VCSEL with polarization

OF in [26]. It is well-known that the conventional OF strongly influences the VCSEL dynamics. Therefore, the dynamics of semiconductor lasers subject to the conventional OF [27, 28] have widely been studied both practically and theoretically [27, 29, 30].

The relative intensity noise (RIN) characteristics of semiconductor laser are important parameter in many applications and needs to be kept low, for example in optical communications [31]. Fluctuations in photon densities result in the intensity noise observed at the output of the laser [32]. RIN of -135 dB at a low feedback level between -45 dB to -35 dB has been reported, which is degraded by about 20 dB at a high feedback level of -10 dB [33]. However, a theoretical model of a semiconductor laser has demonstrated a significant reduction in RIN from -124.8 to -149 dB/Hz when using OF [34]. Despite of a rich varieties of dynamics in VCSELs provided by the conventional OF, the dynamics of rotated polarization angle θ_p of the OF are considerably different [35]. This technique can lead to a complex dynamics, such as the chaotic behaviour, which could be exploited in optical communications for security reasons. In recent years we have seen the application of chaotic systems in optical communications because of the chaos dynamic, which is continually unstable and is difficult or impossible to predict its system behaviour. This feature adds more security in communication systems [11].

This thesis includes an intensive experimental works about the dynamics of variable polarization optical feedback (VPOF) for the polarization characteristics of VCSEL, which gives more insight and assessment of the VCSEL characteristics. The experimental results agreed well with the theoretical results obtained and it demonstrated the recent theoretical analysis in literature. Interestingly, in this work different properties have been considered including PS, threshold current, RIN characteristics and nonlinearity of the VCSEL. It has been found that these parameters

are drastically affected by the orthogonal OF with rotated θ_p. On the other hand, selective OF is also applied, when the difference between the feedback strengths of the two modes is great enough the OF assumes the dominant role on the polarization properties. The VCSEL with a strong feedback level requires a smaller θ_p to implement PS. Moreover, preserving OF is considered, the polarization properties is different compared with selective OF, the PS was not observed for the whole range of the OF levels that were used in the measurements.

A novel way was used in this thesis to suppress harmonic distortion of VCSEL based on T-shaped polarization OF. It is demonstrated that the power peaks of the spectrum are strongly dependent on the type of the polarization that is being pumped back into the VCSEL. The harmonic distortion decreases and the spectrum peaks (2^{nd} and 3^{rd}) were completely suppressed when using the orthogonal polarization OF. For the RIN characteristics, it is show that RIN level strongly depends on the PS position and modulation signal. It is found that VPOF with modulation signal leads to increased oscillations of the signal and a change the RIN spectrum.

Furthermore, the VCSEL properties under VPOF combine with important parameter of modulation signal, frequency and modulation depth have also been demonstrated in this work. These modulation parameters can be used to eliminate PS of VCSEL. In terms of the chaotic dynamic of the VCSEL under VPOF, a clear relationship has been found between achieving a higher value of chaotic synchronization and both θ_p and OF level based on VPOF. A correlation coefficient function has been used to evaluate the chaotic synchronization modes, a maximum value obtained is -0.99 without time delay between the two modes. As far as we know, this is a better value for practical work. Moreover, a complex dynamics and high dimension chaos synchronization have been demonstrated for the polarization modes of VCSEL under VPOF.

1.2 Research Motivation

A huge number of experimental works have been reported on the characteristics of VCSELs and how it can be improved. However, their polarization dynamics have not been fully understood [36-38]. In the literature, several works describing the operation characteristics of VCSELs with VPOF have been demonstrated [39-42]. However, the dynamics of VPOF, which influence the polarization dynamics of VCSEL, are still under investigation because the dynamics consequences of VPOF are not fully understood yet. Therefore, better understanding the VCSEL's dynamic and addressing un-solved issues will ultimately lead to improved VCSEL performance for polarization-sensitive applications such as optical switching and optical wireless communications [42]. OF can lead to increased polarization inversion and mode competition of the VCSEL and involving multiple switching which destabilizes the laser modes emission and its dynamic solution. Interestingly, VPOF is recently proposed for the external cavity feedback as an effective tool to control the polarization instability of VCSEL [41, 43]. Still, the experimental studies on VPOF are yet inconclusive. The motivation for this thesis is to carry out several experimental investigations for comprehensive characterization of the polarization dynamics of VCSELs.

The PS phenomenon has unwanted effects in many applications, such as communications systems and networks because it can affect the noise level thus leading to a reduced signal to noise ratio (SNR) [44]. However, PS features are attractive in a number of applications including optical switching, high capacity data processing and information storage systems [45, 46]. The polarization modulation of the laser is one of the most attractive schemes for a communication links [47]. This is because of the polarization beam is the most stable characteristic while propagating through the atmosphere [48].

In data communication there is a growing need for high security in order to prevent hacking of information and systems intrusions. There are a number of ways in dealing with information security including digital signature, quantum key distribution (QKD), the spread spectrum technique and synchronization of chaotic signal [49-51]. Interestingly enough VCSELs exhibit unpredictable chaotic and dynamic properties especially when it is subject to an external OF, which can be fully exploited in chaotic optical communications [49]. A crucial point is to identify the laser operating conditions that provide the best quality synchronization conditions and those which provide the optimized message extraction. Therefore, the need for further investigation of the VCSEL's to address the issues associated with chaotic optical systems and how it will fulfil the basic performance requirements for optical wireless communication systems is required.

1.3 Research Objectives

The VPOF can significantly alter the bi-stability properties of VCSELs [40]. It has also been shown that the irregular dynamics of the polarization mode of VCSEL are drastically modified using selective-optical feedback [52]. In this thesis, the polarization characteristics of VCSEL with VPOF are intensively investigated. The goal of this thesis is to provide a detailed experimental study and mathematical model for polarization dynamics of VCSEL under effects of VPOF.

Polarization instability in a VCSEL can cause mode-partition noise when used in an optical communications [53]. Therefore, possible ways of improving the stable polarization mode operation using external control mechanisms i.e., VPOF are investigated in this thesis. In addition, the effect of the laser bias current on the PS

properties of the VCSEL is also investigated to show their influence and who it is change the PS position.

A number of researches addressing the RIN properties of the individual mode of a semiconductor laser have been reported [8, 30, 44, 54-56]. However, these findings offer a limited insight to the important problem of noise properties of the polarization mode in many applications that used polarization light. Such applications are including wireless communication systems. Thus the need for further research works on the RIN properties of the polarization modes of VCSEL. Furthermore, VCSEL with VPOF exhibit characteristics, which can be exploited as chaotic synchronization source for a secure communication system. In this thesis a complex dynamics and high dimension chaos synchronization with VPOF are investigated to demonstrate the potential of the VCSEL based chaotic communications.

1.4 Original Contributions

i. In Chapter 3, experimentally demonstrating the induced hysteresis loop (HL) using VPOF and determining dependency conditions the HL, the results have been published in [57].
ii. In Chapter 4, practical verification of polarization characteristics of VCSEL in terms of its instabilities has been presented.
iii. The modulation signal is demonstrated as a new tool to control the polarization switching properties of the VCSEL, which is demonstrated in Chapter 4, the results have been published in [58].

iv. For the first time, a novel way has been proposed in Chapter 5 to elimination the nonlinearity associated with the VCSEL by the way of employing orthogonal polarization optical feedback, the results have been published in [59, 60].

v. Investigation of the relative intensity noise (RIN) characteristics of the two polarization modes in VCSEL has been provided in Chapter 5. Determining what the optimal condition to achieve a minimum value for RIN with variable polarization optical feedback (VPOF), the results have been published in [61, 62].

vi. Identifying an optimal operating condition for the high-quality of polarization-resolved chaos synchronization of VCSEL's polarization modes under VPOF, the results have been published in [63, 64].

vii. Experimentally obtained a perfect chaotic synchronization of transmitter with correlation coefficient of -0.99 with a zero time delay over a wide range of θ_p. The last two point's achievements (vi and vii) have been presented in Chapter 6, [63, 64].

1.5 List of Publications

1.5.1 Journal Papers

[1] **S. Nazhan**, Z. Ghassemlooy, K. Busawon, and A. Gholami, "Investigation of polarization switching of VCSEL subject to intensity modulated and optical feedback," *Optics & Laser Technology,* vol. 75, pp. 240-245, 2015.

[2] **S. Nazhan**, Z. Ghassemlooy, K. Busawon, and A. Gholami, "Suppressing the Nonlinearity of Free Running VCSEL Using Selective-Optical Feedback," *Photonics Technology Letters, IEEE,* vol. 28, pp. 185-188, 2016.

[3] **S. Nazhan,** Z. Ghassemlooy, and K. Busawon, "Chaos synchronization in vertical-cavity surface-emitting laser based on rotated polarization-preserved optical feedback," *Chaos: An Interdisciplinary Journal of Nonlinear Science,* vol. 26, p. 013109, 2016.

[4] **Nazhan, Salam**, Ghassemlooy; Zabih and Busawon, Krishna "Harmonic Distortion-Dependent on Optical Feedback, Temperature and Injection Current in Vertical Cavity Surface Emitting Laser," Journal of Physics D: Applied Physics 49.14 (2016): 145107.

1.5.2 Conference Papers

[5] **S. Nazhan,** Z. Ghassemlooy, K. Busawon, and J. Perez, "Hysteresis properties induced by variable polarization angle in the polarization switching of VCSELs," in Communication Systems, Networks & Digital Signal Processing (CSNDSP), 2014 9th International Symposium on, 2014, pp. 325-329.

[6] **S. N. Ahmed,** Z. Ghassemlooy, K. Busawon, and S. Zvanovec, "Relative intensity noise of vertical-cavity surface-emitting lasers subject to variable polarization-optical feedback," in Optical Wireless Communications (IWOW), 2014 3rd International Workshop in, 2014, pp. 21-24.

[7] **S. Nazhan,** Z. Ghassemlooy, K. Busawon, and J. Perez, "Polarization RIN of VCSEL subject to modulation signal with variable polarization angle of optical feedback," in Optical Wireless Communications (IWOW), 2015 4th International Workshop on, 2015, pp. 65-68.

[8] **S. Nazhan,** Z. Ghassemlooy, K. Busawon, and A. Gholami, "Variable-polarization optical feedback induced high-quality polarization-resolved chaos synchronization in VCSEL," in Science and Information Conference (SAI), 2015, 2015, pp. 1052-1055.

[9] **Salam Nazhan,** Z. Ghassemlooy and Krishna Busawon."Investigation of current modulation effects on threshold current of an 850nm single-mode VCSEL," Proceeding of the Northumbria Research Conference, Newcastle, UK, 21-22 May 2014.

[10] **Salam Nazhan,** Josep pericas, Zabih Ghassemlooy and Krishna Busawon "Chaotic regime modulation in VCSEL based on Rotated Polarisation-Preserved Optical Feedback" photonics global conference 2015, (PGC), 28 June to 03 July, Singapore.

[11] **Salam Nazhan,** Z. Ghassemlooy and Krishna Busawon "High-quality Chaos Synchronization in VCSEL polarization modes under Optical Feedback" , (poster), Proceeding of the Northumbria Research Conference, Newcastle, UK, 21-22 May 2015.

[12] **Salam Nazhan**, Z. Ghassemlooy and K. Busawon "Polarization properties of Vertical-Cavity Surface-Emitting Lasers subject to variable polarization angle of optical feedback" Second Scientific Conference, Diyala, Iraq, 16 – 17 December 2015, (In press).

1.6 Thesis Outline

The thesis is composed of seven chapters, Chapter 2 gives an overview of the VCSEL characteristics including, light-current (L-I) curve, OF mechanism, polarization switching, hysteresis properties and bi-stability, relative intensity noise, nonlinearity, chaotic dynamics and VCSEL under direct current modulation. On the other hand, the chapter describes the equations used to obtain the numerical results presented in subsequent chapter. A model is developed based on the rate equations, which describe how OF effects, particularly VPOF with selective and preserve OF, are included in the formulation. Identical and practical parameters values of VCSEL are considered in the Simulink model to investigate the polarization properties. The developed model consists of a carrier and photon rate equation as well as a field equation for each polarization mode.

Chapter 3 present the VCSEL properties in the absence of external OF (free running operation) and with external OF. These properties included L-I characteristics, hysteresis properties and bi-stability. Additionally, the polarization extinction ratio of the polarization modes of the VCSEL with OF is presented.

Chapter 4 considers the PS properties of VCSELs, VPOF with selective and preserve OF. In two configurations, A and B depending on the OF type, (selective and preserve OF), the influence of VPOF on the polarization properties of VCSELs is investigated theoretically and experimentally. The experimental data were used as real parameters in theoretical model. Further investigation of PS of VCSEL subject to intensity modulated and Optical Feedback are also presented in this chapter. Influences of the modulation frequency and modulation depth have been presented as well as the effect of changing bias current.

Chapter 5 investigates the effect of parallel and orthogonal optical feedback, (POF) and (OOF) respectively, on the dynamic range and the harmonics characteristics of VCSELs. The possibility of suppressing the nonlinearity of the polarization mode of VCSEL has been demonstrated. Temperature and drive current effects are also investigated in terms of the nonlinear dynamics. The chapter also outlines the study of VCSEL noise characteristics considering the modulation parameters of frequency and amplitude. The RIN characteristics have been provided under the effect of VPOF.

Chapter 6 considers the effects of VPOF on the chaotic characteristics of VCSEL over a wide range of θ_p and feedback levels. The possibility of achieving complete synchronization between the polarization modes of VCSEL with VPOF is demonstrated. The VPOF achieve a complex dynamics and polarization mode hopping in VCSELs with high-quality chaos synchronization over a wide range of θ_p is also reported. Simulation results and Simulink model are provided in this chapter.

Chapter 7 summarizes the main results of this research and outlines the future works.

Chapter 2

Free Space Optics and VCSELs Characteristics Overview

2.1 Introduction

The FSO communications technology depends on the propagation of the laser beam through the channel. In the past decade, the FSO technology has been used for applications such as satellite-to-satellite cross links and among mobile or stationary terminals to provide high bandwidth wireless communication links. FSO will be a powerful technique and one of the most unique tool to address the issues that have been created in high speed communication such as bandwidth limitation and security [65-67]. The FSO based interconnect is the most promising scheme that could lead to increased speed, reduced size and compact packaging in future ICs [68].

In general, FSO systems uses the wavelength range between 750 and 1600 nm owing to the optical energy that travels through atmosphere have similar properties at these wavelengths (visible and near-IR wavelength) [69]. However lower and higher wavelength are also being considered for specific applications. The wavelengths between 780-850 nm are the most popular because of readily available and inexpensive components, which have an attenuation of less than 0.2 dB/km [69]. The majority of FSO systems designed to operate at a transmission window located at a wavelength range of around 780–850 nm. Laser devices that emit 780 nm are available and inexpensive, but have short lifespan so must be considered during system design. At

850 nm, high-performance transmitter, inexpensive and reliable, therefore they are commonly used in network and transmission systems. Furthermore, there are many devices that operate in this wavelength, such as avalanche photodiode (APD), highly sensitive silicon (Si) and VCSELs.

The optical sources used for such systems are light emitted diode or laser. Both light emitting diodes and laser diodes (LD) are used in FSO communications. LDs are mainly for outdoor and medium to long range applications, however the latter is ideal for high speed line of sight links both in indoor and outdoor application [69, 70]. With increasing demand, high security transmission data over a network, Chaos based FSO communications technology is one of the most promising technique to prevent all kinds of hacking information [65]. The message can be encoded with spectrum of the chaos and be sent through an FSO channel. In the past few years, the chaotic dynamics of VCSELs with OF has been the subject of great interest for researchers theoretically and experimentally [11, 12]; particularly, for secure optical communications. Recently, chaotic synchronization of the orthogonal polarization modes of VCSEL has received wide attention as a means of offering a secure communications [13, 14]. In this context, chaos-based optical communications using laser polarization modes intensity have attracted intensive research interest due to its encryption capabilities [15]. The information signal is used intensity modulate the VCSEL, which is set to operate in the chaotic oscillation of the polarization mode, and can be retrieved at the receiver upon synchronization with an identical VCSEL [11, 16].

This chapter contains an overview about the VCSEL characteristics for FSO and optical chaos dynamics in Sections 2.2 and 2.3, respectively. Polarization properties of VCSEL studied in this thesis which includes; optical and electrical properties, light-current (L-I) properties and polarization switching (PS) in Section 2.4, 2.5 and 2.6 respectively,

principle OF mechanism in Section 2.7, a brief introduction about the hysteresis and relative intensity nose (RIN) are resented in Section 2.8 and 2.9 respectively, a short background about the nonlinearity and VCSELs under current modulation are presented in Sections 2.10 and 2.11,respectively. Finally in section 2.12 theoretical analysis including the rate equations and the polarization dynamics analysis of VCSEL subjected to VPOF are outlined.

2.2 VCSELs for Free Space Optics

Since 1992, VCSELs based on GaAs have been extensively studied. Some devices exhibiting sub-milliampere threshold were demonstrated by improving the quality of the active region and the laser cavity [4, 71]. From 1999 and onwards, VCSELs based optical transceivers have been introduced into Giga-bit/sec Ethernet and high-speed local area network. VCSELs are being applied in various optical systems such as optical fibre networks, parallel optical interconnects laser printers, and high density optical disks [17]. Recently, VCSEL array has been proposed as a concept of a compact FSO communications terminal thanks to their high reliability and high-speed modulation (2.5 Gb/s) under high optical power operation [65].

VCSELs are relatively recent type of semiconductor laser devices, which are attractive for a number of applications from sensors to telecommunications. VCSEL is a SL, which has a resonant cavity that is vertically formed with the surfaces of the epitaxial layers. Typically SLs devices consist of semiconductor layers grown on top of each other on a substrate. Usually the growth processing is achieved in a molecular-beam-epitaxy (MBE) or metal-organic-chemical-vapor-deposition (MOCVD) growth reactor. Figure 2.1 show the oxide-confined VCSEL top-emitting structure. The construction of

VCSEL is particularly different from other lasers, an active layer sandwiched between highly reflectivity mirrors in range of about 99.5 to 99.9%, which is placed at the bottom and top of the device structure as shown in the figure 2.1. These mirrors consist of distributed Bragg reflectors (DBRs), which is made up of several quarter-wavelength-thick layers of semiconductors. These layers have alternatively high and low refractive indexes. The VCSEL emission can be from the top or bottom of the device [72]. There are several categories of VCSELs based on the optical and electrical confinement techniques, active layer design and wavelength emission. The most important issue in fabrication such devices is the optical confinement factor, because of the conversion efficiency of the electrical-to-optical signal.

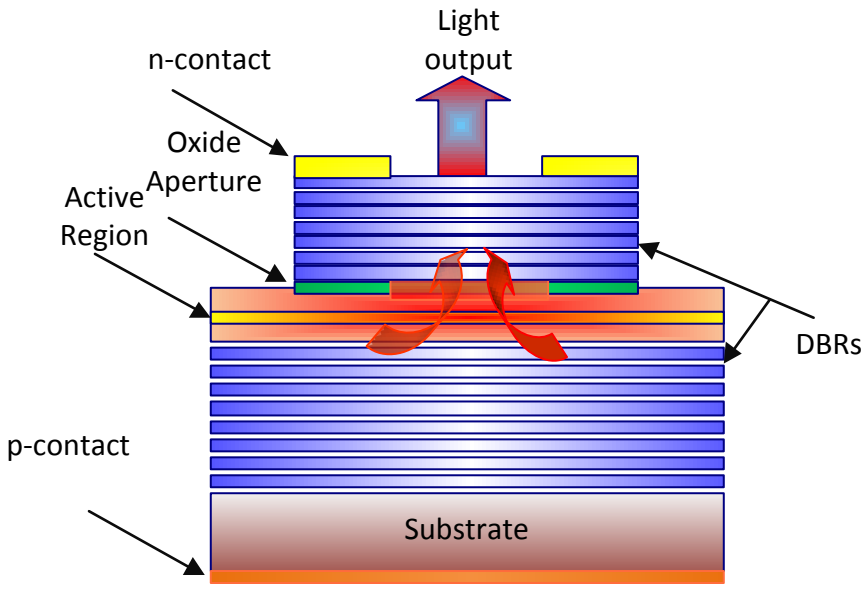

Figure 2-1: VCSEL with a selectively-oxidized top-emitting structure.

VCSEL has become a very important source, which effectively displacing EELs for applications such as high speed data communication and chaos for local area networks [8]. VCSELs consist of a small active volume (few μm) and these have a very low threshold current (few μA) compared with EELs (~300 μm) [73]. This is one of the attractive features that give the higher reliability than edge-emitters devices. This

chapter contains a background of the VCSEL characteristics that were investigated in this thesis and theoretical analysis for these properties with OF effects.

2.3 Optical Chaos Characteristics for Communications

In recent years the application of chaotic system in optical communications have become attractive because of the chaos dynamic, which is continually unstable and is difficult or impossible to predict system behaviours. This feature adds more security in communication systems. There is a need to increase the security protection of data being transmitted in order to prevent hacking of information and systems intrusions. VCSELs exhibit unpredictable chaotic and dynamic properties especially when it is subject to an external OF, thus making them a promising candidate for transmission sources in chaotic optical communication systems [74, 75]. The chaotic communication system has three main parts, as depicted in Fig. 2-2, transmitter (Tx), channel (Noise) and receiver (Rx). The time delay between the two chaotic synchronization waveforms is the key to distinguish massage from these two signals of synchronization. It is important to match the corresponding parameters (internal and external) of Tx and Rx to achieve a complete synchronization. External parameters such as bias current, temperature and so on of both Tx and Rx can be controlled easily; however, the internal parameters such as optical loss, gain and quantum efficiency are difficult to be accurately controlled. Under the additive chaos modulation encryption scheme, the encoded messages can be successfully extracted based on a good synchronization oscillation between the Tx and Rx signal. At the Tx a chaotic carrier is employed to improve the overall security of the system. The modulated chaotic carrier signal is transmitted over the communication channel. At the Rx detection is carried out using exactly the same chaotic oscillator as in the Tx to ensure successful recovery of the information signal.

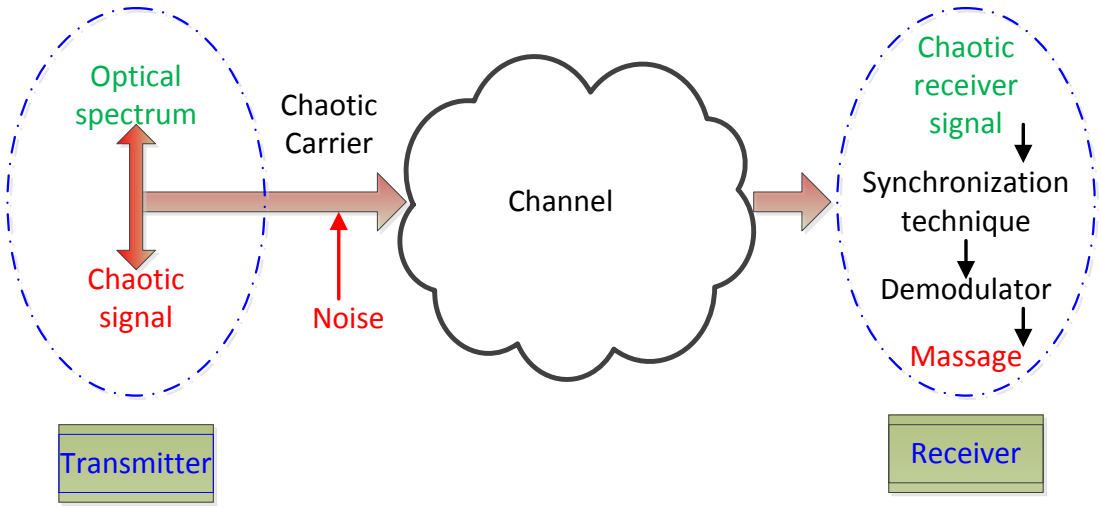

Figure 2-2: Block diagram of chaotic communication system.

Successful message encoding/decoding in an unpredictability-enhanced chaotic VCSELs system is achieved numerically via the chaos-shift-keying technique. Using two VCSELs, which are subject to VPOF, and polarization-preserved optical injection, are adopted. Improved decoding performance is achieved by choosing a proper polarizer angle, and the security is, to some extent, enhanced owing to the VPOF [76]. Message encoding and decoding using the chaotic VCSELs has been experimentally demonstrated in [77].

2.3.1 Chaos Synchronization in VCSEL

Chaotic synchronization based on semiconductor lasers and their applications in secure communications have attracted considerable attention. The first demonstration of chaos synchronization was by Pecora and Carroll [78]. Recently, chaos synchronization in optical communications systems employing SL diodes has been a hot topic in applications where security is paramount. In such systems, a message is encoded into a noise like signal generated by laser source with chaotic behaviour [79]. In this context, chaos-based optical communications have attracted intensive research interest due to its encryption capabilities. A popular optical source adopted in such systems is the

VCSELs because of their unique features especially when subjected to VPOF. Furthermore, a different chaotic pattern and complex dynamics can be achieved under rotated-polarization angle of OF [11, 35, 80, 81].

Nowadays, we have seen a number of experimental and theoretical research activities on chaos, chaos synchronization and communication characteristics of VCSELs. Synchronization of the chaos is achieved experimentally in un-directionally coupled external-cavity vertical-cavity surface-emitting SLs operating in an open-loop regime. The polarization of the injected beam was perpendicular to that of the free-running receiver (x polarization). The injected beam and the y-polarized component of the receiver show good synchronization [11, 76, 77, 82-88]. It has been shown that two VCSELs can be synchronized under appropriate conditions. However, synchronization is lost at a higher mirror reflectivity (i.e., 50%).

In contrast, a higher external reflectivity leads to a more chaotic behaviour in the output power of VCSELs. VCSEL's dynamic can be driven into the chaotic regime by means of an external OF. The synchronization has been observed over a range of values of the coupling parameter such as the drive current, external reflectivity and coupling coefficient [82]. Solitary VCSEL can exhibits strong anti-phase dynamics between own orthogonal polarization modes [14]. However, one study has presented an anti-phase oscillation between transverse electric (TE) and transverse magnetic (TM) modes in a SL with polarization-rotated OF. It has achieved a maximum value of correlation coefficient of the synchronization modes of -0.68 (-0.99) experimentally (theoretically) with zero time lag between the orthogonal modes under appropriate conditions [42]. Polarization-resolved dynamics of VCSEL has been used in this work for the chaos synchronization technique. To best of our knowledge no experimental work has been

found in the literature has done a correlation coefficient of -0.99 with zero time delay of the orthogonally polarization modes of VCSEL as demonstrated here in this thesis.

2.4 Optical and Electrical Properties of VCSELs

As discussed above the structure of VCSEL is completely different from other semiconductor structures devices that have been realised so far, such as distributed feedback laser (DFB) or EELs [17]. What makes VCSEL structure unique is that the emitting light is perpendicular to the surface of the laser. Consequently, this dramatic difference in the VCSEL structure makes a similar design technique impossible for convention facet emitting lasers. Because of the main concern in these devices is to achieve high-longitudinal side-mode suppression, which is completely disregarded in the VCSEL design [89].

VCSELs gained a reputation as a superior technology for applications such as fibre-channel, Gigabit Ethernet and intra-systems, free space optical communications, optical fibre communications and optical recording [90-92]. However, VCSELs have a number of problems based on large frequency chirp and polarization insensibility, which limit their performance in fibre-optic communication systems, as well as causing limitations in transmission distances and speed [53]. Such drawbacks are related to the laser noise properties and also depend on polarization mode fluctuation [56]. VCSELs are very sensitive to the effects of optical feedback (OF) and optical injection because of their high gain and very short cavity length [21]. In the next few sections these problems will discussed and more insight will provided.

2.5 Light-current (L-I) Curve Characteristics

VCSEL when operating near threshold current usually lases in a single polarization mode [93]. However, VCSEL can oscillate with the orthogonally polarized simultaneously, owing to their circular symmetry structure [94]. VCSEL emit mainly linearly polarized light. However, its orientation is not well distinguish because of the laser cavity and the gain medium are quasi isotropic in the active layer. In most sensing applications and data communications, a polarization stability of VCSEL and how it can be controlled is essential [95]. Consequently, the polarization mode linearity of VCSELs when modulated is of critical concern; particularly, in applications such as optical communications and optical memory [96]. One of the essential parameter of a SL is light-current (L-I) curve, the laser efficiency can be predicted from the L-I curve properties [97]. The polarization-resolved L-I curve properties have been studied in details with VPOF in Chapter 3.

2.6 Polarization Switching

Most VCSELs devices typically emit linearly polarized light. In fact, instability is a common features in VCSELs devices owing to weak material and cavity anisotropies [41], therefore polarization instability can happen without external perturbation. However, under some conditions - such as when the bias current is increased or an external OF is introduced - the linearly polarized state switches to the orthogonal linearly polarized state. This usually occurs due to changes in the gain and loss of the orthogonally polarized modes [98], and changes in the operating temperature as well as the magnitude and directionally of the bias current [99]. Based on the relevant studies in the literature, experimental and theoretical works on VCSELs have shown that increasing the injection current and the OF level can lead to increased polarization

inversion and mode competition between the laser polarization modes. Mode competition is involving multiple switching, which destabilizes the laser emission and dynamic solutions. Interestingly, variable polarization based OF was recently proposed for external cavity feedback as an effective tool to control the polarization instability of VCSEL [41].

The PS features of SLs are of interest for a wide range of applications including optical switching, storage system and high capacity data processing. It has been observed that PS can occur under the fixed bias current and OF conditions [39]. In VCSEL the position of PS is mainly determine by three factors; the net gain of the two polarization modes, the electric field and the injection current [52]. A critical issue in developing such laser devices is how to determine and control their polarization instability. Controllable PS has been investigated in [27, 93, 100] by considering the effects of a number of parameters including the OF strength, optical injection and frequency detuning.

The first experimental work that demonstrated the PS in VCSELs was reported in 1993 [101], using optical injected. Since that time the polarization bi-stability of VCSELs has been the subject of extensive research from both theoretical and experimental perspective. However, the majority of previous studies have focused on influences of conventional OF on the dynamics and polarization characteristics of VCSELs [28, 102, 103]. The polarization properties of SLs subject to the OF with non-rotated [27, 28, 52, 93, 94, 100, 102, 104-108] and variable rotated polarization angles have been studied experimentally and theoretically in [39, 40, 57, 80, 109, 110]. It has shown that a laser under the OF effect can emit in certain polarization mode and increasing the level of OF dose lead to supressed the polarization instability. Controllable PS of VCSEL has also

been investigated in [27, 93, 100], where the effects of a number of parameters such as the OF strength, optical injection and frequency detuning were considered.

Recently, numerical simulations results on the influence of polarization-rotated OF on the polarization properties of VCSEL have been reported in [39]. It has been observed that PS can be occur even for a fixed bias current and an OF level. Furthermore, PS properties are depending on the OF level and the polarization angle θ_p, where smaller θ_{p} is required to implement the PS when the OF level increase. No experimental work on these theoretical findings has been reported yet. In VCSELs it is possible to achieve PS by means of thermal effects [111], optical injection [112], strong enough OF [113] and rotated polarization angle of OF [40]. In the later, it was shown that by employing a polarization controller to obtain the variable polarization angle, VCSEL exhibit dominant PS for a fixed bias current and OF for the case of the selected polarization feedback, whereas in case of preserving the OF the dominant PS is not observed in the entire parameter space.

2.7 VCSELs with Optical Feedback

VCSELs are very sensitive to external OF because of their short cavity length and a large emitting area [114]. OF is normally needed in some applications that use a VCSEL in order to control their polarization properties or to achieve optimum dynamic characteristics for VCSEL applications. As a result, such devices under OF mechanism have been the subject of extensive research, where the polarization properties are studied theoretically and experimentally [19, 22, 25, 27-29, 39]. A schematic diagram of a VCSEL subject to external OF is shown in Fig. 2-3. An external plane mirror with high reflectivity is used to reflect back part of the output laser beam into the internal

cavity of the laser. The reflected beam is called the OF. The external cavity length represents the distance between the laser facet and the external mirror.

The external cavity length of OF and the external mirror reflectivity are important parameter in the mechanism of OF. The dynamic characteristics of a semiconductors laser are found to be dependent on the external cavity length and feedback strength or mirror reflectivity [27, 114].

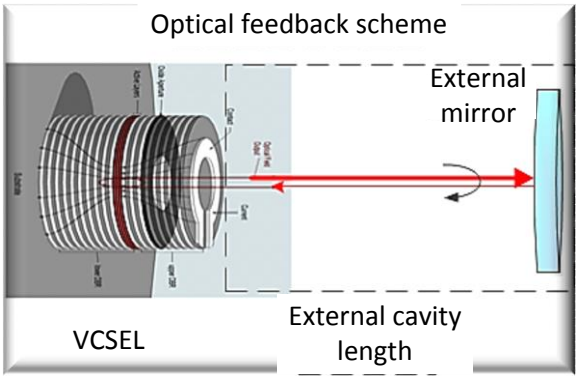

Figure 2-3: Optical feedback scheme for VCSEL.

Five OF regimes have been experimentally assessed in [115] varying from weak (-80 dB) to high (-8 dB) level depending on OF effects. Regime I at the weak level of OF, the laser line emission can be narrowed or broadened depending on the phase of the reflected beam of OF [116]. In Regime II splitting of the emission beam is observed, which arise from the longitudinal mode hopping depending on the OF strength and the distance of the reflector [117]. Regime III, at an approximately feedback level of -45 dB, does not depend on the distance to the reflection, the laser mode becomes narrow and the mode hopping is suppressed. In regime IV where the feedback level is approximately -40 dB, as the feedback increase the laser line width broadens and the coherence length reduces, where the effects of this regime are independent of the phase of the feedback light, this regime termed as “coherence collapse” [118]. In Regime V a strong OF level is needed to achieve stable operation of the external cavity mode.

At highest OF level, usually greater than -10 dB, the antireflection coating of the laser facet is necessary. In this regime the laser operates on a single longitudinal mode with a narrow line width and is relatively insensitive to the additional external optical perturbations. In highest level of OF chaotic behaviours is appearing in the laser dynamics system. Therefore, the laser chaotic dynamics under Regime V operation have attracted considerable attention due to potential application in secure optical communication [19]. The majority of previous studies have focused on the influence of conventional OF on the dynamics and polarization characteristics of VCSELs [28, 102, 103]. However, OF with variable polarization angle does lead to a number of interesting dynamics in VCSEL including chaotic, bi-stabilities, time-period pulsing dynamics etc. [119], and how they depend on OF are interesting topic to study further [52, 120].

2.7.1 Variable Polarization Optical Feedback

The polarization properties of SLs subject to conventional OF [27, 28] have been studied extensively both practically and theoretically [27, 29, 30], which gives rich varieties of dynamics. It is well-known that the OF will strongly influence VCSELs' dynamics and characteristics. However, these characteristics are considerably different when laser is subjected to the rotated angle of polarization OF [35]. In the past ten years, several works have investigated the SL properties with a variable polarization angle of OF both numerically and experimentally [39, 121]. The theoretical prediction of the PS position with the OF level and θ_p is that the PS is dominant at a smaller angle at higher OF levels. It was also predicted that larger θ_p forces the laser to emit via the suppressed mode. In addition, a complex dynamics and route to the chaos have also been observed both experimentally and theoretically depending on the rotation of the polarization OF.

The polarization characteristics of VCSEL with a variable polarization OF (VPOF) will lead to a chaotic behaviour that could be exploited in optical communication for security reasons. Controllable PS has also been investigated with VPOF in many works [39, 100] under different condition as mentioned in section 2.4. The polarization rotation angle can be controlled by a quarter-wave plate [102, 122], polarizer [80], Faraday rotator [81, 123], where all these optical devices have the ability to create polarization-rotated OF. In this thesis, both quarter-wave plate and polarizer devices have been used to achieve VPOF.

2.8 Hysteresis Properties and Bi-stability of VCSEL

In recent years we have seen a growing interest in studying the bi-stability in SLs since its first introduction in 1964 [18, 124]. Because of their attractive properties, SLs have further increased motivation to apply a function of optical devices based on bi-stability properties [17]. An optical bi-stability (OB) system is one which exhibits two stable optical output states for the same single input state as in a Fabry-Perot resonator with an optical cavity filled with materials with intensity-dependent refractive index [124]. The property of gain saturation is considered the main origin of bi-stability [46]. Bi-stability has many advantages, such as inherent optical gain and low optical switching power, therefore, bi-stability is expected to play an important role in future optical switching and communication systems [125]. In optical networks VCSEL devices are good candidates for optical signal processing [46] because of their many advantages over other semiconductor device, including bi-stability and PS characteristics, which can occur in free running VCSELs, as well as being induced by external optical injection [101].

The hysteresis can occur in PS of the free-running VCSEL using injection current sweep rate. OB is applicable to a numerous applications including optical memory [46], optical transistor [126], all-optical switching [127], optical flip-flop memories, and among others. In recent years we have seen a growing interest in exploring and realizing OB in nonlinear nanophotonic systems [128]. A theoretical results show that the HL is sensitive to the bias current and the possibility of enhancing the hysteresis size with fast injection current compared to slow injection current [18, 129].

2.9 Relative Intensity Noise of VCSEL

The studies of the intensity noise characteristics of laser diodes are important in many applications, such as optical communication systems. Fluctuations in the photon densities does appear as an intensity noise in output power of laser devices, while variations in the carrier density result in the frequency noise [32]. The relative intensity noise (RIN) can be utilized as a good measure of the laser dynamics [130], since it correlates well with the output power fluctuation of the laser source. VCSELs have played an important role in allowing deployment and optimization of high-speed short-range communication links, thanks to their reduced size, higher speed, lower power consumption, and low cost [8]. VCSEL with the relative noise levels of the their drawbacks based on the large frequency chirp and polarization insensibility, is valid for most practical applications with modulation process [131]. However, such noise level limit their performance in optical fibre communications, as well as causing limitations in transmission distances and data rates [53, 56].

A numerical investigation reported in [120] indicated that RIN of VCSEL with low feedback levels is relatively unaffected except for narrowing and enhancement of the

relaxation oscillation peaks. In [132], it has been found that polarization of the VCSEL mode plays a significant role in determining the noise spectra. The RIN is an important factor, which determines the achievable modulation bandwidth in communication systems. Therefore, it is important to understand the effects of RIN on each individual mode of VCSEL. Different studies have addressed the effects of RIN at individual modes of VCSEL, e.g., application of VCSEL in low noise image processing [133]. In [33] the effects of OF on the RIN of VCSEL was investigated. At the low OF levels of -45 to -35 dB the measured RIN of -135 dB/Hz was reported, while it is degraded of 20 dB/Hz at a high OF of -10 dB. Moreover, lower RIN of -149 dB/Hz using VCSEL was outlined in [34].

As stated in [7], a strong OF can lead to a reduced RIN owing to the phase effect of the reflected light in the laser cavity, provided the light is from a pure single mode oscillation [30]. In this thesis, the RIN characteristics under strong OF and VPOF have been experimentally investigated.

2.10 Nonlinearity of VCSELs

The nonlinear behaviour of SL with modulation signal is a subject of great interest in many researches [134] particularly for optical communication due to, for instance their effects to limit the RF dynamic range of optical devices. The nonlinear behaviour of optical devices such as EEL and VCSEL is a major limiting factor in analogue optical communications [135] and has been widely investigated [43, 136-138]. The nonlinear dynamics of VCSELs as a result of optical injection and OF was investigated in [43]. Noise and different physical mechanisms, such as spatial-hole burning, phase coupling, gain anisotropy and birefringence effects can lead to rich nonlinearity properties in SL. In [139, 140] it was shown that nonlinear induced harmonic distortion can lead to

decreased power efficiency of VCSEL. Recently, special attention has been paid to light polarization in VESCELs [43].

In the VCSELs under current modulation (CM) the nonlinear dynamics and chaos are easily realized due to the mode competition or polarization mode switching [141]. Furthermore, in semiconductors laser the nonlinear distortion appears when the laser is being driven near threshold current [140]. High nonlinearity in the L-I curve of VCSEL devices has been reported when the laser is biased near the threshold current at high modulating frequency [136], which has led to harmonic distortions. Nonlinear gain saturation of the lasing transition produce a nonlinear behaviour in the L-I characteristics of VCSELs devices, which lead to increase the relaxation oscillation damping and eliminate the light intensity through the reduction of differential gain [142].

2.11 VCSEL under Current Modulation

In a number of applications such as communication systems, high pump sources and optical fibre communication systems, the EEL diodes are the most widely used source. However, with EELs there is the requirement for optical fibre coupling and waveguides owing to its large divergence angle. A potential alternative light source for such applications would be VCSELs with their unique features such as low cost, circular output beam, higher data rate and lower power consumption [143, 144]. VCSELS are also considered to be ideal for gigabit Ethernet and optical interconnects [90, 145, 146]. Consequently, the polarization mode linearity of VCSELs when modulated is of critical concern particularly in applications such as optical communications and optical memory [96].

There has been also several works dealing with the polarization properties of VCSELs when subjected to current modulation. VCSEL with a high frequency modulation current and subjected to weak OF have been theoretically investigated [147]. It was shown that applying small signal modulation does not induce PS, except for the low frequency range of 1 Hz to 100 kHz. However, under large signal modulation, the situation is different, where for certain modulation frequencies PS may occur by adjusting the modulation amplitude. On the other hand, the influence of low frequency modulation (1 Hz~100 KHz) on PS of VCSELs subject to the weak OF level (-39 dB) has been investigated with no PS being observed [148]. It has been shown that depending on the OF level [110] and the drive current [100] the laser favours the suppressed mode emission. In this thesis, modulation parameters such as frequency and modulation depth have been used in presence of high level of OF (-7 dB) and VPOF which presented in chapter 4.

2.12 Theoretical Analysis of VCSELs

2.12.1 Rate Equations

In order to assess VCSEL performance theoretically and to investigate their properties, it is imperative to utilise rate equations describing the time variation of the carrier and photon density.

2.12.2 Carrier and Photon Density Dynamics

These equations are shown below describing the rate equations for the carrier decay N and the photon decay S as a function of time t. These can be written as the subtracting carrier recombination rate via laser emission $G\,v_g S$, and loss mechanisms N/τ_c, from

the carrier generation rate $\eta_i I/qV$, by stimulated and spontaneous emissions [32, 80, 136]:

$$\frac{dN(t)}{dt} = \frac{\eta_i I}{qV} - \frac{N(t)}{\tau_c} - G\,(t)v_g S(t), \tag{2. 1}$$

The sources of photons are stimulated and spontaneous emissions. However, only a small fraction of the spontaneous emission is coupled into a given laser mode and this component may often be neglected. Losses of photons are governed by a photon lifetime τ_p, is given by:

$$\frac{dS(t)}{dt} = G\,(t)v_g S(t) + \Gamma\beta_{sp}\,R_{sp} - \frac{S(t)}{\tau_p}, \tag{2. 2}$$

where I is the current density, η_i is the injection efficiency, V is the active volume, q is the unit charge, G is the gain coefficient, $\tau_c$is the carrier lifetime, v_g is the photon group velocity, Γ is the confinement factor, $ß_{sp}$ is the spontaneous emission factor, and R_{sp} is the spontaneous recombination rate. The gain coefficient is assumed to be a linear function of carrier density and can be expressed as:

$$G(\mathrm{t}) = g_o \frac{N(\mathrm{t})-N_{\mathrm{o}}}{1+\epsilon S(\mathrm{t})}, \tag{2. 3}$$

Here g_o is the linear gain coefficient, ϵ the gain saturation coefficient, and N_{o} is the carrier number at transparency. At the study-state condition, the gain of a laser above threshold should always equal the threshold gain, otherwise optical amplitude continues to increase which cannot happen in the steady-state. The same argument is valid for the carrier density in the steady-state because of both G and N are combine in the cavity of the laser, so [149]:

$$G = G_{\mathrm{th}}, \qquad (I > I_{\mathrm{th}}) \tag{2. 4}$$

$$N = N_{\text{th}}, \qquad (I > I_{\text{th}}) \tag{2. 5}$$

At the study state condition, gain = loss and can be assumed to be constant, therefore we have:

$$G_{th} = \frac{1}{\tau_p}, \tag{2. 6}$$

where I_{th} is the threshold current. The average modal gain can be written as:

$$< G >_{th} = \Gamma G_{th} = < a_i > + \frac{1}{L} ln\left(\frac{1}{R}\right), \tag{2.7}$$

Where L is the total cavity length, R is the mean mirror reflectivity, for simplicity the mirror loss term ($\frac{1}{L} ln(\frac{1}{R})$) is abbreviated as a_m and the photon loss ($\frac{1}{\tau_p}$) is defined by:

$$\frac{1}{\tau_p} = \nu_g(< a_i > + a_m), \tag{2.8}$$

The internal cavity loss of the laser is ($a_i + a_m$), a_i is the photon losses, and a_m is the mirror loss parameter.

$$\Gamma G_{th} = \frac{1}{\tau_p \nu_g} = < a_i > + a_m, \tag{2. 9}$$

At the study state condition and from equation 2.1 the photon density above threshold can be written as:

$$S = \frac{\eta_i (I - I_{th})}{qVG_{th}\nu_g}, \qquad (I > I_{th}) \tag{2. 10}$$

To obtain the output power of the laser we have to extract the total optical energy inside the cavity E_{in}, which is defined in terms of the energy loss rate through the mirrors ($\nu_g a_m$) as:

$$E_{in} = Sh\nu\, V_c, \tag{2. 11}$$

$$P_{out} = Sh\nu\, V_c \nu_g a_m, \tag{2.12}$$

where V_c is the cavity volume, and $h\nu$ is the photon energy. Substituting from Eq.(2.10) and (2.9) and using $\Gamma = V/V_c$ in Eq. (2.12), now the laser out power can be written in a common expression as [150],

$$P_{out} = \eta_i \frac{a_m}{a_i + a_m} \frac{h\nu}{q} (I - I_{th}), \tag{2.13}$$

The differential quantum efficiency is given by:

$$\eta_d = \eta_i \frac{a_m}{a_i + a_m}, \tag{2.14}$$

We can simplify Eq. (2.13) to be as:

$$P_{out}(t) = \eta_d \frac{h\nu}{q} (I(t) - I_{th}), \tag{2.15}$$

When a laser is subject to direct modulation current, the total injection current is given by:

$$I(t) = I_{dc} + I_m(t), \tag{2.16}$$

I_{dc} is the bias current (time-independent), and $I_m(t)$ is the modulating current (time varying), which could be given in a sinusoidal form as:

$$I_m(t) = I_m\, e^{if_m t}, \tag{2.17}$$

where f_m is the modulation frequency (Hz).

2.12.3 Basic Schemes of the Polarization OF

The principles schemes for the selective and preserve polarization OF that are used in this thesis with rotated polarization angle for VCSEL are illustrated in Fig. (2-4). For preserve OF, both component (XP and YP) re-injected into VCSEL, see Fig. (2-4(a)),

while in the selective OF scheme, only one component (XP or YP) was selected to be re-injected into VCSEL, see Fig. (2-4(b)). The quarter-wave plate (QWP) is inserted into the external cavity to rotate polarization OF. The fast axis (0°) of the QWP is defined as the pure XP OF and the 45° as the pure YP OF. Figure 2-4(a) shows the polarization-preserve OF where the polarization of the reflected light is the instantaneous of the original emission light of VCSEL. Figure 2-4(b) displays the polarization-selective OF, where the polarization beam splitter (PBS) is used to select one of the polarization modes of the VCSEL. The external mirror (M) with high reflectivity is used to provide the OF to the laser. The laser beam is collimated and focusing using an objective lens.

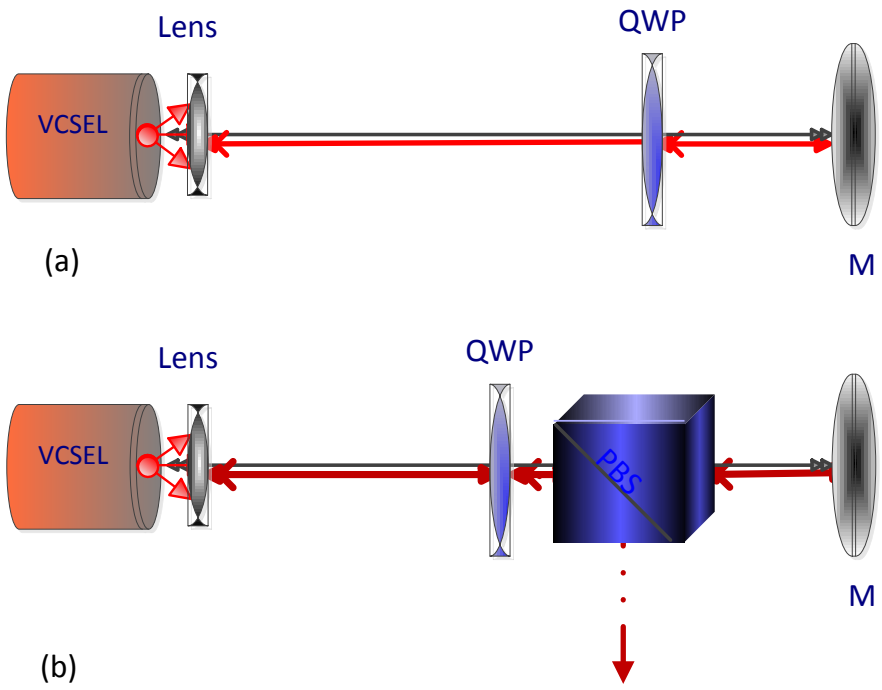

Figure 2-4: Principle schemes of (a) preserve OF and (b) selective polarization rotating OF.

2.12.4 The XP and YP Dynamics with VPOF

Several models accounted for two polarization mode dynamics in SL and widely used with rotated polarization angle of OF [39, 80, 151-153]. VCSELs usually exhibit single polarization mode emission with high orthogonal mode suppression when lasing as a standalone laser without external perturbation. We modified the flowing rate equations for a single mode VCSEL with VPOF in order to describing their dynamical properties. The OF is provided by an external cavity using high reflectivity mirrors where part of the output light is rotated using QWP and re-injects back into the laser. The OF delay time τ is given by the external cavity length L_{ext}, where $\tau = \frac{2L_{ext}}{C}$, and c is the velocity of light in vacuum. It should be mentioned that, the case of θ_p = 0° corresponds to pure XP feedback and the case of θ_p = 90° corresponds to pure YP feedback. The equations take the form (the subscripts (x, y) indicate the XP and YP modes, respectively) [39, 80]:

$$\frac{dE_x(t)}{dt} = \frac{1}{2}[G_x(t)(N(t) - N_o) - \gamma_x]E_x + k_x E_x(t-\tau)\,cos(\theta_p) + \sqrt{\beta_{sp}\xi_x} \quad (2.18)$$

$$\frac{dE_y(t)}{dt} = \frac{1}{2}\left[G_y(t)(N(t) - N_o) - \gamma_y\right]E_y + k_x E_x(t-\tau)\,sin(\theta_p) + \sqrt{\beta_{sp}\xi_y} \quad (2.19)$$

$$\frac{d\phi_x(t)}{dt} = \frac{\alpha}{2}[G_x(t)(N(t) - N_o) - \gamma_x] - k_x \frac{E_x(t-\tau)}{E_x(t)} cos(\theta_p) - \sqrt{\beta_{sp}\xi_x} \quad (2.20)$$

$$\frac{d\phi_y(t)}{dt} = \frac{\alpha}{2}\left[G_y(t)(N(t) - N_o) - \gamma_y\right] - k_x \frac{E_x(t-\tau)}{E_y(t)} sin(\theta_p) - \sqrt{\beta_{sp}\xi_y} \quad (2.21)$$

Equation (2.1) can be rewrite as below to compensate for OF:

$$\frac{dN(t)}{dt} = \frac{\eta_i I}{qV} - \frac{N(t)}{\tau} - (N(t) - N_o) \times G_x(t)|E_x(t)|^2 + G_y(t)\left|E_y(t)\right|^2 \quad (2.22)$$

$$\Delta\emptyset(t) = -\Delta\omega_{x,y}t + \omega_{x,y}\tau + \emptyset_y(t) - \emptyset_x(t-\tau) \quad (2.23)$$

Here E_x and E_y are the varying amplitudes of the XP and YP mode respectively, $k_x$and k_y are the feedback strengths of XP and YP mode respectively, $\beta_{sp}$is the strength of the spontaneous emission, $\xi_{x,y}$ is independent Gaussian white noise sources with zero mean and unit variance for XP and YP mode, $\emptyset$ and ω are the phase and the angular frequency, respectively.

For preserve OF case, both XP and YP mode are utilized to pass through the external cavity and then be re-injected into VCSEL. Due to the rotation of polarization angle, the feedback strength for XP and YP components can be expressed as [122]:

$$k_x = k \times \sqrt{\frac{1+cos^2(\theta_p)}{2}} \quad (2.24)$$

$$k_y = k \times \sqrt{\frac{1+sin^2(\theta_p)}{2}} \quad (2.25)$$

The rate equations for preserve-OF can be expressed as follows:

$$\frac{dE_x}{dt} = \frac{1}{2}[G_x(N(t)-N_o) - \gamma_x]E_x + k_x E_x(t-\tau_1)\,cos(\theta_p) - k_y E_y(t-\tau_2)\,sin(\theta_p) + \sqrt{\beta_{sp}\xi_x} \quad (2.26)$$

$$\frac{dE_y}{dt} = \frac{1}{2}\left[G_y(N(t)-N_o) - \gamma_y\right]E_y + k_x E_x(t-\tau_1)\,sin(\theta_p) + k_y E_y(t-\tau_2)\,cos(\theta_p) + \sqrt{\beta_{sp}\xi_x} \quad (2.27)$$

The feedback strength k can be calculated from the feedback ratio F (in dB) used in the experiment as [115, 154]:

$$k = \frac{1-R_o}{\tau_{in}}\sqrt{\frac{R_m}{R_o}} \quad (2.28)$$

where $\tau_{in} = \frac{2L_{in}\, n_o}{c}$ is the internal round-trip delay time (s), n_o is the refractive index, L_{in} (m) is the internal cavity length, R_o is the facet reflectivity, and R_m represents external reflectivity and can be expressed as $R_m = 10^{F/10}$ (in dB) is the feedback ratio used in the experiment.

2.13 Conclusions

In this chapter, an overview to FSO and polarization properties of VCSEL including of optical chaos, optical and electrical properties, L-I characteristics, PS, hysteresis properties, RIN, nonlinearity behaviours and VCSEL under modulation current were presented. In addition, dynamical properties of the two orthogonal polarization modes of VCSEL with VPOF using the rate equation were described. It was known that FSO is a powerful and promising technique to increase the data transmission rat in communication systems. Most FSO systems use a wavelength range between 780 to 850 nm. For this wavelength range, which has a low attenuation less than 0.2 dB/km, optical devices are available and inexpensive. Although, polarization properties of VCSELs have intensively been studied however, they are still under active investigation due to its potential applications as in secure communication and nonlinear optical systems.

The Chapter also in brief described VCSEL problems and the possibility to control polarization instability. In fact, SLs are particularly sensitive to the feedback light, showing a destabilized optical output power. The polarization properties of VCSELs are altered when subjected to OF. The basic concept of OF with proposed technique of this thesis VPOF were presented with previous studies using this technique on VCSELs. Strong OF led to nonlinearity behaviours in the output power of the laser. Hysteresis

properties also presented in brief, where theoretical studies showed that the HL is sensitive to the bias current and enhances with the fast injection current compared to the slow injection current. Hysteresis width was also sensitive to the OF level and sweep of θ_p, where a narrow width could be achieved with a low OF level and a slow swept of θ_p. The RIN level of VCSEL can be reduced using a strong OF owing to the phase effect of the reflected light. This was also presented in details with OF. It was referring that the VPOF is still under active study and their consequences on the polarization properties of semiconductor laser are not fully understood. Such a technique was investigated theoretically for controlling the polarization instability in VCSEL. The dynamical properties of VCSEL polarization modes with VPOF were developed in a theoretical model and discussed in detail using the rate equations, which use to verify the experimental results of this work and to better understanding of the VPOF effects.

Chapter 3

Light-Current (L-I) Characteristics and Hysteresis Properties under VPOF

3.1 Introduction

SLs with their attractive properties have further increased motivation to apply functions of optical devices based on bi-stability properties [128]. Typically VCSELs devices exhibit unstable polarization properties due to inherent structures, such as PS, which appear at the laser output power and can be exploited it in many applications such as optical memory and data storage [46, 94]. In VCSELs it is possible to achieve PS of the polarization modes by using an optical injection [112, 155], strong enough OF [156] and rotated polarization angle of OF [40], as well as thermal effects [111]. The hysteresis can occur in the PS of the two polarization modes of VCSEL at free-running operation using injection current sweep rate [18]. It is well-known that the OF level would strongly influence VCSELs's dynamics. Theoretical and experimental investigations demonstrated that OF induce attractive properties in VCSELs such as chaos and bi-stabilities and how they are depending on OF strength [52, 120]. A theoretical study based on the framework of the spin-flip model (SFM) has demonstrated that the hysteresis width is modified by the frequency detuning of the VCSELs' polarization modes [157]. It has shown that the hysteresis loop (HL) is sensitive to the bias current and the possibility of enhancing the hysteresis size with fast

injection current compared to slow injection current. In this chapter the L-I curve properties of VCSEL is describe with and without OF in section 2.3. After that the influence of VPOF on the PS properties of a VCSEL has been investigated experimentally and the results are presented in section 2.4. In section 3.5, the polarization extinction ratio of the polarization modes of VCSEL is presented using VPOF effects.

3.2 VCSELs Devices under Study

In this thesis several VCSELs devices have been used, which were provided by different companies, their optical and electrical properties are provided in Table 3-1. All these devices were used in the experiments and their properties were investigated. These devices offer different optical and electrical properties, such as threshold current, output power, emission wavelength, relative intensity noise, polarization stability, etc. However, they are emitting a single transverse and longitudinal mode with a slight deference in the emission wavelength, which is between 850 to 852 nm. The VCSELs under study are lasing in a linear polarized mode near the threshold current and they exhibit different I_{th} values of 0.5 mA, 1.5 mA, 2.9 mA and 3.9 mA with various output powers which reaches up to 2 mW. All VCSEs devices are emitting stable polarization (no PS occur under free running operation), except for one VCSEL that exhibits two types of switching (PSI and PSII) at free running operation (see Fig. 3-3), this will explained later in the next section. The next section provides the L-I curve characteristics of the free running VCSELs under study as well as the L-I curve characteristics under OF effects.

Table 3-1: Optical and Electrical Characteristics of VCSELs devices

Avalon Photonic Devices	Ray Can Devices	Thorlabs Devices	Philips Devices
Premium 850 nm single mode VCSEL,TO46	850 nm single mode VCSEL,RC12xxx1-T	Single mode VCSEL 850 nm	Single mode VCSEL 852 nm
Medium oxidation process	Side mode suppression 25 dB	Oxidation process	Side mode suppression 30 dB
No polarization flips Gaussian beam profile	High speed high performance communication application	Flat window	3dB modulation bandwidth 1GHz
Operating voltage 2.2 V	Operating voltage 3 V	High speed 2.5Gbps	RIN -130 -120 dB
Threshold current 3.9 mA	Threshold current 3 mA	Threshold Current 1.5 mA	Threshold current 0.5 mA
Max. optical output power 0.5 mW	Max optical output power 0.7 mW	Max Optical Output power 2 mW	Max optical output power 1 mW
Side mode suppression 20 dB	Operating temperature Range 0 to 85 ºC	Operating Temperature Range 5 to 80 ºC	Operating temperature Range -20 to 80 ºC

3.3 Free Running (L-I) Curve Characteristics of VCSELs

In this section the optical properties of the L-I curve characteristics of the VCSELs that were used in this thesis are presented including the polarization-resolved output power with and without OF. The standalone VCSELs lase in a fundamental mode with two orthogonal polarization modes for the entire range of bias current I_b used in the experiments. Fig. 3-1, displays the experimental setup for the free running L-I curve measurements of VCSELs. The laser is driven by laser diode driver (Newport, 505B) and is temperature controlled by temperature controlled with a thermoelectric temperature controller (TED 200C) to within 0.01^{o}C. The laser output is collimated using objective lens (Aspheric Lens, f = 4.51 mm). A half wave plate (HWP) (Zero-Order Half-Wave Plate) and a polarization beam splitter (PBS) (Cube, 620 - 1000 nm) are used to direct the orthogonal polarizations of the VCSEL to the photodetectors (PD) (New Focus Nanosecond photo detector, model No). 1621. The HWP and PBS are used only when measured the VCSEL polarization-resolved L-I curve using an optical power

meter (Anritsu, ML9001A) and then removed when measuring the total output power (I_T). The L-I plots were obtained using LabVIEW controlled by a personal computer.

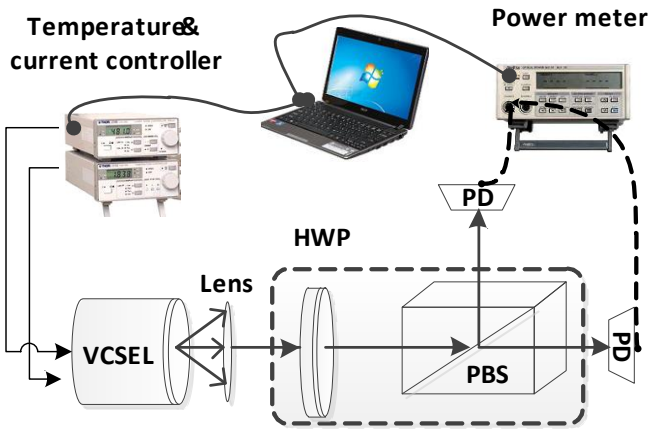

Figure 3-1: Experimental setup to measure output power properties of VCSELs, half wave plates (HWP), polarization beam splitter (PBS) and photo detector (PD).

Fig. 3-2 displays the L-I characteristics of standalone VCSELs under study, where in Fig. 3-2(a) the total output power and in Fig. 3-2(b) the polarization-resolved output power of the VCSEL are presented. The first lasing mode in Fig. 3-2(b) with a full square black line refers to the X-polarization (XP) and the suppressed mode with a full dot red line corresponds to the Y-polarization (YP) mode. For all VCSELs (except one) no PS was observed over the whole I_b range. Fig. 3-3 shows the total output power (a) and the polarization resolved output power (b) of the standalone VCSEL combined with two PS without any external perturbation. PS occurs between the orthogonal polarization modes of the VCSEL when I_b increase from zero to 9 mA. The first type of switching (PSI) occurs at ~ 6.3 mA from the high-frequency mode (XP) to the mode with low frequency (YP). While the second type of switching (PSII) is observed at I_b of ~ 7.6 mA corresponding to PS from the XP (low frequency mode) to the orthogonal

mode (YP) with the high frequency mode, as depicted in Fig. 3-3(b). Both types of switching (i.e., PSI and PSII) are defined and studied in detail in [158].

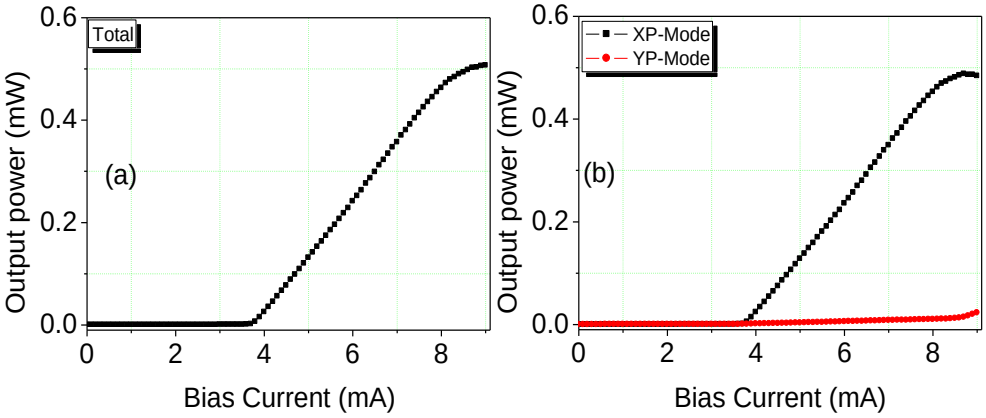

Figure 3-2: light-current characteristics of free-running VCSELs under study (a) the total output power and (b) the polarization-resolved output power.

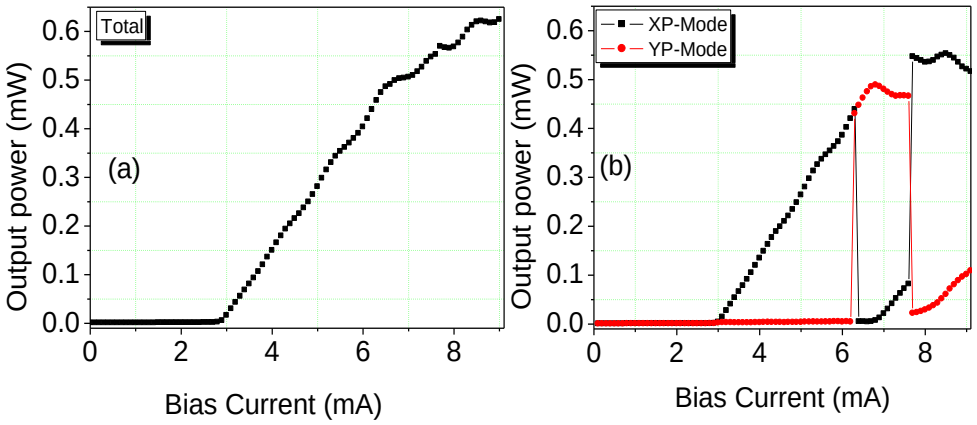

Figure 3-3: The L-I characteristic of standalone VCSEL, (a) total output power, (b) polarization-resolved output power with two PS.

3.3.1 Threshold Current Reduction and L-I Curve Characteristics under OF

As we mentioned earlier in Chapter 1 that the OF can reduce I_{th} value of the laser due to reduced losses inside the cavity of the laser and the intensity noise [22, 23]. A lasing threshold reduction in VCSEL is observed under strong OF. Fig. 3-3 displays the L-I curve characteristics of VCSEL subject to -5.5 dB of OF. Fig. 3-4(a) shows I_T under rotating the YP mode by 90° and reinjecting it back to the VCSEL. In this figure, clearly

we can see the VCSEL start lasing at I_{th}~3.45 mA, with the threshold current reduction I_{thR} of ~ 11.5% compared with that of standalone VCSEL (3.9 mA). However, VCSEL exhibits low output power and slop efficiency compared with the standalone VCSEL, as displaying in Fig.3-4(a). I_{thR} is defined by:

$$I_{thR} = \frac{I_{th}Free\ running - I_{th}under\ OF}{I_{th}Free\ running} \times 100 \tag{3.1}$$

Fig. 3-4(b) shows the polarization-resolved output power of VCSEL subject to the orthogonal OF. The VCSEL display two PS and mode fluctuation at higher values of I_b. The first and second PS occurs at I_b of ~7.5 mA and ~8.6 mA, respectively.

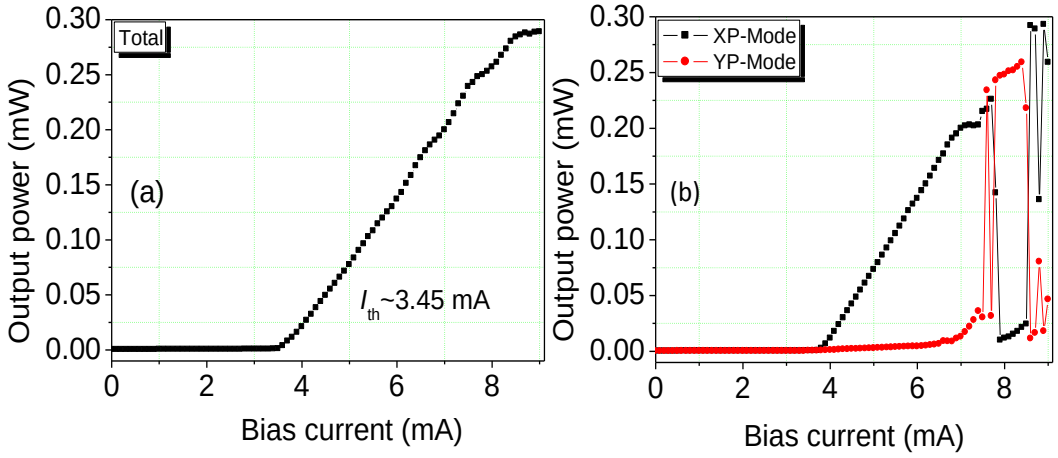

Figure 3-4: light-current characteristics of VCSELs under-5.5 dB OF (a) the total output power of VCSEL with YP OF, (b) the polarization-resolved output power of VCSEL under VPOF.

3.4 Hysteresis Properties and Bi-Stability in the Polarization Mode of VCSEL

Recently, bi-stability properties of VCSELs with VPOF have been studied theoretically [39, 40]. It was shown that the HL width is depending on the sweep rate of θ_p and the feedback delays and the feedback strength can significantly affect the size of HL. However, the polarization bi-stability properties of such devices subject to VPOF have

not yet been experimentally reported. VPOF provides different ways and more flexibility of controllable polarization properties of SLs, which justifies in depth investigation.

The results of this investigation show that the hysteresis size is significantly affected by the OF levels. For higher OF level of -6.4 dB the HL width is much narrower than that of the lower OF level of -8.3 dB, which agrees with the theoretical investigation in [40] and experimental study in [52]. In this chapter the hysteresis properties are investigated using a different technique, which is VPOF mechanism compared with the experimental studies reported in the literature [52].

3.4.1 Experimental Configuration for HL Measurements

Fig. 3-5 displays the experimental setup for the delayed VPOF to measure the HL properties. The system is composed of an 850 nm single mode VCSEL (Avalon photonics UK Components Ltd) with a threshold current of ~3.9 mA at free running operation. The VCSEL is driven by a DC source (7651 YOKOGAWA) and is temperature controlled with a thermoelectric temperature controller (TED 200) to within 0.01^{o}C. Both beam splitters (BS1&2) 50/50 splitter. A polarizer is used to select the polarization direction in which measurements are carried out the output of which is measured using a photodetector (PD) (New Focus Nanosecond photo detector, model No. 1621). An optical power meter (OPM) is used to measure the optical output power and the feedback light from the feedback loop.

A half wave plate (HWP1) is used to select the orthogonal polarization (YP) direction, which is injected back into the VCSEL, whereas HWP2 is used for rotating the polarization direction of YP from 0^{o} to 90^{o}. Note that 0^{o} and 90^{o} are defined as the 1^{st} and 2^{nd} polarization modes i.e., XP and YP, respectively. An optical isolator (ISO) (> 40

dB) is utilized to ensure that the beam is rotating clockwise within the loop; 5^o rotation in HWP2 is equivalent to 10^o rotation the polarization. The intensity of the beam within the loop is adjusted using the neutral density filter (NDF) (OD: 0-2.0, ARC: 650 - 1050 nm). Finally M1-3 is used to establish the optical loop. θ_p is varying from 0^o to 90^o pure parallel an orthogonal OF respectively, with respect to XP of the standalone VCSEL. Basically θ_p controls the strength of fixed feedback to both modes of XP and YP. The OF level that used here is within regime V, as reported in [115], to study the HL properties of the VCSEL.

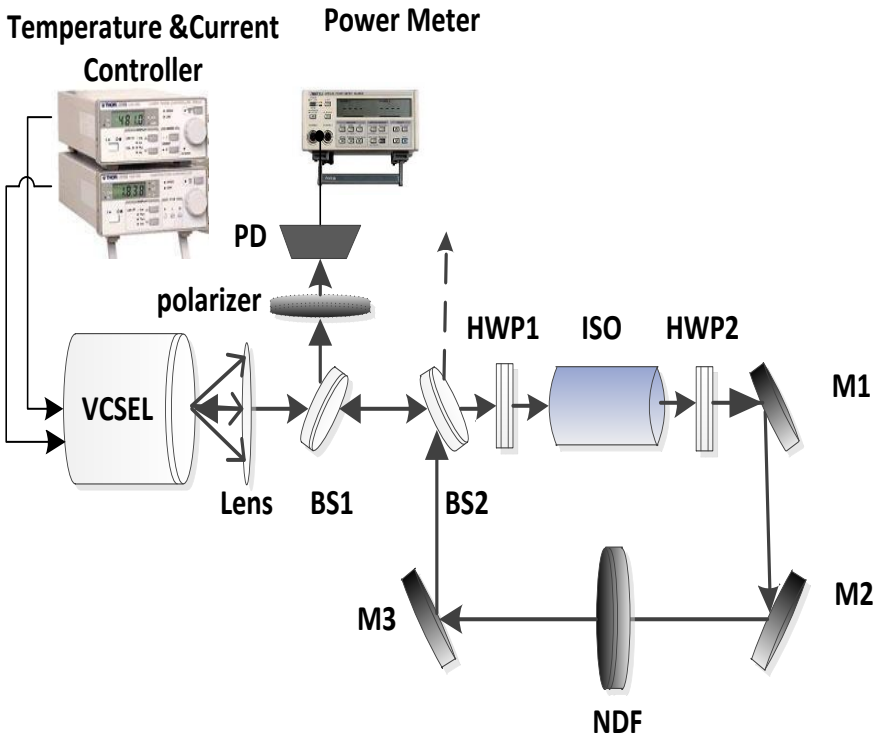

Figure 3-5: Experimental setup; VCSEL with external cavity included, non-polarizer beam splitter (BS), polarizer, photo detector (PD) and optical feedback loop which consist of mirrors (M1, 2, 3), BS2, half wave plates (HWP1, 2), optical isolator (ISO) and neutral density filter (NDF).

3.4.2 Results and Discussion

At high levels of OF, VCSEL exhibits an abrupt PS when θ_p is swept from 0^o to 90^o and vice versa. We observe a HL beyond the polarization angle of 45^o, which is barely

affected by the level of the feedback. Fig. 3-6 displays the polarization resolved L-I characteristic of the free-running VCSEL. For the XP-mode the characteristics is that of a typical laser devices with I_{th} of around 3.9 mA where as for the YP-mod there is no obvious threshold knee beyond the maximum limited injected current. Thus, the figure shows that the YP-mode is being suppressed. Therefore, no PS is observed in the free running VCSEL. Orthogonal polarization feedback (YP) has been employed to obtain polarization bi-stability under a high OF level. In this case of investigation I_b was fixed at 6 mA for all experimental measurements. The polarization angle θ_p is increased linearly from 0^o to 90^o in an upward scan and then decreased from 90^o to 0^o in a downward scan.

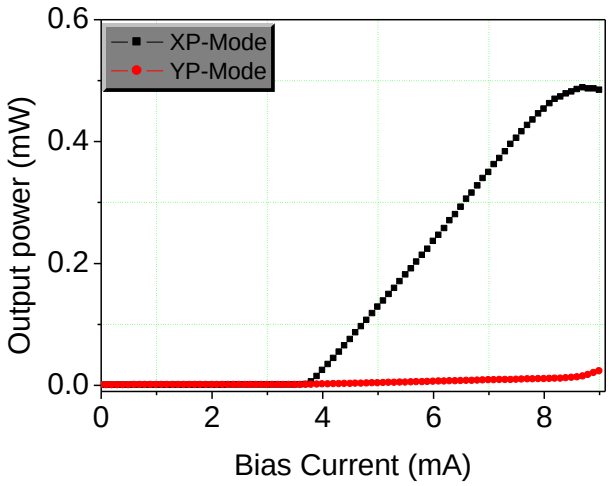

Figure 3-6: Polarization-resolved L-I curve of the free-running VCSEL, the square black line is the XP mode and the dot red line is the YP mode.

Fig. 3-7 displays the polarization resolved intensities of VCSEL as a function of θ_p for the XP and YP modes when subjected to an OF level of -11 dB. The OF level here is defined as a ratio of the feedback power (measured at BS2) to the total VCSEL output power (measured before BS1), see Fig. 3-5. As shown in Fig. 3-7 the VCSEL output intensity displays low sensitive to the polarization variation of OF with no evidence of

lay PS over the given range of polarization angle. The VCSEL lases with the dominant mode (i.e. XP) and the YP mode is being suppressed. This is because the OF plays less important role when the feedback effect is smaller than the gain effect of the mode as a demonstrated in Ref [39].

However, when the OF level increase their influence is clearly observed in the output power of the polarization modes. Fig. 3-8 shows the optical intensity as a function of θ_p for the XP and YP mode for OF of -8.3 dB. Both reference levels (-8.3 and -6.4 dB) in Figs. 3-8(a) and (b) selected are within the well-defined feedback regime V, which is the highest level feedback power ratio, as in [115].

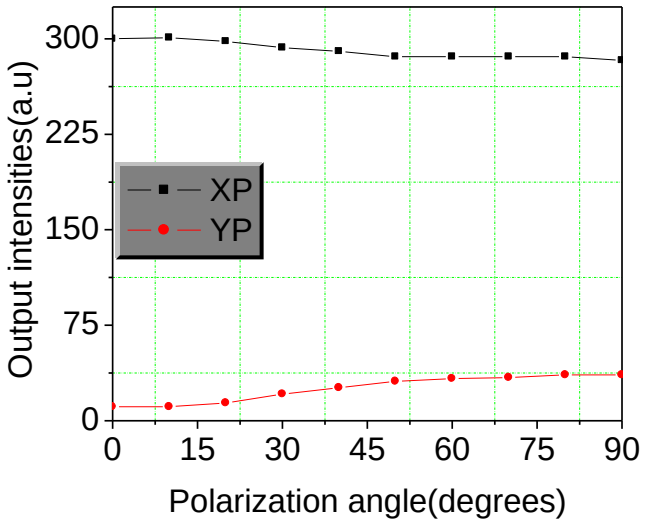

Figure 3-7: Polarization-resolved intensities as a function of the polarizer angle, XP and YP mode. The external optical feedback is Fixed at -11 dB.

At these levels of the feedback the XP is the dominant mode switching to the YP mode after 45° of rotation of θ_p. This is due to as θ_p increases the XP mode losing more and more feedback while the YP mode is gaining more feedback [39].In Fig. 3-8(a), for the optical feedback level of -8.3 dB, PS occurs at 60° (θ_{pu1}) and 69.9° (θ_{pu2}) in upward scan of θ_p from 0° to 90°, while in the downward scan from 90° to 0° PS occurs at

different angles of 89.7° (θ_{pd1}) and 70° (θ_{pd2}) that causes variation in the hysteresis width. In this case the width *W* of HL is 11.6°. Correspondingly, in Fig.3-8 (c) for the feedback level of -6.4 dB, PS take place at θ_{pu1}= 60° and θ_{pu2} = 69.6°, for the upward scan and θ_{pd1} = 79.8° and θ_{pd2} = 70° for the downward scan.

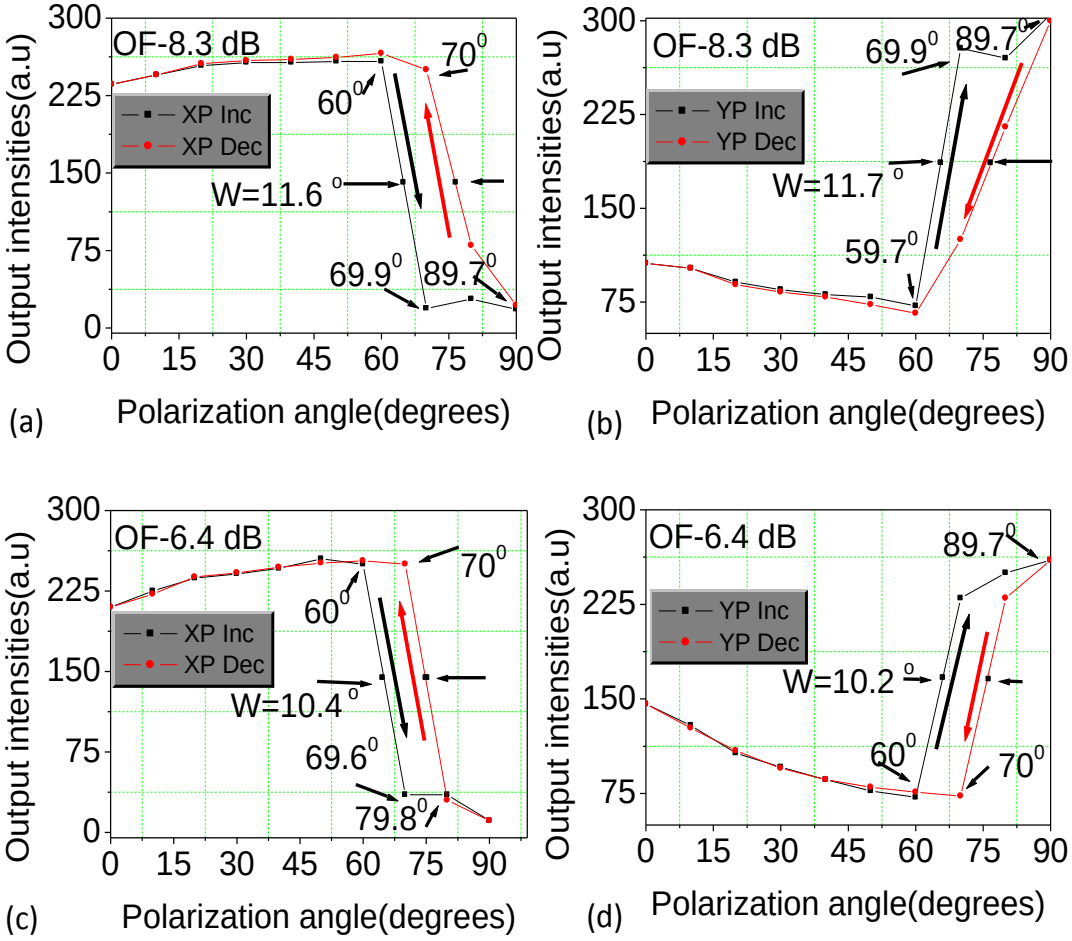

Figure 3-8: Polarization-resolved intensities as a function of polarization angle, (a) represent the XP mode, the arrow down (up) corresponds to increasing (decreasing) θ_p and (b) represent the YP mode, the arrow up (down) corresponds to increasing (decreasing) θ_p, The external optical feedback fixed at -8.3 dB, (c) represent the Xp mode, the arrow down (up) corresponds to increasing (decreasing) θ_p and (d) represent the YP mode, the arrow up (down) corresponds to increasing (decreasing) θ_p, The external optical feedback fixed at -6.4 dB.

The HL width *W* is 10.4°. Note that in Figs. 3-8(a) and 3-8(c) θ_{pu1} are equal and θ_{pd} is more sensitive to the OF than θ_{pu}, which is quite similar to the numerical calculations

reported in [40].The results show that changes in the size of HL are depending on the OF strength. We observe that narrow and wide HLs takes place for higher and lower levels of OF, respectively. Variation of the polarization OF can cause HL in output power of the VCSEL depending on the level of OF. The results in Figs. 3-8(b) and (d) show the intensity of the YP-mode against θ_p for the feedback levels of -8.3 and -6.4 dB, respectively. In Fig. 3-8(b), for the upward scan of the YP mode switch to XP mode at θ_{pu1} =59. 7^o and θ_{pu2} = 69.9^o, while in the downward scan the PS occur at θ_{pd1} = 89. 7^o and θ_{pd2} = 59.7^o.

However, for the feedback level of -6.4 dB, see Fig. 3-8(d), the upward scan of θ_p display different position for the switching point than Fig. 3-8(b) where θ_{pu1} and θ_{pu2} are 60^o and 89. 7^o, respectively and for the downward scan the values are 89.7^o and 70^o, respectively. The width of HL is 11.7^o at -8.3 dB and 10.2^o at -6.4 dB. These results verify that larger feedback levels do lead to a narrower HL.

3.5 Polarization Extinction Ratio of Polarization Modes of VCSEL

VCSELs offer very attractive features, such as very low threshold current (μA) low cost and circular output power beam. However, polarization stabilization remains an issue in such devices due to their inherent structures, which lead to instability polarization gain [52]. The PS between the orthogonally modes easily occurs by changing the injection current of the laser. Recently, several works have investigated the polarization modes properties of VCSELs with rotated polarization angle of OF both theoretically and experimentally [39, 57, 88, 159]. Polarization extinction ratio (PEX) is an important factor in modulation amplitude requirements for error-free data transmission [160].

For this investigation the influence of rotated polarization OF (RPOF) on the polarization resolved light-current (L-I) characteristics of VCSEL is examined experimentally. The two orthogonally polarization modes (XP and YP) of the VCSEL are rotated and re-injected individually to the VCSEL using a T-shaped external cavity OF. The VCSEL is subjected to rotating the parallel and orthogonal polarization OF, RPOF and ROOF respectively. Polarization stabilization of the VCSEL is evaluated using the L-I curve measurements and PEX. It has been show that the output power of the VCSEL is strongly modified by the ROOF, which is enforces the laser to emit in certain polarization mode. However, RPOF does have a less important effect on the polarization properties and the extinction ratio values of the VCSEL.

As mentioned above, in two cases of the feedback based on the T-shaped scheme the polarization properties have been examined. M1 (M2) and QWP are provided RPOF (ROOF).

3.5.1 Results and Discussion

The schematic diagram of the experimental setup is shown in Fig. 3-9. The ROOF is attained with M2 (M1 is closed) and the RPOF is achieved with M1 (M2 is closed) as display in the setup. We refer to polarizations parallel and orthogonal light to that of solitary device light. VCSEL operating at 850 nm was used in the experiment with a similar L-I curve characteristics that were presented in section 3.4. A QWP and NDF are used to rotate θ_p and control the feedback level, respectively. The collimated laser beam was reflected back to the VCSEL using two mirrors placed at ~ 40 cm away from the VCSEL. The laser output power decomposed in two orthogonally polarized modes using a cube PBS. An optical power meter was used to measure the output power variation using after passing through a linear polarizer (P), which is used to select the polarization mode.

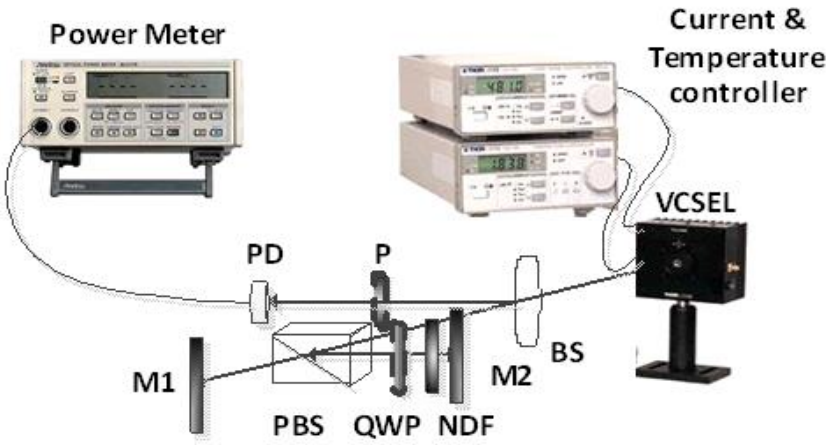

Figure 3-9: T-shaped feedback scheme for parallel and orthogonal polarization feedback, non-polarizer beam splitter (BS), polarizer (P), photo detector (PD), mirrors (M1, 2), quarter wave plates (QWP), and neutral density filter (NDF).

The feedback ratio is defined as the ratio of the power fed back into the VCSEL relative to the total output power of the free running operation of the laser. In this study we defined $\theta_p = 0^o$ to a maximum power of the XP OF and $\theta_p = 90^o$ to a maximum power of the YP OF. PEX is defined as the optical power ratio between the two orthogonally polarized XP and YP modes.

For the two polarization feedback schemes the L-I curve characteristics of the VCSEL have measured under feedback level of ~ -6 dB. The maximum PEX of the free running VCSEL is ~16.8 dB. This is strongly affected by the ROOF scheme as we can see in Fig 3-10. This figure shows the output power response of the VCSEL subject to both XP and YP OF with only rotating θ_p of the parallel mode (XP). For this case of the feedback VCSEL start lasing with the orthogonal polarizations mode (YP), which become the dominant mode. The PEX degraded to 10 dB at 0^o. The two orthogonal polarization states are degenerated at 0^o, while they are well separated at 90^o. The VCSEL emits two modes simultaneously for several mA, after that the YP become the

dominant mode. The YP mode gain is strong enough to let the mode become the dominant mode, while at 90^o the XP mode loss the feedback light and becomes suppressed [39, 159]. The results are also indicated that I_{th} of the VCSEL decreased by several μA combine with decreasing the slope efficiency of the output power [29].

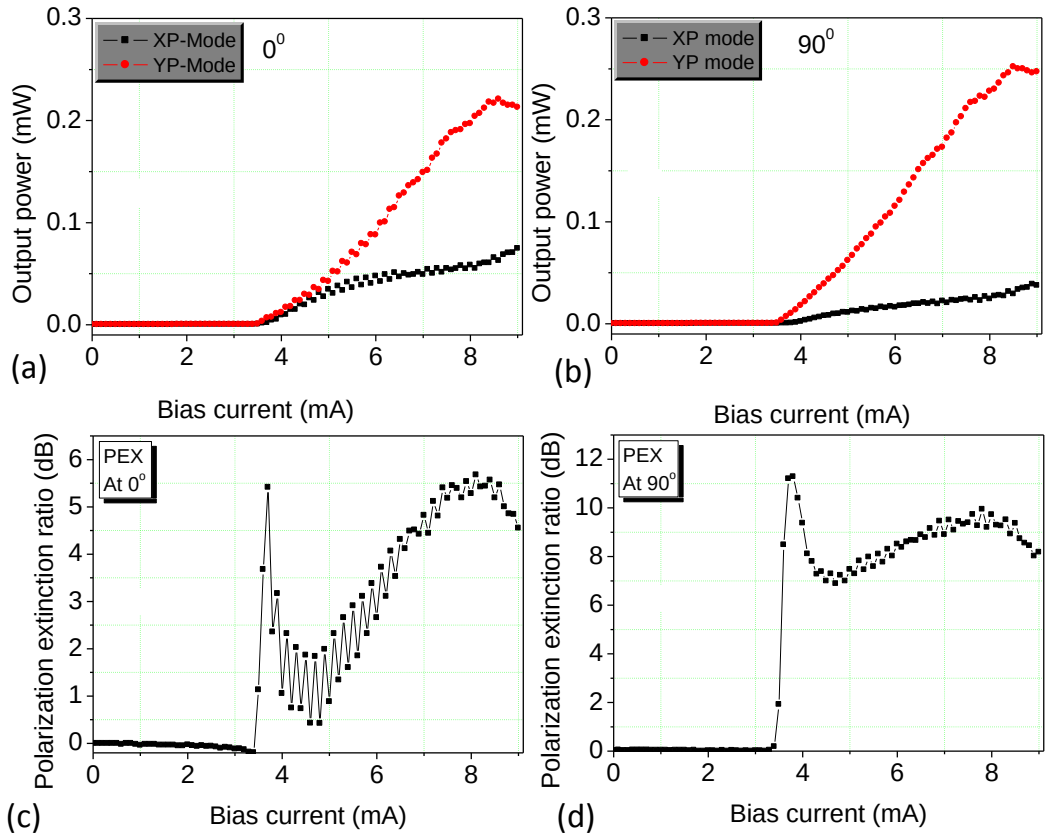

Figure 3-10: Measured output power response of VCSEL with rotated XP mode of the optical feedback and fixed YP mode at (a) 0^o and (b) 90^o; (c) and (d) display corresponding extinction ration measurements of (a) and (b) respectively.

In case of RPOF, the orthogonal OF (YP) is closed, no PS is observed and the laser lases in the XP mode over the entire range of I_b, see Fig. 3-11(a & b). The maximum value of PEX is 17.8 dB at 0^o, while it is 14.5 dB at 90^o of θ_p. The polarization direction selectivity is enhanced at $\theta_p = 0^o$ and the PEX value increases by 1 dB compared with that of the free running results.

However, when θ_p = 90°, which mean the XP mode loss the OF, the YP mode starts increase especially at higher values of I_b, which lead to the PEX values deteriorated. This is because the XP mode obtain the maximum feedback light at 0° with no feedback for the YP mode [39].

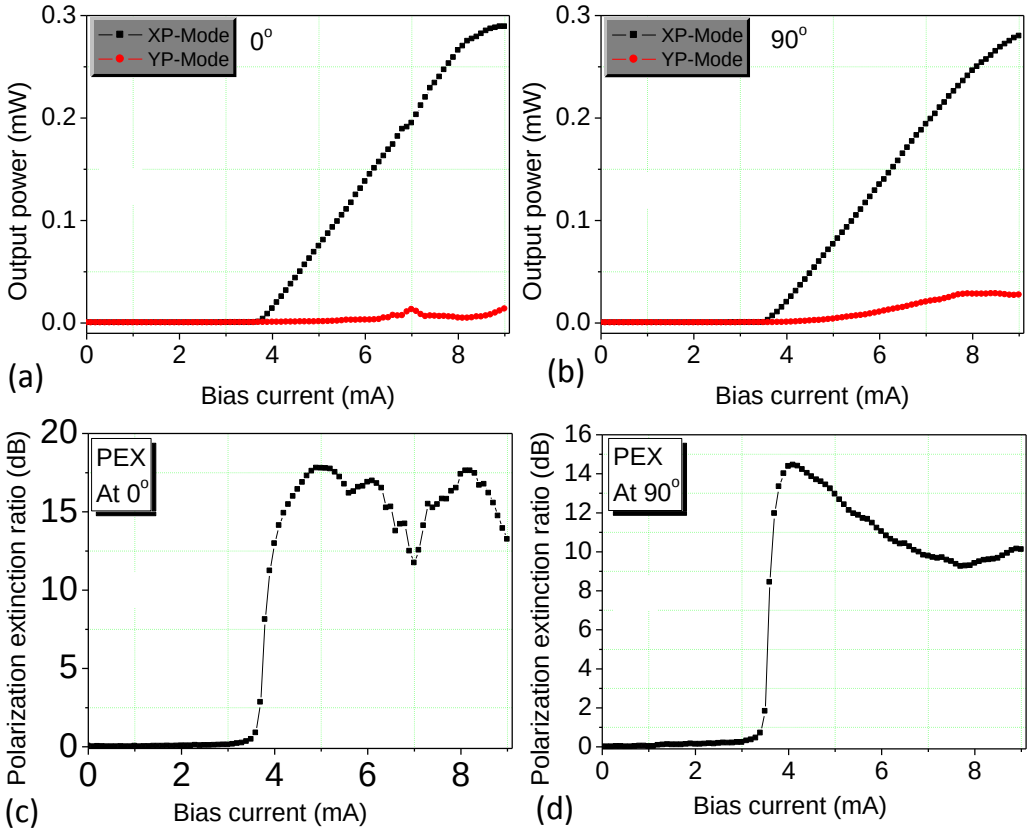

Figure 3-11: Measured the output power response of VCSEL with rotated the XP mode of the optical feedback and closed the YP feedback at (a) 0° and (b) 90°; (c) and (d) display the corresponding extinction ration measurements of (a) and (b) respectively.

The results indicated that the orthogonal polarization OF forces the laser to emit in certain polarization state. Whiles the parallel polarization OF can enhance the corresponding polarization mode of standalone VCSEL, which in turn lead to increase PEX between the two orthogonal modes.

Next, the polarization intensities of the VCSEL under the effects of VPOF of the parallel and orthogonal polarization modes are investigated. In this case, both the

feedback level and I_b are fixed at 6 dB and 6.8 mA respectively, while the QWP angle is varied from 0^0 to 180^o. In Fig. 3-12(a) displays the results of RPOF (the orthogonal OF is closed), clearly can be seen that the rotated only the parallel OF does not have significant effect on the VCSEL polarization emission over the entire range of θ_p.

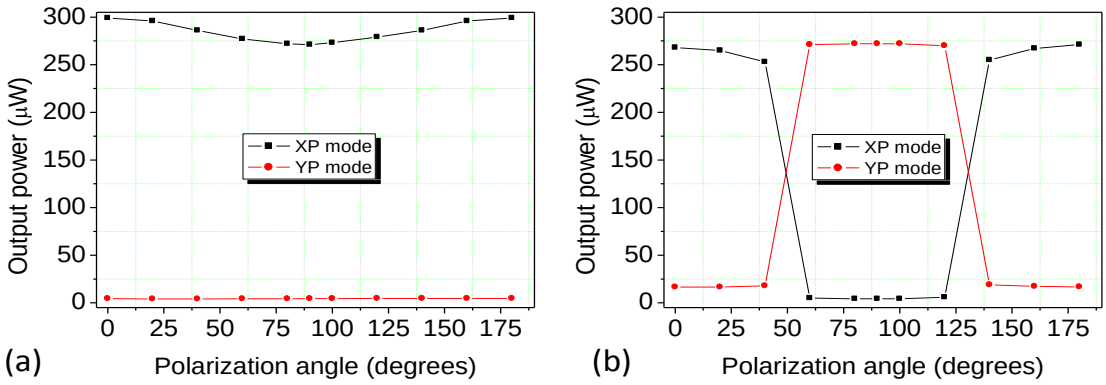

Figure 3-12: Polarization-resolved intensities of VCSEL versus polarization angle, (a) subjected to XP feedback (block the YP feedback), (b) subjected to YP feedback (block the XP).

However, when the ROOF is applied the polarization stabilization has changed dramatically depending on the sweep of θ_p. PS occurs after 45^o and 135^o of θ_p, which is verified the theoretically predicted results reported in [39]. The polarization selectivity increase when applied the ROOF especially for the higher degrees of θ_p and after the PS of the VCSEL modes.

3.6 Summary and Conclusions

In this chapter in section 3.3.1, the experimental results demonstrated that the threshold current of VCSEL emission can be reduced under the orthogonal polarization OF. Under rotating the suppressed polarization mode (YP) by 90^o and re-injected back to the

VCSEL, the laser threshold current I_{th} reduce to about 11.5%. In addition, when the VCSEL subjected to strong OF (-5.5 dB), two PS at higher value of the bias current I_b were exhibited combining with the modes fluctuations.

Another properties described in section 3.4 was the hysteresis properties of the polarization mode as a results of PS of the VCSEL which induced by VPOF. The hysteresis properties were experimentally investigated. It was demonstrated that VPOF induced HL and the feedback level can modify the hysteresis properties significantly. Hysteresis cycles were observed beyond 45^o of θ_p with OF level greater than -8 dB. The result showed that the hysteresis width for the higher feedback level -6.4 dB is much narrow than that of the lower feedback level -8.3 dB. In addition, the result showed that θ_{pd} of the PS of the downward scan was more sensitive to the feedback level than θ_{pu} of PS of the upward scan. These results were closely resembled theoretical demonstration in Ref [40].

In section 3.5, polarization extinction ratio of the polarization modes of VCSEL was presented. The results showed that the orthogonal polarization OF forces the laser to emit in certain polarization mode. Whiles the parallel polarization OF enhanced the corresponding polarization mode of VCSEL. This led to increase PEX between the two orthogonal polarization modes. The polarization selectivity increased with ROOF especially after the PS beyond 45^o of θ_p. An external OF with the variable polarization angle can significantly alter the bi-stability properties of the PS in VCSELs. VPOF can provide a new method to obtain the controllable bi-stable PS in VCSELs, which is extremely useful for applications that use the optical bi-stability.

Next chapter illustrated the PS properties with selective and preserved polarization OF with rotated θ_p. These properties are presented both experimental and numerical results.

Chapter 4

Polarization Switching Properties of VCSEL under VPOF

4.1 Introduction

In chapter three the polarization properties of VCSEL including L-I curve characteristics with and without OF and hysteresis properties under VPOF were presented. In this chapter the influence of VPOF on the PS properties of VCSEL is investigated theoretically and experimentally in two configurations. In the next section (4.2), selective and preserved OF with rotated θ_p have been considered. Selective OF is demonstrated in configuration A (CA), where only the parallel polarization mode (XP) to that of the light emitted by the solitary device is selected and re-injected into the VCSEL. While in preserved OF, which is demonstrated in the configuration B (CB), both the parallel and the orthogonal polarization modes (YP) are re-injected into the VCSEL.

For CA, it is demonstrated that PS between the orthogonal polarization modes of VCSEL can occur for a fixed feedback level and a bias current with variable θ_p of OF. However, In CB PS takes place only for certain values of θ_p, particularly when intensities of the two polarization modes become comparable with each other. For both feedback configurations, the experimental results of the two polarization modes (XP and YP) of VCSEL are found to agree well with the numerical simulations and recent theoretical study reported in literature [39]. Under rotating VPOF VCSEL can exhibit

PS for a fixed bias current and OF. The VCSEL with a greater feedback level requires a smaller θ_p to implement PS. For CB feedback, PS was not observed, nevertheless, the modes intensities were found to be close to each other at higher feedback levels, due to the comparable feedback strength between them.

Following investigation of the PS properties with VPOF using selective and preserved OF are studied considering the intensity modulation parameters, frequency and amplitude, under VPOF in section 4.3. Elimination of PS of VCSEL is achieved under certain values of the modulation frequency and amplitude in presence of the OF. The bias current effect is also investigated in Section 4.3.2.5. It is shown that for a fixed OF level a smaller θ_p is required to ensure PS when the bias current is increased.

4.2 Influence of VPOF Using Selective and Preserved Optical Feedback on the Polarization Properties of VCSEL

In this section, to study PS properties of VCSEL subject to VPOF consideration is given for two different feedback configurations; termed CA and CB with selective and preserved OF respectively, as illustrated in Fig. 4-1.

4.2.1 Experimental Arrangement

A premium 850 nm single mode VCSEL (Avalon photonics UK Components Ltd) was used with a threshold current of about 3.9 mA at free running operation. The VCSEL was driven by DC source (7651 YOKOGAWA) and was temperature controlled with a thermoelectric temperature controller (TED 200) to within 0.01^{o}C. With regards to CA, Fig. 4-1(a), a HWP1 was used to select the parallel polarization direction (XP), and an optical isolator (ISO) of > 40 dB attenuation was utilised to ensure that the beam from

the VCSEL passed though the OF loop in one direction, and was then re-injected back into the VCSEL.

The HWP2 was used to rotate the polarization direction from 0^o (maximum power passed through HWP2) to 90^o, by rotating 5^o of the HWP2 every time to obtain θ_p value until 45^o (equal 90^o of θ_p). The OF strength was adjusted using NDF. The optical power meter (PM) was used to measure the feedback level as explained previously in Chapter 3.

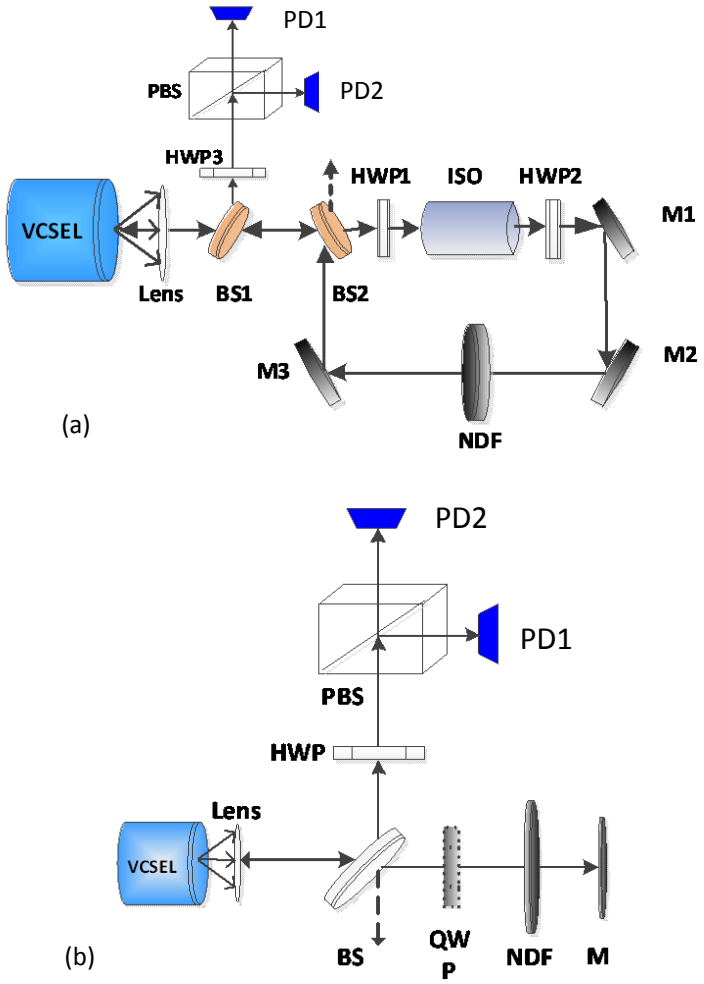

Figure 4-1: Experimental setups (a) Configuration A (CA) *and (b) Configuration B* (CB)*; BS: beam splitter. HWP: half wave plate. ISO: optical isolator. M: mirror. NDF: neutral density filter. PBS: polarized beam splitter. PD: photo detector. QWP: quarter wave plate.*

The laser output power is measured using two optical detectors, PD1 and PD2 (Newport model AD-70xr, 6 GHz bandwidth), via HWP3 and PBS. BS1& BS2 directed the VCSEL output power to the measurement and OF loop, respectively. In contrast, with CB, see Fig. 4-1(b), a QWP was used to rotate both polarization modes (XP and YP) prior to re-injecting both of them back into the VCSEL via OF loop.

4.2.2 Results and Discussions

In this section for both configurations (CA and CB), two parameters have been considered; the OF level and variable of θ_p. These parameters effects on the PS properties of VCSEL are studied experimentally and then verified theoretically. Equations 2.18 until 2.28 that were presented in Chapter 2 are used to obtain the numerical based simulation results.

4.2.2.1 Effect of the Feedback Levels

First of all, in CA consideration has given to the polarization properties of VCSEL for different values of θ_p subject to varying feedback levels from ~ -27 dB to -13 dB as shown in Fig. 4-2. The parallel polarization, (i.e., parallel to solitary VCSEL mode (XP)), is selected to re-inject back into the VCSEL. It should be noted that the maximum feedback level achieved in CA is about -13 dB due to losses associated with components etc., used in the experimental setup. The feedback level (ratio) was defined previously in Chapter 3, section 2.4.2, and the polarization resolved L-I characteristics of the free-running VCSEL under study were also presented in this section of Chapter 3. The bias current I_b was fixed at 5.8 mA for all the experiments whose results are contained in Figs. 4-2 to 4-6. In this way it was ensured that the YP mode was significantly suppressed relative to the XP mode. Fig. 4-2(a) shows that when θ_p is zero the VCSEL emits a single XP mode over the entire range of the feedback level with

completely suppressed YP mode. This is because with θ_p= 0° the dominant mode (XP) obtains all the feedback light. When θ_p = 45°, as shown in Fig. 4-2(b), the intensities of both modes has increased, but the XP mode remains the dominant mode. For this value of θ_p, the OF is shared equally between the XP and YP modes as theoretically demonstrated in [39].

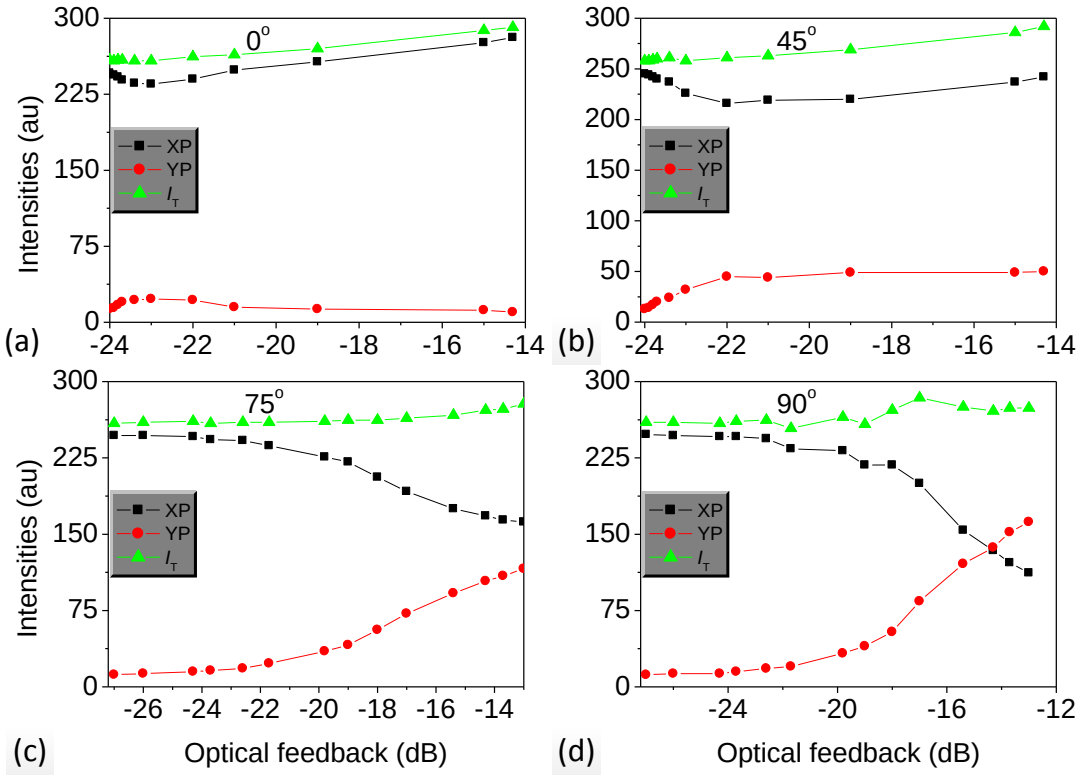

Figure 4-2: Polarization-resolved intensities versus optical feedback for CA (XP-optical feedback) for polarization angle fixed at (a) 0°, (b) 45°, (c) 75° and (d)90°.

For θ_p greater than 45°, as the feedback level increases the intensity of the XP mode decreases and the intensity of YP mode increase, see Fig. 4-2(c). In this case the XP loses the feedback light whiles the YP obtains the feedback light, thus resulting in PS as shown in Fig. 4-2(d). This is because, in contrast to the XP mode, the YP mode has experienced higher level of feedback with increased θ_p.

For CB feedback, the intensities of XP and YP mode versus the feedback level from about -18 dB to -6 dB are shown in Fig. 4-3. For θ_p = 0° as in Fig. 4-3(a), VCSEL exhibits the dominant polarization mode (XP) and the same tendency as shown in Fig. 4-2(a). However, the YP mode emission is increased compared with that of the Fig. 4-2(a). This is because of the feedback alignment. The XP mode is the dominant mode and is subjected to strong feedback. Recalled that I_b was fixed at 5.8 mA to ensure that the YP mode was highly suppressed, therefore no light is reflected back into the YP mode, thus leading to zero feedback.

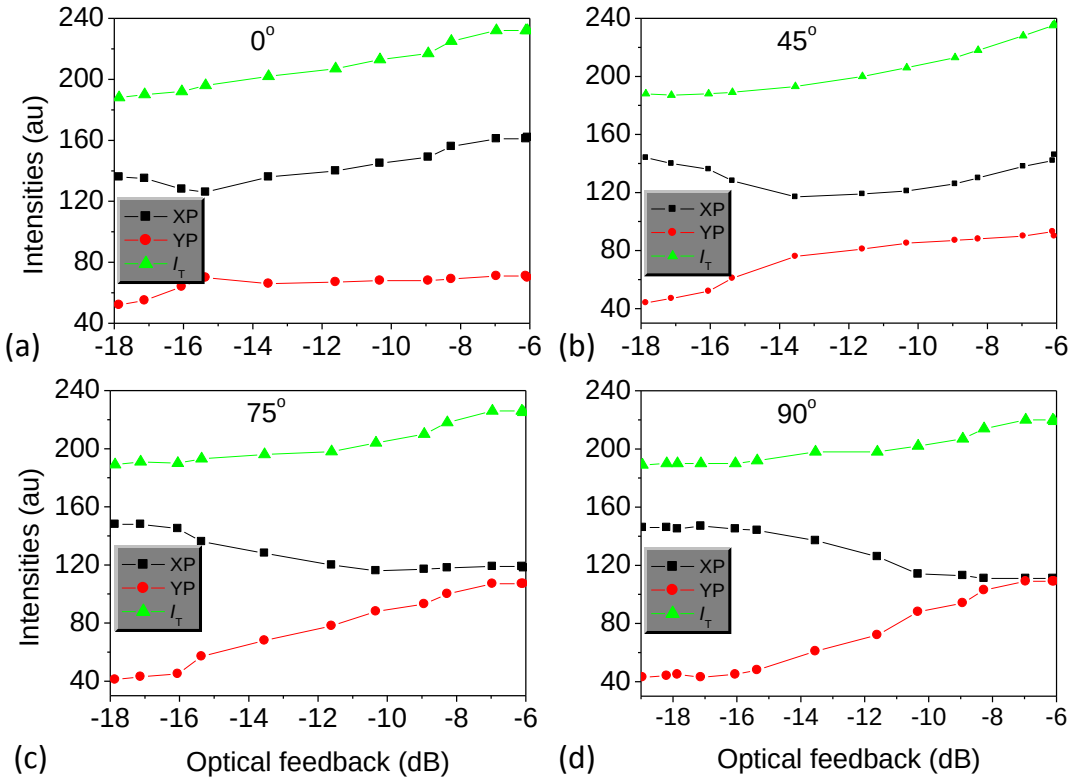

Figure 4-3: Polarization-resolved intensities versus optical feedback for CB (XP and YP optical feedback) for polarization angle fixed at (a) 0°, (b) 45°, (c) 75° and (d) 90°.

In Fig. 4-3(b) both intensities of the XP and YP modes exhibit similar behaviour, gradually increasing in intensity with increasing feedback levels. This is because for θ_p= 45° both modes are subjected to the same feedback level. Furthermore, as θ_p

increases the XP (YP) mode loses (obtains) more feedback light, therefore the comparable feedback strength achieved by the XP and YP modes leads to similar intensity profiles of both modes.

Fig. 4-3(c-d) illustrates further the enhancement of the YP mode by ~6 μW when the feedback level increased by 5 dB, as well as the total intensity for θ_p= 75° and θ_p= 90°, whilst the XP mode intensity decreases slightly by ~3×10^{-3} mW when increasing the feedback level by ≈ -4.7 dB in the entire region. For the entire feedback level considered here, the XP mode is always the dominant polarization mode for all values of θ_p, and no PS is observed. Similar finding was demonstrated theoretically in [39], which is attributed to the gain of the YP mode being less than the gain of the XP mode, (see Fig. 4-6). Next subsection will presented the second parameter effect on the PS properties, which is θ_p.

4.2.2.2 Effects of Variable Polarization Angle

Next we consider the effects of VPOF on the polarization properties of VCSEL for a range of feedback levels of -15.6, -15, -14, -13 dB. In this case, both the feedback level and I_b are fixed and θ_p is varied from 0° to 90°. For CA feedback, the polarization-resolved intensities as a function of θ_p are shown in Fig. 4-4 for different feedback levels. Fig. 4-4(a-d) shows that the XP (YP) mode decreases (increases) gradually with θ_p. Moreover, a larger feedback level, as shown in Fig. 4-4(c) and Fig. 4-4(d), lead to a PS whose position is dependent on the feedback level. The total emission intensity began to decreases at higher values of θ_p. The results illustrate that a smaller θ_p is required to realize PS for a large feedback level. These experimental results confirm the results of previous theoretical analysis in [39], which predicted that for relatively larger feedback the OF effect and gain compete for the dominant effect.

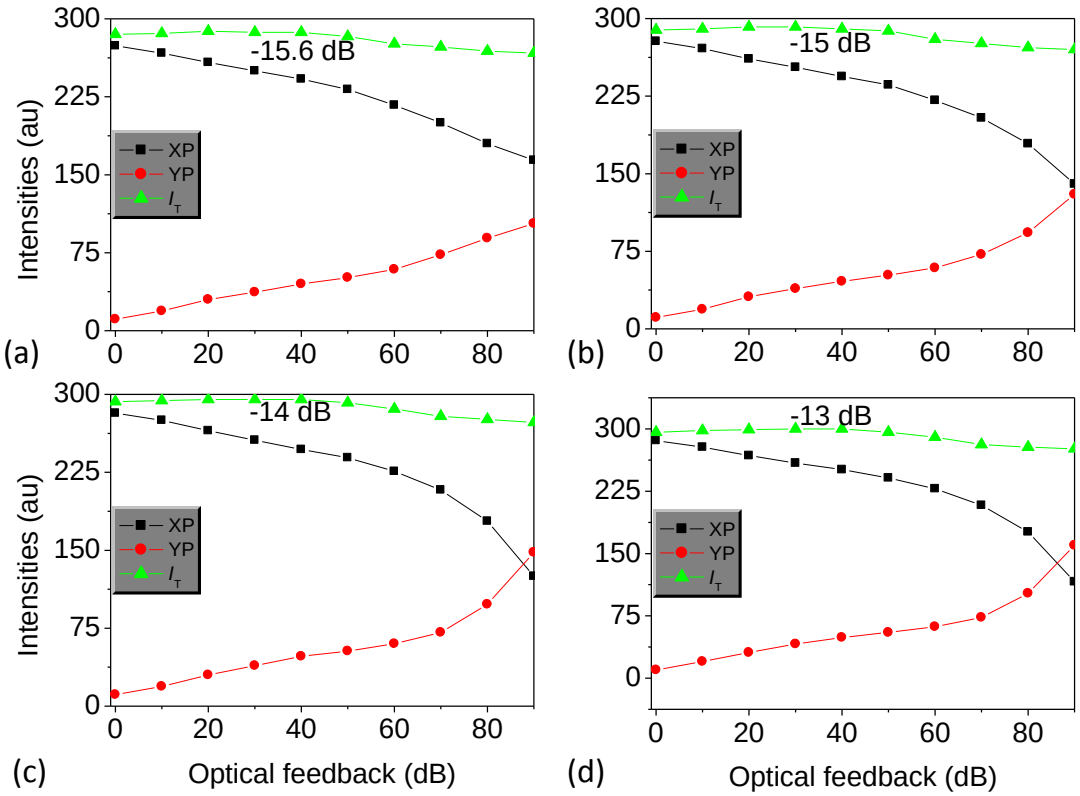

Figure 4-4: Polarization-resolved intensities versus polarization angle for CA, (XP optical feedback) for a fixed feedback level at (a) -15.6, (b) -15, (c)-14 and (d) -13dB.

Fig. 4-5 displays the polarization resolved output intensities as a function of θ_p for the VCSEL subject to CB feedback. It can be observed from Figs. 4-5(a-d) that as θ_p is increases in the range of $0° \leq \theta_p \leq 20°$, the intensity of the XP mode decreases, whilst that of the YP mode increases. Further increase of θ_p beyond 20° results in the decrease in the intensity of the XP mode and the total intensity, thus leading to PS occurring between the orthogonal modes. On the other hand the intensity of XP and YP modes becomes saturated after the PS point, see Fig. 4-5(c, d). The gain of the XP mode (dominant mode), at a relatively low optical feedback level (-12 dB to -11 dB) is higher than the gain of YP mode.

However, for larger feedback level the polarization properties are different compared with lower feedback level. For the feedback levels of -7.6 dB and -6 dB, the PS occurs between the two modes and their intensities become closer to each other. Furthermore, the location of the PS point is somewhat different and is located at about θ_p = 76° in Fig. 4-5(c) and at about θ_p = 74° in Fig. 4-5(d) for the feedback levels of -7.6 and -6 dB, respectively. This result illustrates that a VCSEL with larger feedback requires a smaller θ_p to achieve PS, which attributed to the same reason above in Fig. 4-4 (The optical feedback and gain compete for the dominant effect).

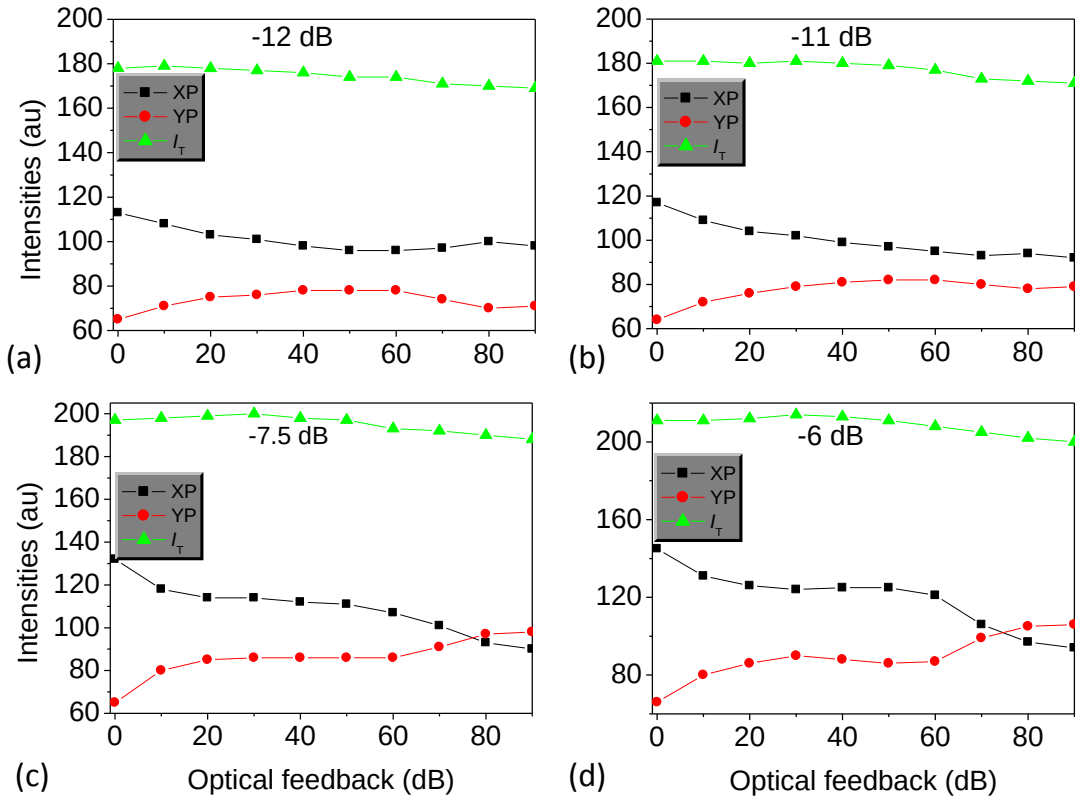

Figure 4-5: Polarization-resolved intensities versus polarization angle for CB (XP and YP optical feedback) for optical feedback fixed at -12, -11,-7.5 and -6 dB in (a), (b), (c) and (d) respectively.

Further explanation for Fig. 4-5 can be obtained via consideration of the feedback strength variation when θ_p increase from 0° to 90° as depicted in Fig. 4-6. The feedback

strength of the two polarization modes of the VCSEL have a sinusoidal dependences on θ_p, where increasing of polarization angle leading to decrease (increase) in the feedback strength of XP (YP) mode. Here, at relatively smaller optical feedback levels of -12 and -11 dB the OF plays less important role than the gain of the XP mode, thus leading to the intensity of XP mode still being dominant as depicted in Figs 4-5(a, b). Fig. 4-6(b) shows that for strong feedback (-5.5 dB), when θ_p increases, the feedback strength of both modes become closer to each other. This is because of the fact that the feedback strength of the XP mode and the YP mode becomes comparable [39], and the OF and the gain compete for the dominant effect. VCSEL polarization properties have been studied theoretically in [41] with variable polarization OF. It was show that PS can occur with the sweep of θ_p from zero to 90^o, which is barely affected by the frequency detuning of the polarization modes.

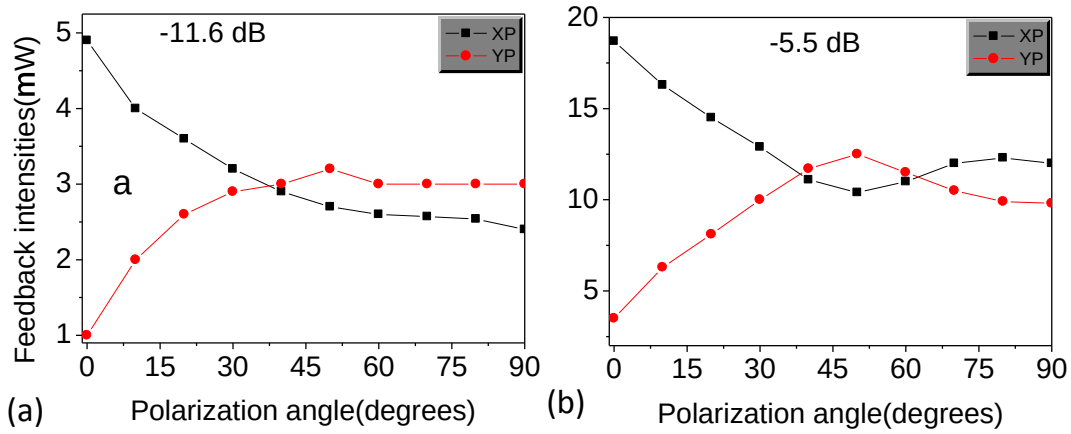

Figure 4-6: Feedback strength variation versus the polarization angle for CB (XP and YP optical feedback).

Now we will show the numerical results corresponding to the above investigation of the PS properties using the experimental parameters and typical values of VCSELs [39, 52].

4.2.2.3 Numerical Results of CA Feedback

Figure 4-7 shows the result of the numerical simulations of the average intensities of the XP and YP modes versus the feedback level in the CA feedback scheme. It can be observed that the numerical results are in agreement with the experimental results provided in Fig.4-2. Note that there is slight difference between the experimental and numerical results, which can be attributed to the feedback alignment issues.

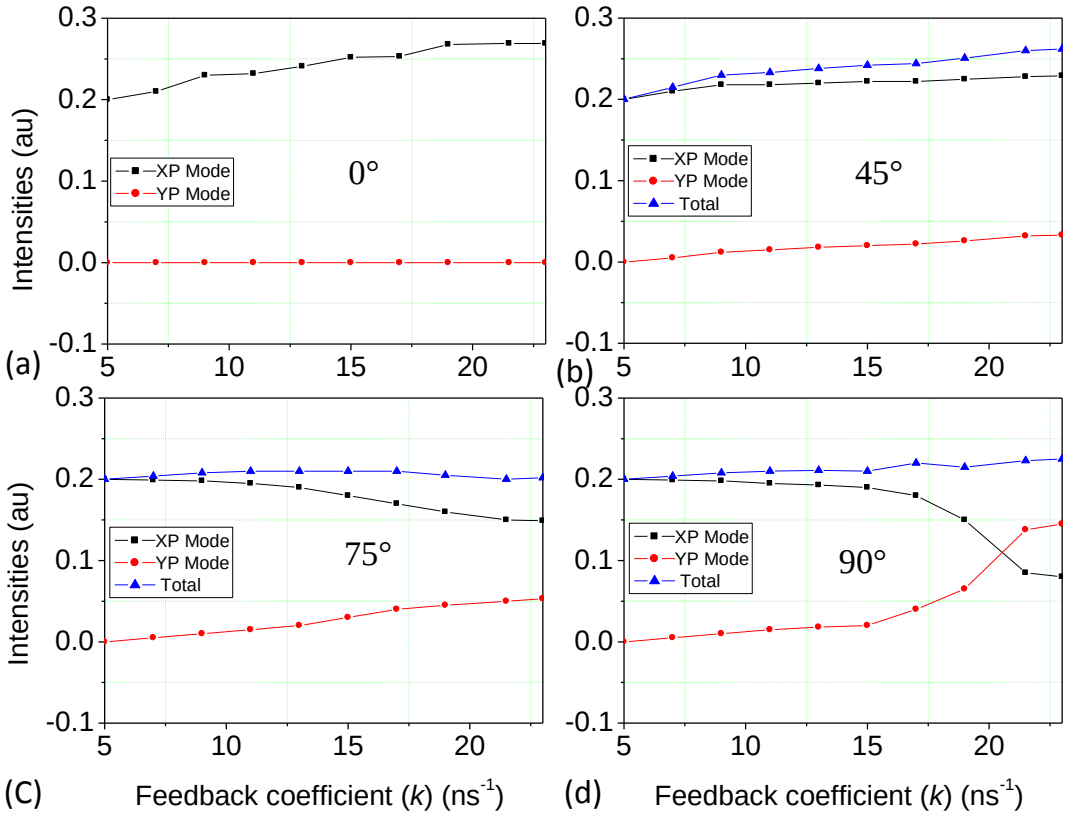

Figure 4-7: Numerical results of the polarization-resolved intensities of the XP and YP mode with total output intensity as functions of the feedback level for θ_p fixed at (a) 0°, (b) 45°, (c) 75° and (d) 90°, for CA feedback. The circles (stars) line corresponds to the intensity of XP (YP) mode and the blue line is the total intensity. The curves for XP mode and total output in (a) are overlapped.

When θ_p = 0° the XP mode is dominant and the YP mode is suppressed. The two polarization modes exhibit the same tendency for the other θ_p values, where the PS occurs at a similar value of θ_p in the practical results at almost the same feedback

level. Furthermore, for CA feedback, Fig. 4-8 shows the numerical results for polarization-resolved intensities as a function of θ_p for the VCSEL subject to relatively low and high feedback levels from 17 ns^{-1} (-16 dB) to 24 ns^{-1} (-13 dB). It is shown that for the feedback coefficient k = 17 ns^{-1} the XP mode is the dominant mode and the YP mode is suppressed. When the feedback increases to the maximum feedback level of 24 ns^{-1}, PS occurs at $\theta_p \cong 86^o$, which is the same as that observed in the experiment (see Fig 4-4). Based on the results obtained for CA feedback, there are good agreements between numerically predicted and experimental results.

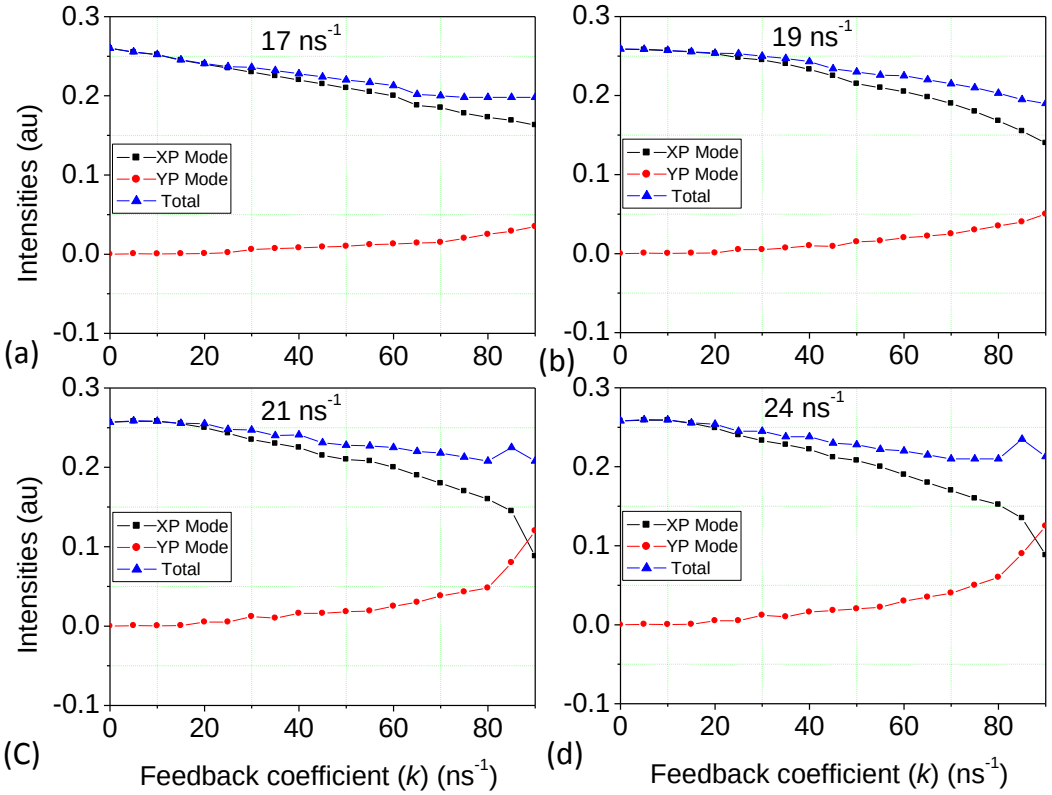

Figure 4-8: Numerical results of the polarization-resolved intensities of the XP and YP mode as functions of θ_p for the feedback level fixed at (a) 17, (b) 19, (c) 21 and (d) 24 ns^{-1} for CA feedback. The other descriptions are the same as in Fig. 4-7.

The typical and experimental values that were used in the simulation and Simulink models (in Chapter 6) are provided in Table 4-1[39, 80, 147, 151, 161].

Table 4-1: Parameter values for VCSEL under study

Parameters	**Values**
$k_{x,y}$ (Polarization feedback coefficient)	variable
β_{sp} (Strength of the spontaneous emission)	10^{-5} ns^{-1}
$\gamma_{x,y}$ (Inverse of photon lifetime for XP &YP mode)	7.692×10^{11} s^{-1}
τ_x (Feedback delay for XP mode)	6.4 ns
τ_y (Feedback delay for YP mode)	2.6 ns
G_o (Difference between XP and YP gain coefficients)	5×10^{-13} m^3/s
G_y (Gain coefficient for YP mode)	2×10^{-12} m^3/s
N_o (Carrier density at transparency)	2.5×10^{24} m^{-3}
$1/\tau$ (Inverse of carrier life time)	1×10^{9} ns^{-1}
λ (Wavelength of laser)	850 nm
Δf (Frequency detuning of XP and YP modes)	40 GHz
R_o (The phase reflectivity)	0.995
n_o (The reflective index)	3.5
R_m (The external reflectivity)	$10^{F/10}$
L (Laser cavity length)	2 μm
$\propto$ (Line-width enhancement factor)	3.0

4.2.2.4 Numerical Results of CB Feedback

With reference to the experimental results in Fig 4-3, the numerical results for the intensity of the XP and YP modes as a function of the feedback level for CB feedback are presented in Fig. 4-9 for θ_p of 0°, 45°, 75°, 90° similar to that used in the experiment. When θ_p= 0° the intensity of the XP and YP modes in Fig. 4-9(a) exhibit similar tendency to that of Fig. 4-3(a). The XP mode remains dominant for all θ_p values for the entire region of the feedback. The two modes have comparable feedback strength at θ_p of 45° and they become closer to each other, especially at higher values of θ_p for a strong feedback coefficient (k) of 55 ns^{-1} (equivalent to ~ -7 dB). For the whole range of

θ_p beyond 45° the intensity of both modes become closer to each other with no PS being observed for the entire range of θ_p, which is similar to that of the experimental results.

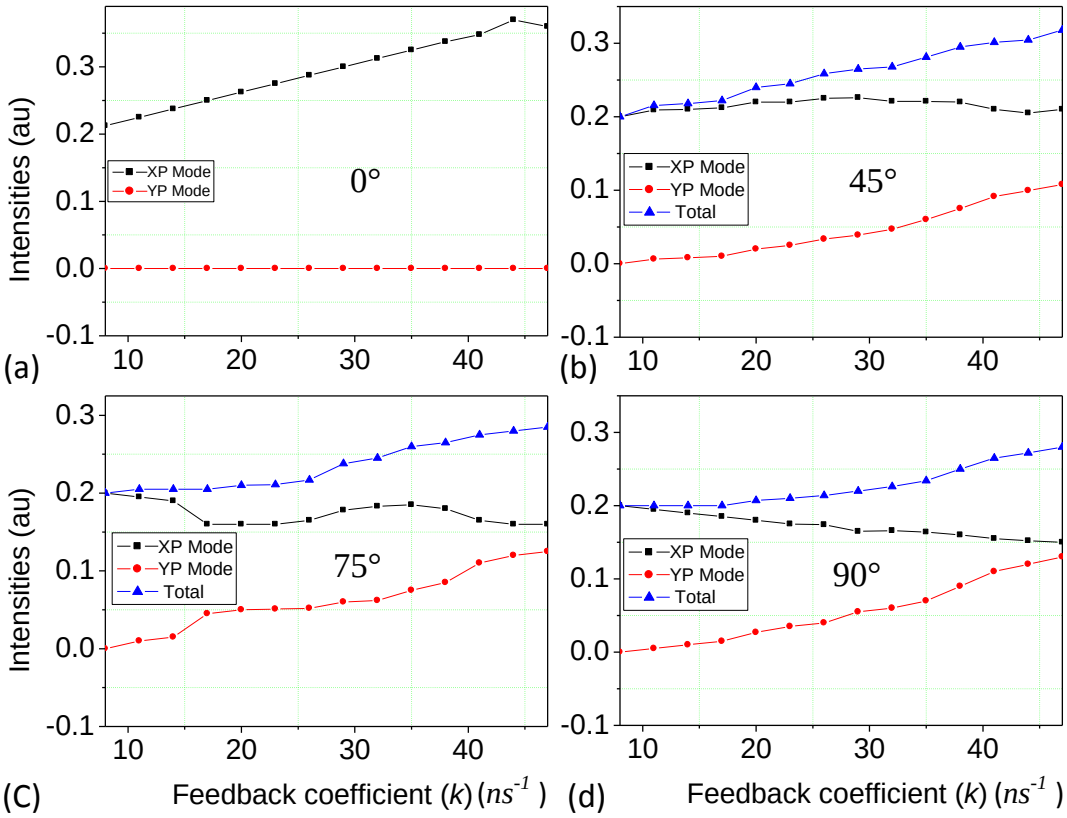

Figure 4-9: Numerical results of the polarization-resolved intensities as functions of θ_p for different polarization angles of (a) 0°, (b) 45°, (c) 75° and (d) 90° for CB feedback.

Fig.4-10 presents the numerical simulations results of the polarization resolved intensities of the XP and YP of the VCSEL as a function of θ_p for different feedback coefficient values of 20, 30, 45 and 55 ns^{-1} with CB feedback. In terms of the modes behaviours, the numerical simulations results are in line with the corresponding experimental results as in Fig. 4-5. However, the PS occurs at different points. In numerical simulation with the feedback coefficient of 55 ns^{-1} the PS occurs at θ_p value

of about 68°, while in the experimental results it happen at about θ_p= 73° for a feedback level of -6 dB.

In practical environments especially when the feedback level is strong, potentially error may occurs due to multiple reflected feedbacks reflected that needs considering.

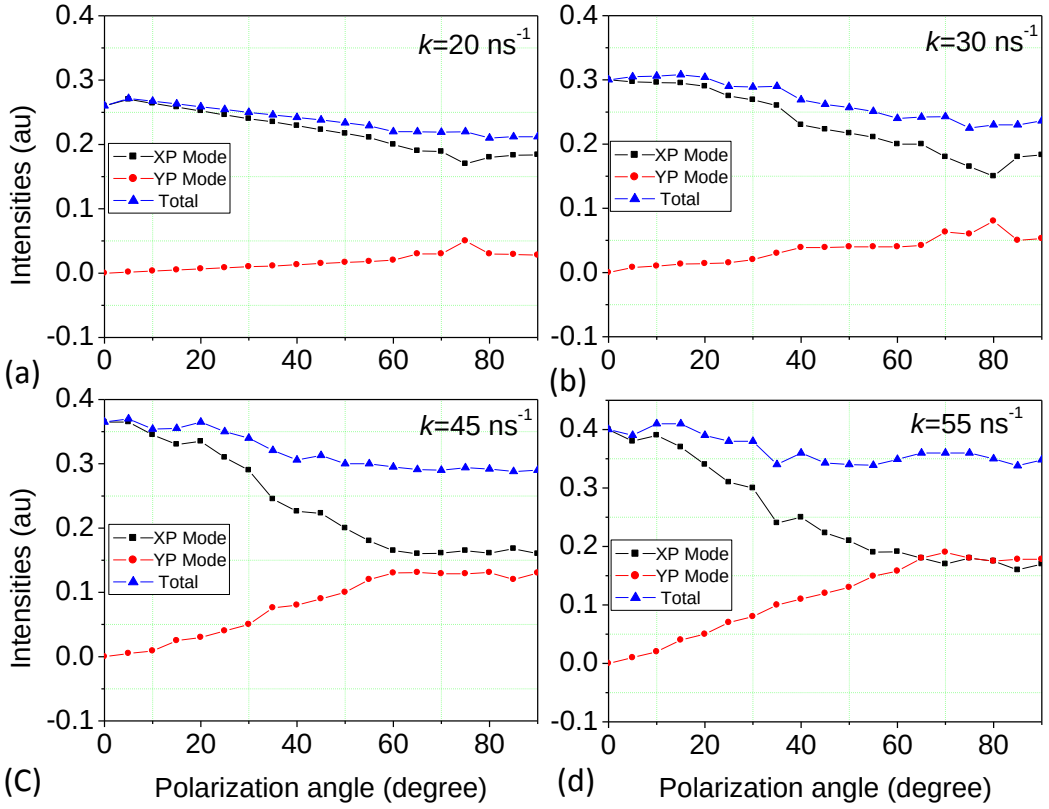

Figure 4-10: Numerical results of the polarization-resolved intensities as functions of θ_p for different feedback level, of (a) 20, (b) 30, (c) 45 and (d) 55 ns^{-1} for CB feedback.

4.3 Investigation of Polarization Switching of VCSEL Subject to Intensity Modulation and Optical Feedback

Further investigations on the PS properties using another VCSEL with different characteristics than that used in section 4.2 carried out are outlined in this section. This study presents the results of an experimental investigation of the PS of VCSELs using the polarization-rotated OF mechanism. In particular, the experiment is performed by

changing the laser drive current, OF level, modulation signal parameters such as frequency and modulation-depth in order to assess their influences on the PS of VCSEL. Similar finding to that outlined in section 4.2 are established when assessing the parameter effects of the OF level and θ_p. To realize PS with increasing the level of OF smaller θ_p should be used. Moreover, for a fixed OF level and increased bias current smaller θ_p is also need to ensure PS. However, to the best of our knowledge this is the first time for using modulation parameters to eliminate PS in VCSEL in presence of OF.

Here, the PS properties is investigated by changing the OF level, varying the polarization angle by means of applying the modulation signal, and varying the bias current. The results give more insight and a controllable tool into PS dynamics of VCSEL with OF and modulation signal.

4.3.1 Experimental Arrangement

The experimental set up is shown in Fig. 4-11. A commercial 850 nm single mode VCSEL with a threshold current I_{th} of ~1.5 mA at the free running operation was used. The VCSEL was driven by a DC source and temperature controlled using a thermoelectric temperature controller (TED 200) to within 0.01^{o}C. An external signal generator (Tektronix AFG3252C 2 GS/s, 240 MHz) was used for intensity modulation (IM) of the laser source. The laser output beam was collimated using an objective lens prior to being applied to a BS. HWP and PBS were used to direct the orthogonal polarizations of the VCSEL to the two identical optical receivers (OR) for the measurements. The optical beam propagating in the *x* direction is reflected back using a mirror M with high reflectivity to the VCSEL via NDF, QWP and BS, thus providing the OF signal.

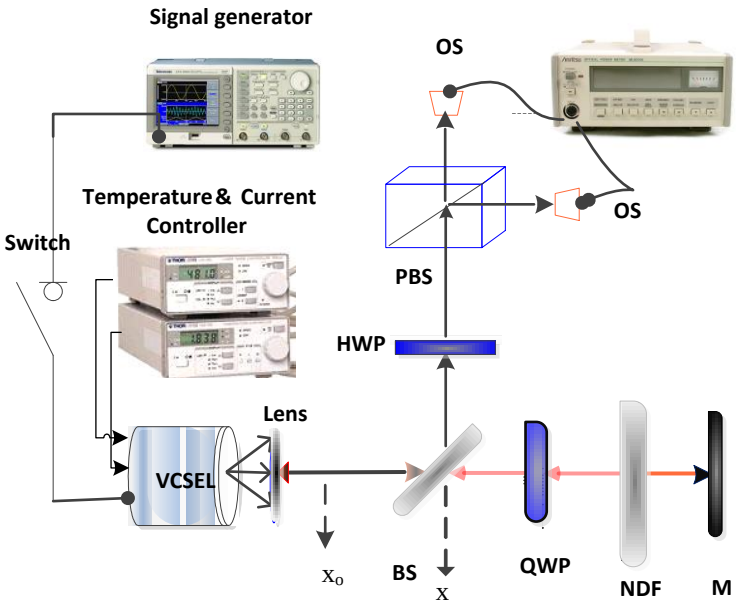

Figure 4-11: Experimental setups; VCSEL, Lens, BS: beam splitter. QWP: quarter wave plate. NDF: neutral density filter. M: mirror. HWP: half wave plate. PBS: polarized beam splitter. OS: optical sensor, Power meter.

QWP was used to rotate the VCSEL polarization XP and YP modes, i.e., parallel and orthogonal, respectively. NDF was used to adjust the OF level. The switch shown in Fig. 4-11 symbolises IM state of the VCSEL.

For this setup, the OF power level measured at the point "x" in Fig. 4-11 is normalized to the total output power measured at the point "x_o". Note that, θ_p of 0° and 90° corresponds to XP and YP feedback signals, respectively. In this study the OF level is within the regimes IV and V, which previously introduced in Chapter 2. In these regimes it was reported that the laser operation was insensitive to the phase effects and other external optical perturbations [22]. Here we investigate the influence of VPOF on the PS properties when considering effects of the OF level with and without IM, and the bias current.

4.3.2 Results and Discussions

Consideration has been given to preserve OF when rotating θ_p with and without the modulation signal in order to examine their influences on the PS properties of VCSEL. First, Fig. 4-12 shows the polarization-resolved L–I curve characteristics of the free-running VCSEL at a wavelength of 850 nm at the room temperature of 20° C with a threshold current of ~1.5 mA. VCSEL lases at the XP mode (square dots), which is the dominant mode over the entire range of the bias current I_b.

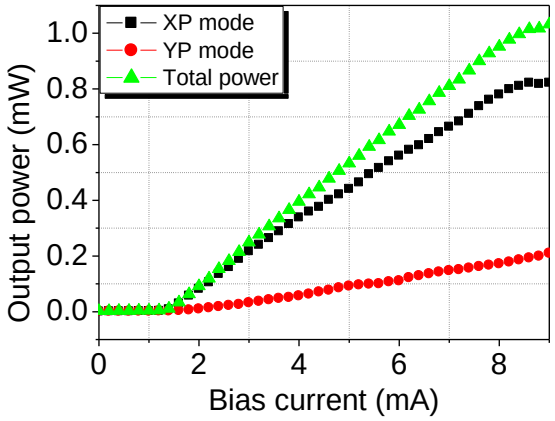

Figure 4-12: Polarization-resolved L-I curve of the free-running VCSEL- XP mode (black), YP mode (red) and total power (green).

The YP mode (round dots), not fully suppressed display lower L-I characteristics than the XP mode. This L-I curve characteristic is different compared to previously reported data on VCSELs in terms of the entirely suppressed polarization mode as demonstrated in earlier sections of this thesis and compared with relevant studies in literature [28, 39, 40, 57, 100]. This is because of the inherent structure of the commercial 850 nm VCSELs used in this work. However, similar tendency and polarization properties have been reported in previous works when using similar parameter for OF, VPOF and the injection current to investigate the polarization mode properties of VCSEL. The L-I curve is linear within ~1.5 < I_b < 8.5 mA with no PS observed. The device was biased

at I_b of 5.2 mA for all figures except Fig. 4-17(a) where I_b of 3.2 mA was used for the purpose of comparison.

4.3.2.1 Effects of Optical Feedback levels on VCSEL's PS Properties

First we investigate the effects of OF on the polarization properties of VCSEL. The polarization-resolved intensities of the VCSEL against θ_p for range of OF levels for I_b of 5.2 mA are shown in Fig. 4-13. The result illustrates that the output power of the XP and YP modes are almost constant for θ_p > 10° for an OF level of -17 dB. For OF levels of -10, -8 and -7 dB, the optical power for XP (YP) decreases (increases) with increasing θ_p at rates of 2.3×10^{-3}, 4.1×10^{-3} and 4.3×10^{-3} mW per degree, respectively for both polarization modes. As shown in Fig. 4-13(a) at the OF level of -17 dB, both XP and YP modes are emitted simultaneously with no PS.

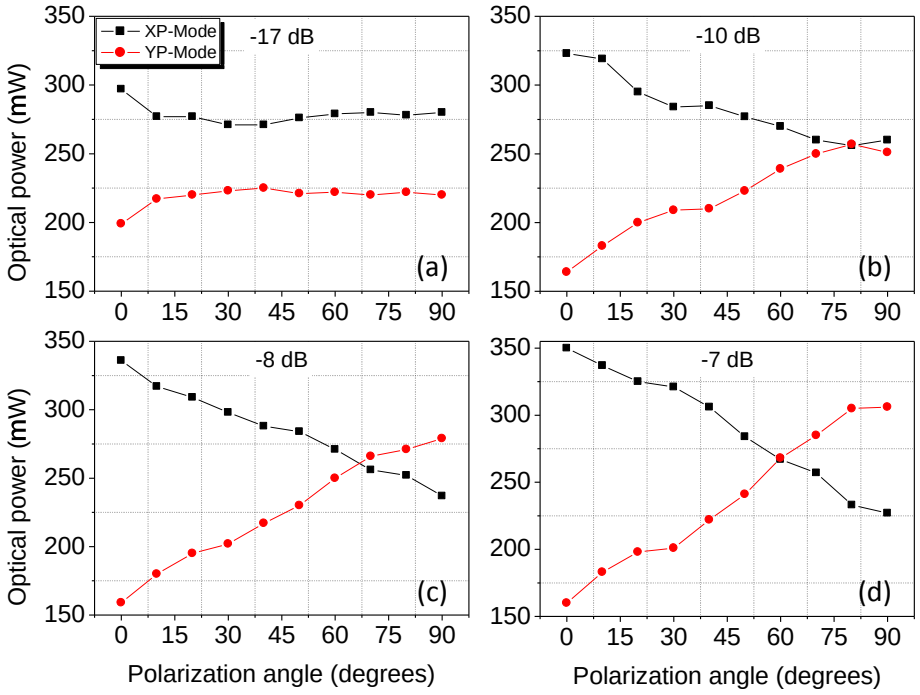

Figure 4-13: Polarization-resolved intensities vs. the polarization angle at a bias current of 5.2 mA with no modulation for OF levels of -17 dB (a), -10 dB (b), -8 dB(c), and -7 dB (d).

This is because at low level of OF the XP mode gain is higher than the YP mode, this is because the XP mode is the dominant mode and get most the feedback light [39]. At higher OF levels the plots display linearly increasing and decreasing trends for XP and YP, respectively with PS, see Fig. 4-13(b, c, d). The position of PS depend on the OF level as predicted in [39]. The PS positions observed are at θ_p of 78^o, 66^o and 60° for OF levels of -10, -8 dB and -7 dB, respectively. Increasing θ_p results in both XP and YP modes experiencing reduced and enhanced feedback light, respectively. The results demonstrate that PS can be achieved at smaller values of θ_p when the OF level increases. In [39] it was shown that for θ_p > 45° the OF level between the two polarization modes should be large enough to let the suppressed mode to be the dominant mode. Furthermore, PS can also take place when the net gain between the two orthogonally polarization modes of the laser is equal to zero [52].

4.3.2.2 Effects of OF on VCSEL's PS Properties with Intensity Modulation

In this section we investigate PS properties of the VCSEL with IM. Polarization-resolved intensities versus θ_p for I_b = 5.2 mA, frequency f_m of 12 MHz, modulation-depth M_d of 55.5 % for OF levels of -17, -10, -8 and -7 dB are depicted in Fig. 4-14. The XP and YP profiles are almost similar to Fig. 4-13 for all OF levels except for lower rate of change of power of 3×10^{-4}, 2×10^{-3}, 2.1×10^{-3} and 3.3×10^{-3} mW per degree for OF levels of -17, -10, -8 and -7 dB, respectively. However, PS take place at lower values of θ_p = 75° and 66° at OF values of -8 dB and -7 dB, respectively. This position differences can be attributed to the modulation power effect [147].

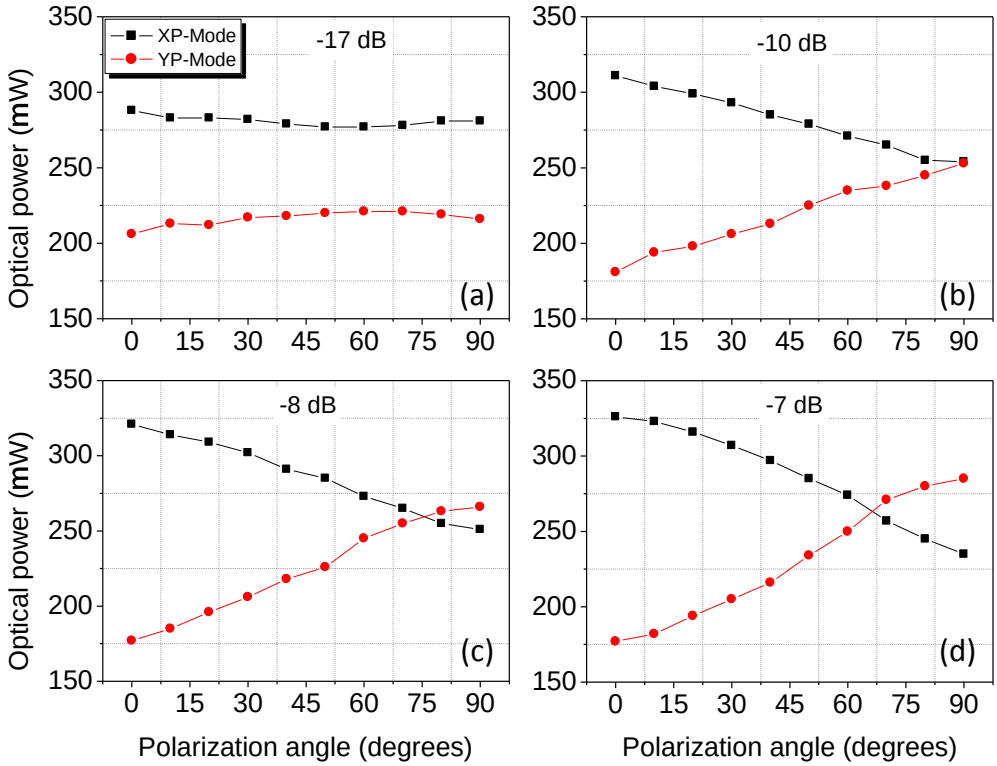

Figure 4-14: Polarization-resolved intensities versus the polarization angle at a bias current 5.2 mA with fm of 12 MHz and Md of 55.5% for OF levels of -17, -10, -8 and -7 dB, respectively.

4.3.2.3 Effects of Modulation-Depth

Next, we investigate effects of M_d on PS of VCSEL. Fig. 4-15 illustrates the optical output power of XP and YP modes as a function of θ_p for a range of M_d. We have used I_b, f_m, and OF of 5.2 mA, 12 MHz and -7 dB, respectively. As shown in Fig. 4-15(a-d) the positions of PS depends on M_d, increasing (i.e., to higher values of θ_p) with M_d. The rate of change of power for both polarization modes are 3.6×10^{-3}, 3.3×10^{-3}, 2.6×10^{-3} and 2.1×10^{-3} mW per degree for M_d of 55.5 %, 68.26 %, 78 % and 78.66 %, respectively.

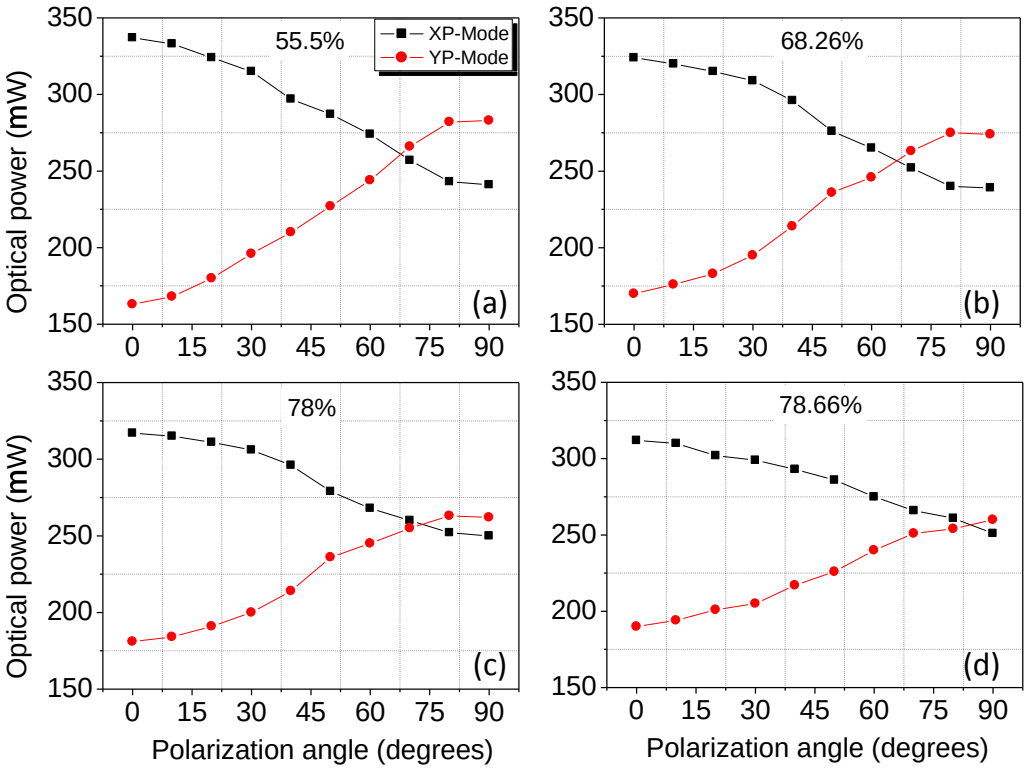

Figure 4-15: Polarization-resolved intensities versus the polarization angle at a bias current of 5.2 mA with internal modulation, fm of 12 MHz and with Md of 55.5%, 68.26%, 78% and 78.66%. The OF level is -7 dB.

4.3.2.4 Effects of Frequency

For the same conditions as in Fig.4-15 except for M_d of 55.5 % and a range of frequencies f_m of 500 KHz, 12 MHz, 100 MHz and 200 MHz, Fig. 4-16 displays polarization-resolved intensities versus θ_p for M_d of 55.5 % and a range of frequencies f_m of 500 KHz, 12 MHz, 100 MHz and 200 MHz, I_b of 5.2 mA with IM and an OF level of -7 dB. PS is observed at θ_p of 60°, 68° and 85° for f_m of 500 KHz, 12 MHz and 100 MHz, respectively. For $f_m \geq 200$ MHz, there is no PS, see Fig. 4-16(d). The total emission intensity began to decreases and increase for XP and YP modes, respectively, which in line with predicted results given in [148].

For both polarization modes the rate of change of power are 3.3×10^{-3}, 3.5×10^{-3}, 2.9×10^{-3} and 2.2×10^{-3} mW per degree of 500 kHz, 12 MHz, 100 MHz and 200 MHz, respectively of f_m, which are smaller to Fig. 4-15. Results show that there is no PS at $f_m \geq 200$ MHz. The results show that modulation parameters (f_m and M_d) can lead to a significant change in PS properties, thus limiting effects of OF on polarization of VCSEL. As a result of the experiment finding, the modulation signal can be used to control PS in VCSEL. Modulation signals have been used to suppressed the dynamic modes of semiconductor laser with OF, as reported in [108]. The feedback effect is strongly depending on the modulation frequency when the modulation amplitude is constant, as reported in [162].

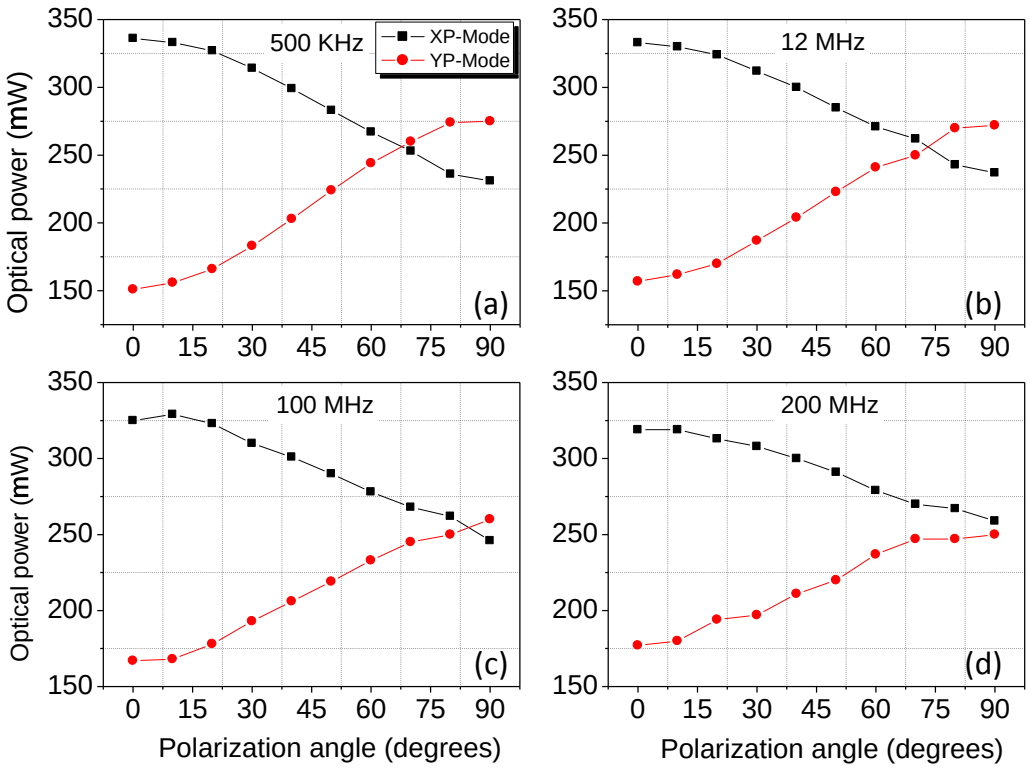

Figure 4-16: Polarization-resolved intensities versus polarization angle at a bias current of 5.2 mA with intensity modulation at fm of 500 KHz, 12, 100 and 200 MHz, respectively and Md of 55.5%. The OF level is -7 dB.

4.3.2.5 Effects of Changing Bias Current

Fig. 4-17 displays polarization-resolved intensities versus θ_p with an OF level of -7 dB and for I_b of 3.2 mA and 5.2 mA. Both XP and YP mode display similar tendency as in other sections. For I_b of 3.2 mA and 5.2 mA, PS is observed at θ_p of 71° and 59°, respectively.

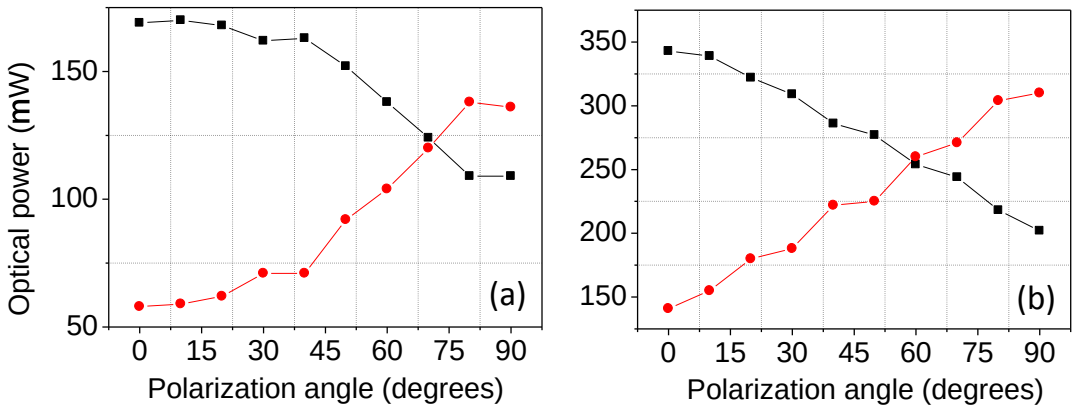

Figure 4-17: Polarization-resolved intensities versus the polarization angle for an OF level of -7 dB and bias currents of: (a) 3.2 mA, and (b) 5.2 mA.

In Fig 4-17(a) for the two modes higher rate of change of power is observed for θ_p > 40°, where it is 2.4×10^{-3} mW/degree. While, in Fig. 4-17(b) the rate increases to 4.9×10^{-3} mW/degree. For higher value of I_b lower θ_p is needed for PS as in line with theoretically predicted data reported in [163]. The results demonstrated that the bias current can affect the PS dynamic of VCSEL.

4.4 Conclusions

In this chapter PS proprieties of the polarization modes of VCSEL were theoretically and experimentally investigated. For first investigation the OF is implemented in two

feedback configurations, CA and CB under the effects of rotating θ_p of OF. The two configurations CA and CB were engaged to rotate the selective and preserved OF, respectively. Additionally investigated were the PS properties of another VCSEL device with different characteristics in terms of the threshold current and polarization emission. Polarization properties were presented by considering the effects of OF level, OF combined with intensity modulation, and finally the bias current.

For the first theoretical and experimental investigation VCSEL was subjected to VPOF. We showed that there a good relationship between the experimental and theoretical results. For CA feedback, the simulation results were agreed well with the experimental results. For CB feedback, the results were slightly different as showed in simulation results in Fig. 4-10, where the PS position was slightly changed. When the feedback level is strong, multiple feedbacks resulting from the setup may need to be taken into account.

Slight differences were found between the theoretical published paper in Ref. [39] and the experimental results. Moreover, the experimental results were demonstrated our theoretical predictions that the larger θ_p lead to the PS takes place and favours emitting the YP mode in CA feedback. For the feedback level applied in the experiment, θ_p could further affect the feedback lights received by XP and YP modes in VCSEL.

The experimental results demonstrated the recent theoretical analysis with VPOF [39], that when the feedback level was relatively small, the OF played a less important role than the gain effect. On the other hand, with regards to the relatively large feedback level, the feedback strength competed with gain for the dominant effect. In the CA feedback finding, when the difference between the feedback strengths of the two modes was great enough the OF assumed to be the dominant role.

For the second investigation in section 4.3, the effects of rotated θ_p of OF on the PS proprieties of VCSEL by considering effects of OF level, OF combined with intensity modulation, and the bias current were presented. It was shown that with the VPOF, similar to the first results obtained in section 4.2, PS was observed for a fixed bias current and OF. However, with modulation signal and OF, PS point shifted to higher polarization angles. Furthermore, a noticeable difference was observed for the rate of change of power for two polarization modes with and without modulation. Interestingly, it was shown that both the f_m and M_d limited the effect of OF on VCSEL and therefore the PS properties. The XP and YP modes experienced no PS when M_d was increased, whereas PS was entirely suppressed for $f_m \geq 200$ MHz. However, the rate of change of power was lower for f_m compared to M_d. Finally, the results showed that increasing the bias current led to PS taking place at lower values of θ_p.

Chapter 5

Nonlinearity Behaviour and Relative Intensity Noise Investigation of VCSEL with VPOF

5.1 Introduction

In chapter 4, the results were presented for theoretical and experimental investigations of effects of the variable polarization angle of the feedback light on the polarization properties of VCSELs. In this chapter, experimental studies of the nonlinearity behaviours and the relative intensity noise of the polarization modes of VCSEL are provided.

The dynamics of SLs with direct modulation have received a considerable attention by the researcher. However, only a limited number of studies have addressed the nonlinear dynamics of VCSELs with direct modulation [43, 134]. Nonlinear effect is a more important factor when laser is modulated [140]. VCSEL with direct modulation exhibit different nonlinear properties such as period doubling, period quadrupling, and chaos [134, 164]. These characteristics are investigated for a range of bias current and up to 4 GHz of modulation frequency [136]. Modulation response of VCSEL have been studied in terms of polarization instability effects based on spin-flip model [165]. Theoretical and experimental investigations was reported in [140], demonstrating nonlinear distortion when the SL is driven near the threshold emission. The spectral properties of

laser are an important characteristic in the applications of communication systems. Temperature variation can caused additional irregular behaviour in the spectral distribution of the laser optical power, which has significant effect on the laser dynamic at a modulation frequency < 100 MHz [166].

In Section 5.2, a novel method has been used to improve the linear dynamic range of VCSEL using the selective OF. More precisely, for the first time an experimental investigation is reported, which shows that the orthogonal optical feedback (OOF) can suppress the nonlinearity associated with the polarization modes of VCSEL. Furthermore, both temperature and injection current effects on the nonlinearity of the polarization modes of VCSEL are also considered in Section 5.2.4. The results obtained show that the nonlinear dynamic is observed as the temperature increases.

In Section 5.3, the relative intensity noise (RIN) characteristics are provided with the influence of VPOF and the modulation signal. RIN is an important factor, which determines the achievable modulation bandwidth in communication systems. Therefore, it is important to understand the effects of RIN on each individual mode of VCSEL. Different studies have addressed the effects of RIN on individual modes of VCSEL, e.g., application of VCSEL in low noise image processing [133]. In [33] the effects of external OF on the RIN of VCSEL was investigated. At low OF levels of -45 to -35 dB the measured RIN of -135 dB/Hz was reported, while it is degraded of 20 dB/Hz at a high OF level of -10 dB. Moreover, lower RIN of -149 dB/Hz using VCSEL was outlined in [34]. A strong OF can led to a reduced RIN owing to the phase effect of the reflected light in the laser cavity, provided the light is from a pure single mode oscillation [30].

The influence of VPOF on RIN of the polarization modes of VCSEL is experimentally investigated and presented in this work. It is shown that the RIN level in the range of

−133 to −152 dB/Hz is achieved under -5.5 dB of OF, which is highly depending on rotating θ_p. More investigations are carried out on the RIN with modulation signal in section 5.3.2. A minimum RIN of -156 dB/Hz is obtained for the dominant polarization mode of the VCSEL over the entire range of θ_p. For both investigations, the RIN level of the dominant mode of VCSEL has a lower values and it's highly depending on the rotating θ_p. Furthermore introducing the modulation signal to the VCSEL results in the increased level of RIN with and without OF, especially at lower frequency range.

5.2 Suppressing the Nonlinearity of Free Running VCSEL using Selective-Optical Feedback

In this work, experimental results are reported on the effects of selective OF to reduce the nonlinearity of the orthogonal polarization modes of VCSEL when subjected to the modulation signal. Parallel and orthogonal optical feedback (POF and OOF), to that of the standalone VCSEL, are employed with variable range of OF and I_b to investigate the nonlinearity of the XP and YP mode. The POF can enhance the harmonics distortion (HD) of the parallel mode of standalone VCSEL, while this mode is entirely supressed when using OOF. Over a wide range of temperature and I_b, the nonlinearity behavior of the VCSEL are studied with results showing a dramatic change with the temperature variation of the laser.

5.2.1 Experimental Arrangement and Discussion

To investigate the effect of selective OF on the VCSEL properties, the following experimental set-up is employed and depicted in Fig. 5-1. A commercial 850 nm VCSEL (Oxidation process) is used in the experiments, which over a range of I_b has a

linear output power. The VCSEL is driven by a low-noise current source (Newport, 505B) and is temperature controlled using a thermoelectric temperature controller (TED 200C) to within 0.01^{o} C. The VCSEL is subjected to current modulation using an external signal generator (Tektronix, 2 GS/s, 240 MHz). The laser output beam is first collimated using an objective lens (Aspheric Lens, f = 4.51 mm, AR: 600-1050 nm), before being detected by OR (Newport, 1 GHz), after passing through a linear polarizer ((P), with N-BK7 Protective Windows, 600-1100 nm), which is used to select the polarization direction of the polarization modes. A 50/50 BS (50:50 UVFS, Coating: 700 - 1100 nm) is used to split the laser beam in two parts, one part is directed to a T-shaped external cavity, which consist of two mirrors (M1, M2). The other part of the light is directed to OR and then stored in a digital oscilloscope (Agilent, 6 GHz) and Network analyser (NA) (Agilent, 13.5 GHz), for further signal processing. HWP (Zero-order half-wave plate) and PBS (Polarizing beam splitter cube, 620 - 1000 nm) are used to direct the orthogonal polarizations modes to M1 and M2. Each branch of the T-shaped is returning light back into its own polarization of the VCSEL. The feedback level adjusted using a neutral density filter ((NDF) OD: 0-2.0, ARC: 650 - 1050 nm). M1 is used for POF (OOF) for the XP (YP) mode and vice versa for M2. For the XP mode, POF and OOF measurements are carried out by blocking M2 and M1, respectively. The VCSEL optical power is measured using an optical power meter (Anritsu, ML9001A). Each of OF branch of the T-shaped is 29 cm length. The standalone VCSEL lases with two orthogonal polarization modes with high XP mode emission compared with YP mode emission over the entire range (0-10 mA) of I_b. The maximum output power of the VCSEL is 1.9 mW at I_b of 10 mA. The polarization-resolved L-I characteristics of the free running VCSEL is shown in Fig. 5-2, at a room temperature of 20^{o}C. It has apparent from the L-I cure that I_{th} is 1.5 mA.

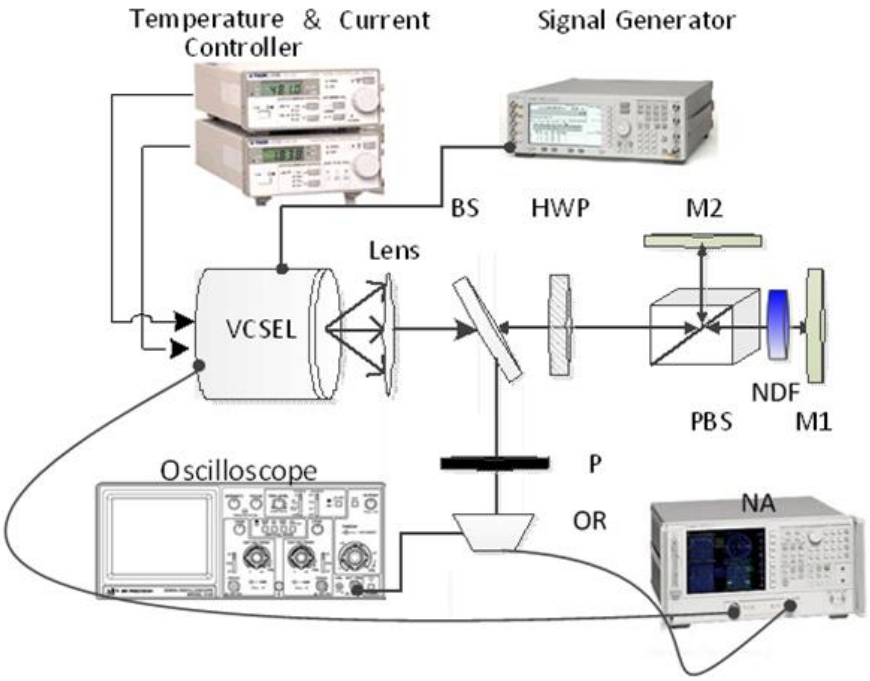

Figure 5-1: Experimental setup to measure power spectrum of the VCSEL, BS: beam splitter. HWP: half wave plate. M: mirror. NDF: neutral density filter. PBS: polarized beam splitter. P: linear polarizer. OR: optical receiver. NT: network analyzer.

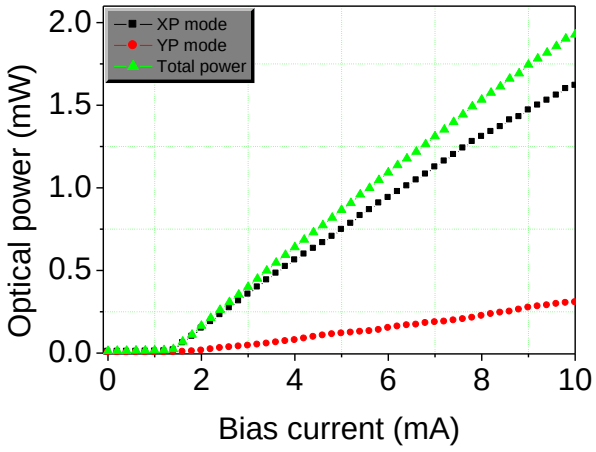

Figure 5-2: Polarization-resolved L-I curve of the standalone VCSEL. Square black and dot red lines correspond to XP and YP mode respectively. The triangle green line refers to the total output power.

The VCSEL starts lasing with the XP mode, which is dominant over the range of I_b although the YP mode starts lasing after fraction of mA, the modes power increasing equally with increasing I_b but the YP mode has lower power emission.

After characterising the L-I curve of free running VCSEL, a sinusoidal modulation signal is applied. The modulation frequency is 1 MHz with 68% of modulation depth. The results obtain at I_b of 3.6 mA and 5.6 mA to demonstrate the finding results over ranges of I_b.

5.2.2 Harmonics Distortion of VCSEL under Selective-Optical Feedback

To study the XP and YP modes nonlinearities of VCSEL, the output power spectra and the harmonics measurement are presented under the polarization-selective OF. In case of the POF feedback and for the XP mode measurement, the OOF light is blocked and the electrical harmonics is measured at I_b of 3.6 mA, as depicted in Fig. 5-3. For free running device, the XP and YP modes spectra are shown in Fig. 5-3(a) and Fig. 5-3(d), respectively. The first harmonic (fundamental (F)), and the 2nd harmonic are clearly visible with different peaks level for both XP and YP modes. The HD arises from the nonlinearity characteristics of the L-I curve of the device. Furthermore, the spatial hole-burning, which arises due to the carrier recombination in the lasing process, also contributes to the output power intensity profile of the VCSEL [139, 150, 167].

For the XP mode measurements, as shown in Fig. 5-3(a, b, c), the high-order nonlinearities are dominant when the POF feedback of -9.9 dB is applied, see Fig 5-3(b). The HD is increased to about 4 dB compared with that of the free running dynamic. However, when the OOF of -9.9 dB is applied, as showed in Fig. 5-3(c), the 2nd harmonic is entirely suppressed and HD is reduced to ~13 dB compared with that of the free running device. For the YP mode measurements, as shown in Fig. 5-3(d, e, f), the nonlinear behaviour is dominant when the POF of -10.5 dB is applied. The 2nd harmonic is enhanced and HD is increased to about 3dB when the POF is applied, as we can see in Fig. 5-3(e). However, when -9.9 dB of the OOF is applied as shown in

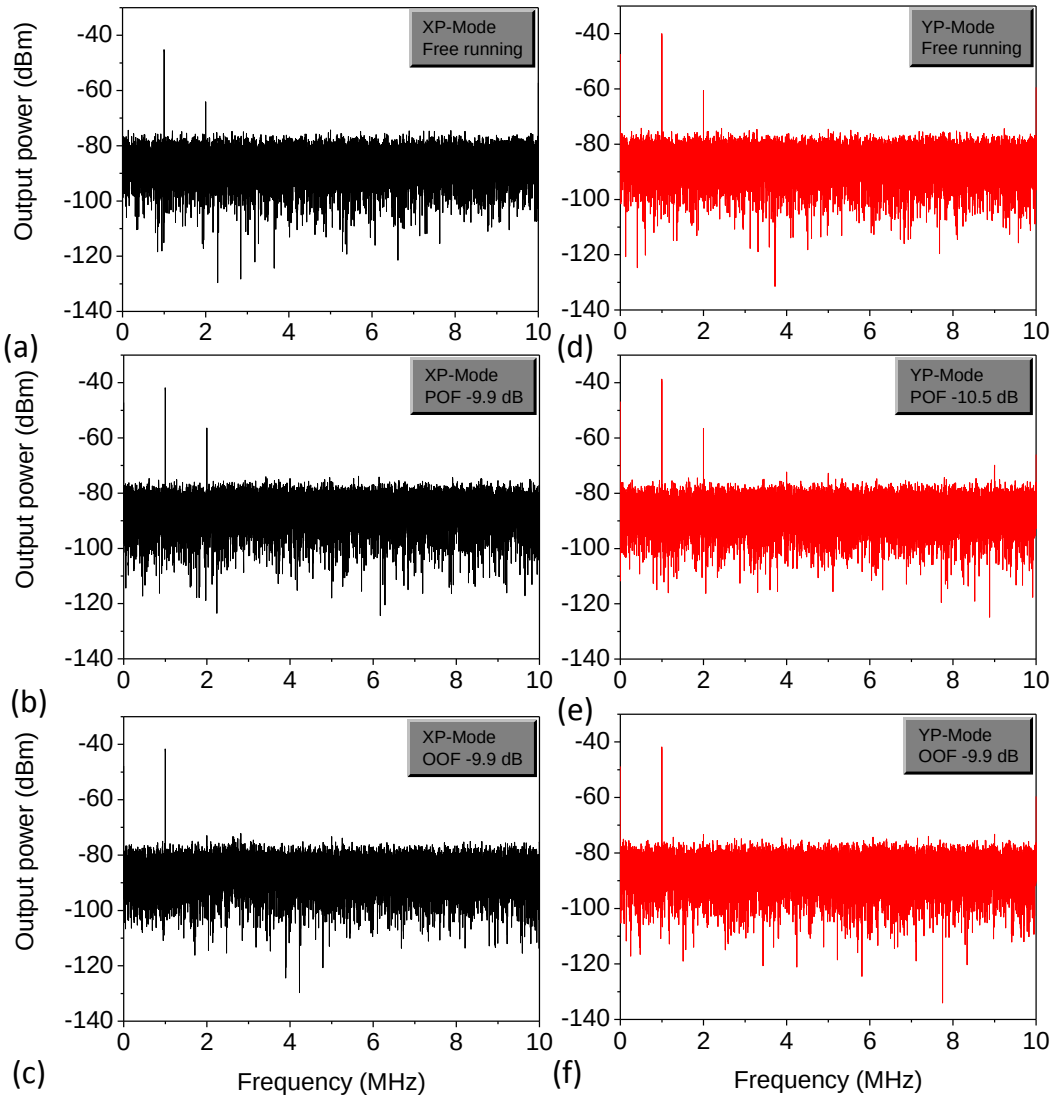

Figure 5-3: Electric power spectra of the XP and YP mode with different levels of optical feedback, (a) and (b) XP and YP mode, respectively at free running VCSEL, (b) and (e) at POF for XP and YP mode, respectively, (c) and (f) at OOF for XP and YP mode, respectively at bias current of 3.6 mA.

Fig. 5-3(f), the 2nd harmonic power is entirely suppressed and HD is reduced to about 11 dB compared to that of the free running operation, see Fig. 5-3(c). It can be notice that the harmonic components have reduced to the noise floor level of -100 dBm. Nonlinearity of the polarization mode can be enhanced (suppressed) by similar (orthogonal) feedback light, as reported in [106]. The harmonics dynamics in the spectrum of the VCSEL with selective-optical feedback could be attributed to the mode

competition, where a certain polarization mode of the optical feedback leads to enhancement of a similar intensity mode and suppressed the other (orthogonal) mode of the solitary VCSEL [168].

Further measurements at I_b of 5.6 mA are showed in Fig 5-4. The VCSEL is subjected to similar condition of the modulation parameters of previous case of I_b = 3.6 mA. For the XP mode measurements, the spectrum is illustrated in Fig. 5-4(a, b, c). Obviously, we can see the harmonics components increase when the POF of -9.9 dB is applied. The HD increases to about 8.5 dB compared with that of Fig. 5-4(a). Here at I_b of 5.6 mA with POF feedback, the 3rd harmonic appears and HD increases to about 5 dB compared to free running. However, when the OOF of -10.4 dB is applied, as seen in Fig. 5-4 (c), the 2nd and 3rd harmonics are entirely suppressed and reach the noise floor. HD reduces to about 9 dB compared with that of the free running device.

For the YP mode measurements, as shown in Fig. 5-4(d, e, f), with POF of -10.4 dB, the peak power of the 2nd harmonic is increased compared with that of the free running operation, where HD is increased to about 5.6 dB. However, when the OOF of -9.8 dB is applied as we can see in Fig. 5-4(f), the 2nd harmonic is completely suppressed and HD is reduced to about 4.5 dB. In case of YP measurements HD due to the 3rd harmonics is almost supressed and does not appear in entire spectrum of the laser mode.

The dynamic range of the VCSEL is improved and the modulation bandwidth is increased by utilizing the OOF. The nonlinearity behaviours of the polarization modes of VCSEL is increased with a similar polarization mode of the OF. The results show that the HD strongly depends on the polarization direction of the OF, where the POF leads to increase in harmonics of the similar polarization mode of the VCSEL. While the OOF leads to entirely supressed harmonics power of the orthogonal mode of

the laser, thus resulting in reduced nonlinearity characteristics in the output power of the laser mode.

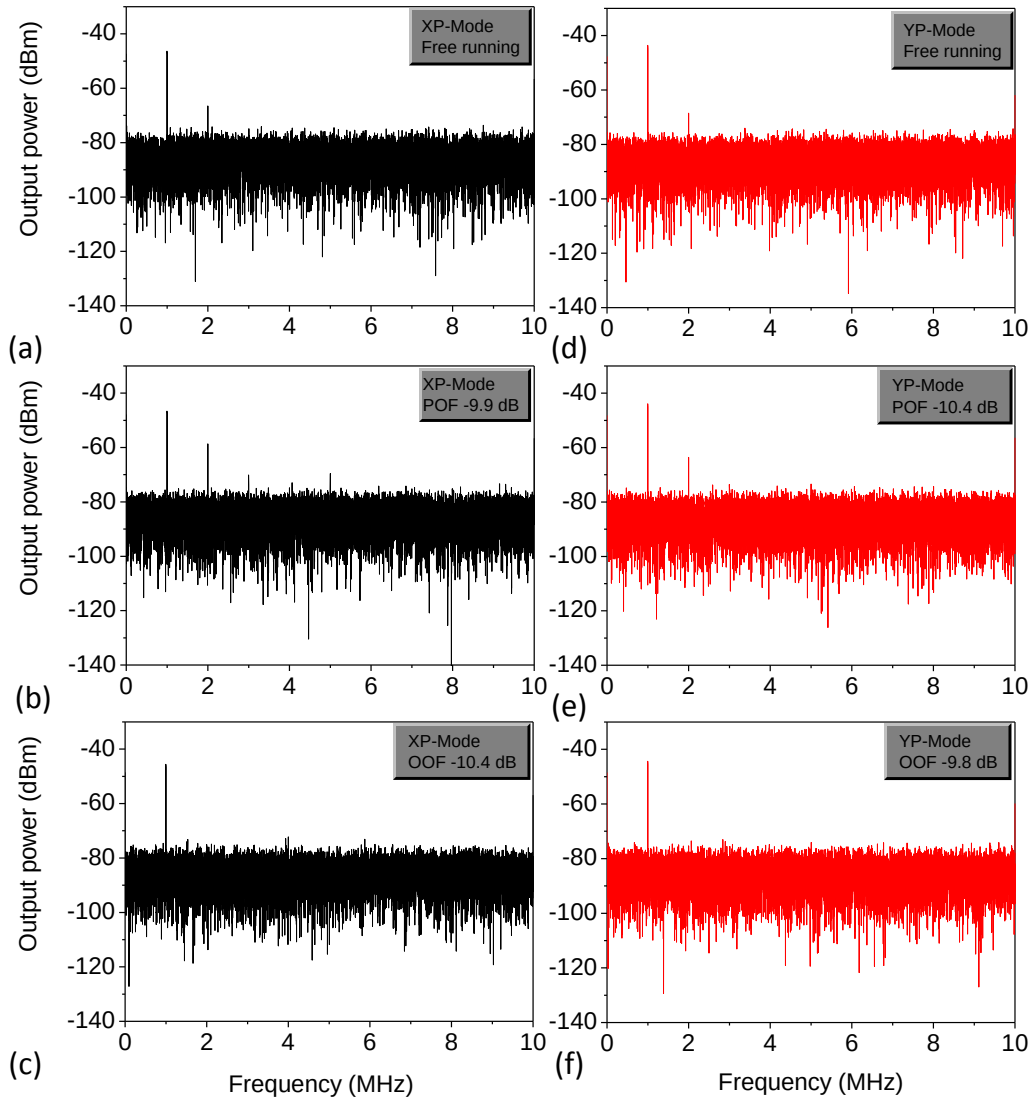

Figure 5-4: Electric power spectra of the XP and YP mode with different levels of optical feedback, (a) and (b) XP and YP mode, respectively at free running VCSEL, (b) and (e) at POF for XP and YP mode, respectively, (c) and (f) at OOF for XP and YP mode, respectively at bias current of 5.6 mA.

Further measurements have been carried out for higher modulation frequency up to 240 MHz. For the XP mode with POF, OOF is blocked; the frequency spectrum for I_b of 3.6 mA is measured as shown in Fig. 5-5(a, b, c). From the frequency spectrum of the

XP mode at the free running condition, see Fig. 5-5(a), the 2nd, 3rd and 4th HDs are ~21, ~24, and ~32 dB, respectively. With POF of -8.2 dB the 2nd, 3rd and 4th HDs has increased by ~2, ~11 and ~9 dB, respectively as shown in Fig. 5-5(b) when compared to Fig 5-5(a). However, with OOF of -8.9 dB the harmonic components is reduced to the noise floor level of -100 dBm, see Fig. 5-5(c).

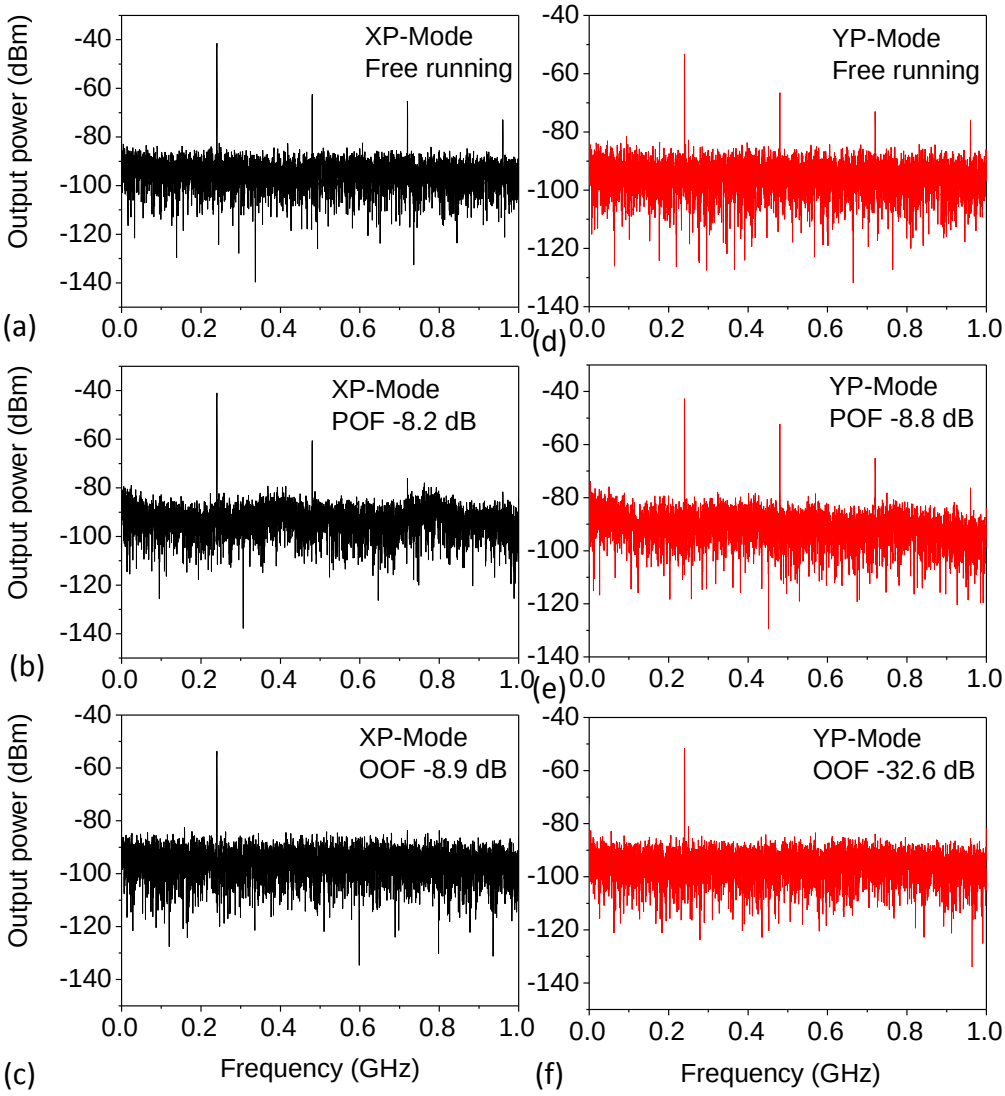

Figure 5-5: Left, the frequency spectrum of the XP mode of VCSEL for: (a) free running, (b) POF of -8.2 dB, and (c) OOF of -8.9 dB. Right, the frequency spectrum of the YP mode of VCSEL for: (d) free running, (e) POF of -8.8 dB, and (f) OOF of -32.6 dB at a bias current of 3.6 mA.

Fig. 5-5(d, e, f) depicts the harmonics spectra of the YP mode measurements. From the spectrum of the YP mode at the free running condition, see Fig. 5-5(d), there is nonlinearity with HDs of ~14, ~20 and ~23 dB for the 2^{nd}, 3^{rd} and 4^{th} harmonics, respectively. With POF of -8.8 dB, the nonlinearity of the YP mode is dominant with HDs of ~10, ~23 and ~40 dB for the 2^{nd}, 3^{rd} and 4^{th} harmonics, respectively. The nonlinearity enhance compared with that of the fee running operation, see Fig. 5-5(e). However, as OOF applied, all harmonic components have suppressed to the noise floor level, see Fig. 5-5(f).

5.2.3 Frequency Response of VCSEL

The frequency response of the polarization modes of VCSEL under POF and OOF are depicted in Fig. 5-6 as well as the free running response. From the frequency response of the XP mode with the OOF as we can see in Fig. 5-6(a), the maximum 3-dB modulation bandwidth can be observed of the solitary VCSEL is ~ 1.3 GHz. This bandwidth is enhanced by 40 MHz with strong OF (-7.6 dB), while it is similar to that of free running when the OF decrease to -25.6 dB.

The frequency response of the YP mode is depicted in Fig. 5-6(b) with the OOF of -20 dB and -8.7 dB. With the latter, the modulation bandwidth is enhanced by ~140 MHz compared with that of the free running VCSEL. However, the bandwidth measurements are limited due to the instruments limitations, OR and the laser circuit bandwidth (up to 1 GHz), see Fig. 5-6(a).

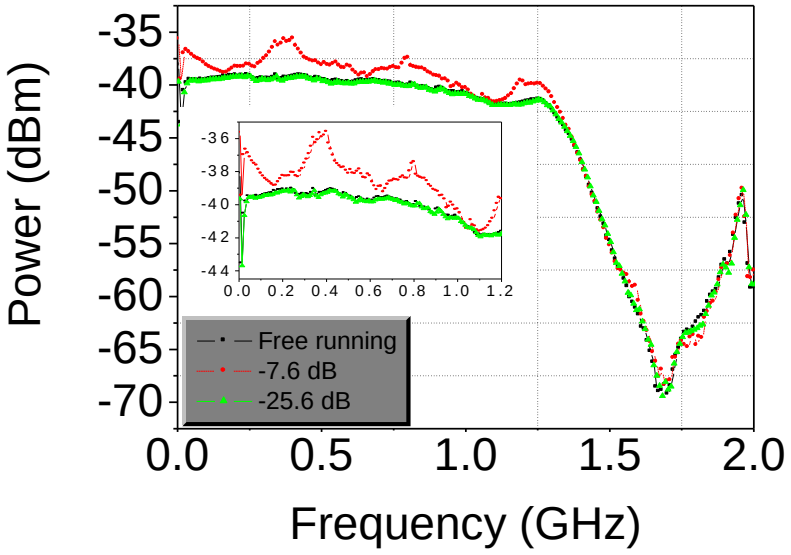

(a)

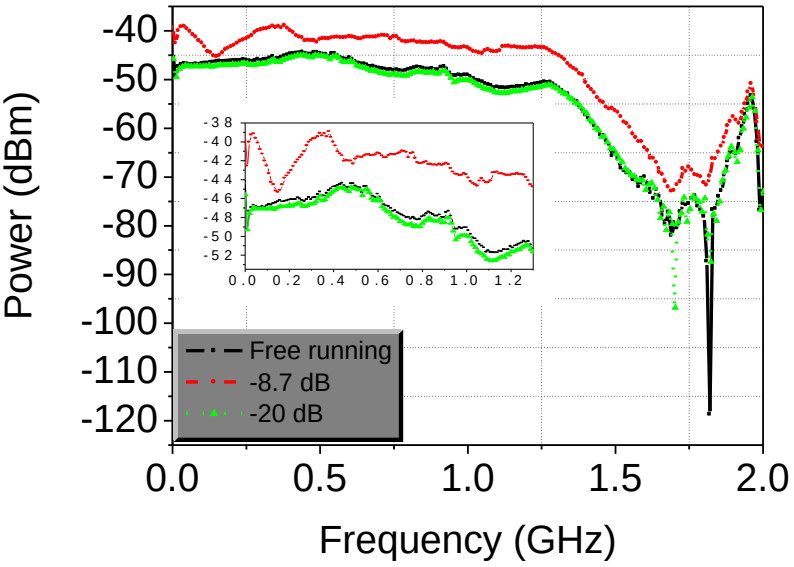

(b)

Figure 5-6: (color lines), (a) frequency response of the XP mode,(b)YP mode at free running VCSEL (soled black), -8.7 dB OF (dashed red) and -20 dB (dashed green) with bias current of 3.6 mA. The inset figure displays enlarge scale until frequency of ~1.2 GHz.

Fig. 5-7 depicts the total frequency response of the VCSEL when subjected to selective OF at I_b of 3.6 mA and 20°C, at free running (black squares), -7.7 dB POF (red dots)

and -8.4 dB OOF (green tringles). The standalone VCSEL has a 3-dB modulation bandwidth of ~1.3 GHz of the total power (XP and YP modes) which enhances with the OOF by 60 MHz as suppressed the nonlinearity of the VCSEL as show in Fig. 5-7. For the same reason above (instruments limitation), laser bandwidth measurements are limited.

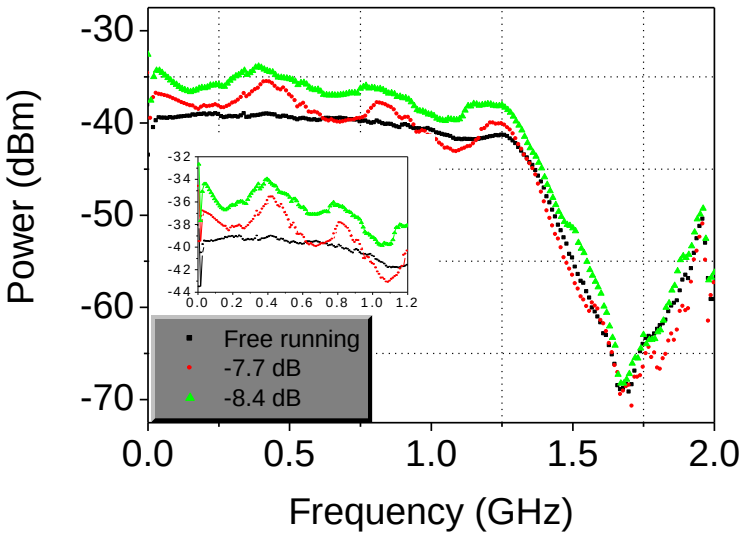

Figure 5-7: (color lines), frequency response of the total power of VCSEL at free running VCSEL, (black squares), -7.7 dB XP OF (red dots) and -8.4 dB YP OF (green tringles) with bias current of 3.6 mA. The inset figure displays enlarge scale until Frequency of 1.2 GHz.

The effect of temperature variation on the VCSEL nonlinearity has been investigated for different values of I_b (2 I_{th}, 2.4 I_{th}, 3.74 I_{th} and 4.4 I_{th}), the measurements results are presented in the next section.

5.2.4 Temperature Effects on the Linearity of VCSEL

As we mentioned above, I_b and the operating temperature can lead to further nonlinearity in SLs devices [140]. Therefore, power spectra of the dominant mode (XP)

of the VCSEL for different values of I_b and the temperature are also investigated. The electrical power spectra of the XP at the free running VCSEL with different I_b and temperature have been considered. The results of the XP mode with I_b of 3, 3.6 and 5.6 mA are depicted in Fig.5-8. First of all, the 2nd and 3rd harmonic levels are almost constant for the temperature range of 5° to 20°. For I_b of 3 mA and 3.6 mA, as temperature increases the 2nd (3rd) harmonic increases (decreases), which leads to increased HD of the XP mode. At I_b of 5.6 mA the 2nd and 3rd harmonics slightly increases with the temperature. The 2nd and 3rd harmonics dynamic are different where the 2nd harmonics power is almost increased with I_b, while the 3rd harmonic dramatically decreases.

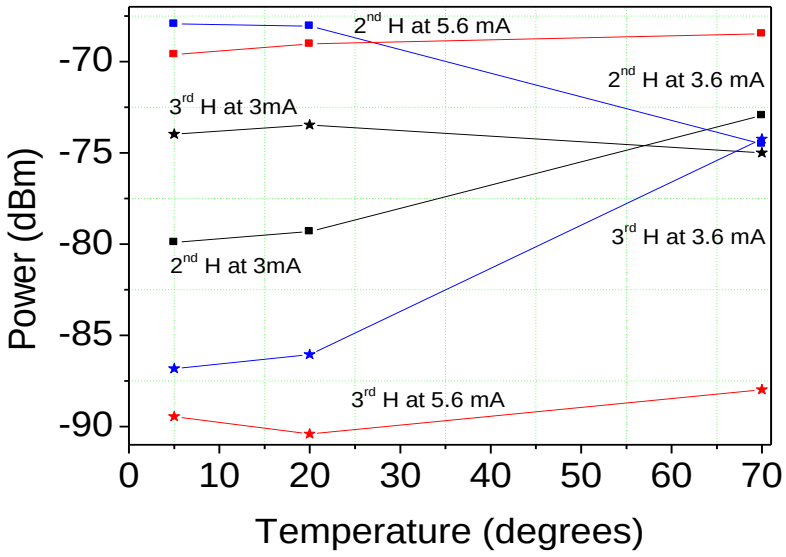

Figure 5-8: (color lines) the electrical power spectrum as a function of temperature of the 2nd (square) and 3rd (star) harmonic of the dominant mode (XP) at the modulation frequency of 1 MHz and modulation depth of 68% without optical feedback and depending on bias current. The black, blue and red lines indicate to 3 mA, 3.6 mA and 5.6 mA, respectively.

The nonlinear dynamic of the polarization modes of VCSEL has been investigated with different values of I_b and temperature, which in general the 2nd (3rd) harmonic

increases (decreases) with both I_b and temperature. At 3.6 mA of I_b, the 2nd (3rd) harmonic increased (decreased) by ~12 dB when the temperature increased from 0^o to 70^o, whilst the 2nd (3rd) harmonic increased (decreased) by ~10 dB when the I_b increased from 3 mA to 5.6 mA. As a conclusion thus far, the experiment results showed how the harmonics peaks varies with the temperature and I_b which leads to changes in the nonlinearity characteristics of VCSEL. This changes were due to the relaxation oscillation and the gain saturation caused by a number of carriers, spatial hole burning and the leakage current [140, 166].

5.3 Relative Intensity Noise Characteristics

Although the RIN characteristics of VCSEL have been studied intensively, however, the RIN of the polarization modes of VCSELs with VPOF and modulation signal has not been reported yet. Two VCSELs devices, with different characteristics, with VPOF have been used to investigate the RIN properties of the polarization modes under rotation θ_p of OF.

In the next section, RIN properties of two orthogonal polarization modes of VCSEL are investigated using a VCSEL with a similar L-I characteristic to that used in Section 3.4.2.

5.4 Relative Intensity Noise Characteristics under VPOF

The influence of VPOF on the RIN of VCSEL is experimentally investigated based on characteristic details outlined in Chapter 3 (section 3.4.2).

5.4.1 Experimental Setup

The experimental setup for the RIN measurements is depicted in Fig. 5-9. To be able to measure the mode intensity and provide an OF, a BS was used to direct the VCSEL output to mirror in order to reflect back the light into the VCSEL and to two PDs (New Focus nanosecond photo detector, model No. 1621) via PBS. The outputs of PD1 and PD2 were captured via a digital oscilloscope (LC564A, 1 GHz, vertical sensitivity 2 mV/div) for further processing.

A HWP and the PBS were employed to adjust the two orthogonally polarized modes (XP - the dominant mode, and YP - the suppressed mode) and enable them to be separately detected using two identical photo-detectors.

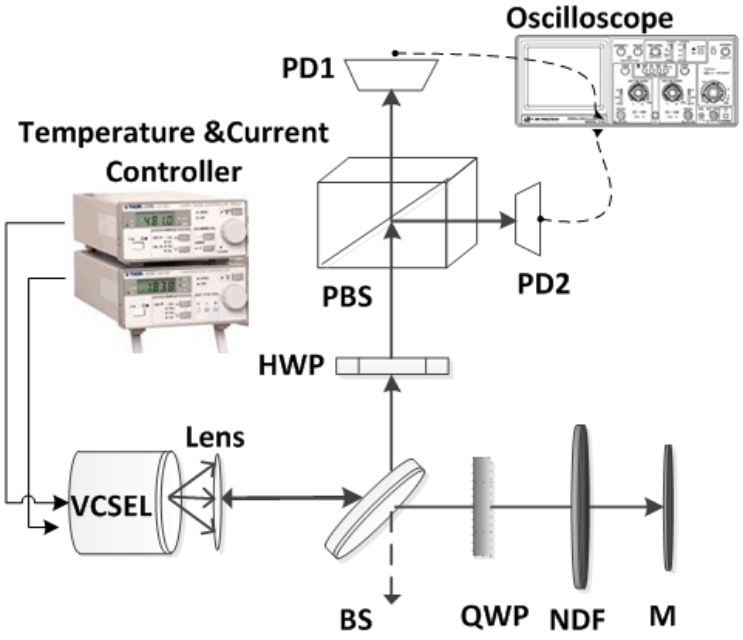

Figure 5-9: Experimental setup to measure RIN of VCSEL polarization modes subjected to VPOF; BS: beam splitter. QWP: quarter wave plate. NDF: neutral density filter. M: mirror. HWP: half wave plate. PBS: polarized beam splitter. PD: photo-detector

A QWP was used to rotate the XP and YP modes and re-inject them into the VCSEL. The QWP was used to rotate θ_p from 0° to 90°. The external cavity length is around 40 cm. The OF strength was adjusted using NDF positioned between M and QWP, see Fig. 5-9. An optical power meter was used to measure the optical level of the feedback signal at the other side of the BS (dashed line in Fig. 5-9).

5.4.2 Results and Discussions

From the L–I curve of the free-running VCSEL, (Chapter 3, section 3.4.2), no polarization switching was observed. Particular consideration has been given to preserving the polarization of the OF with rotated θ_p and their influences on the polarization-resolved RIN of VCSEL. The device was biased under a fixed feedback level of -5.5 dB and a fixed I_b of 6 mA to make sure that the only XP mode is emitted. The RIN is defined as [56]:

$$RIN = \frac{\overline{(P_o(t) - \overline{P_o(t)})^2}}{\overline{P_o(t)^2}} \tag{5.1}$$

where $P_o\ (t)$ is the output power and $\overline{P_o\ (t)}$ is the average output power of the VCSEL. The RIN is averaged over 1 GHz. Time-dependent samples were recorded to calculate the RIN, using 2×10^5 samples for each time trace. The polarization-resolved RIN of the VCSEL subject to a strong OF with VPOF are shown in Fig. 5-10. For θ_p of 0° (defined as the XP mode), the XP mode is the dominant and the YP mode is suppressed. The RIN of the XP mode is 15 dB below that of the YP mode at θ_p= 0°, which indicated that the two polarization modes are well separated at this angle.

The XP mode gain is usually higher than that of the YP mode. This is because XP is the dominant mode. The RIN of the XP mode continues to be lower than that of the YP mode for θ_p in the range of 0° to ~ 45°. In this range the XP mode has more optical

feedback than the YP mode [39]. However, for angles greater than 45°, the RIN of the YP mode is lower by ~4 dB than that of the XP mode. This is because of the gain switching as a result of the polarization switching between the orthogonal polarization mode for θ_p> 45°, and the YP mode becomes the dominant mode, see Fig. 5-11. For θ_p = 45°, the RIN of the XP and YP mode is identical and are approximately equal to −135.6 dB.

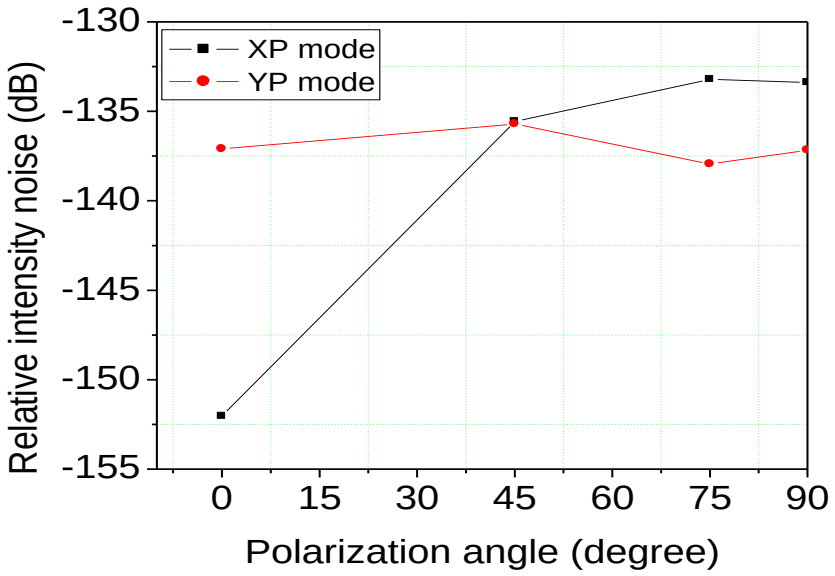

Figure 5-10: Polarization-resolved RIN as a function of polarization angle for XP and YP modes, with the VCSEL subject to −5.5 dB optical feedback level

As θ_p increases from 75° to 90°, no substantial changes in the RIN of the two modes were observed and remaining constant for higher values of θ_p, with the RIN of YP mode 3.7 dB below that of the XP mode. In general, the RIN of the XP mode increases considerably when θ_p increases from 0° to 90°, while the RIN of the YP mode increases slightly until θ_p = 45°, and then decreases.

Fig. 5-11 demonstrates the polarization mode intensities as a function of the time for an OF of −5.5 dB. It can be observed that for θ_p = 0°, the XP mode has a higher intensity

than the YP mode; this is because it is the dominant mode and has a higher gain. Furthermore, the two intensity modes are widely spaced compared with other θ_p values (45°, 75°, and 90°). The results show that rotating θ_p could significantly change the noise and instabilities of the VCSEL modes.

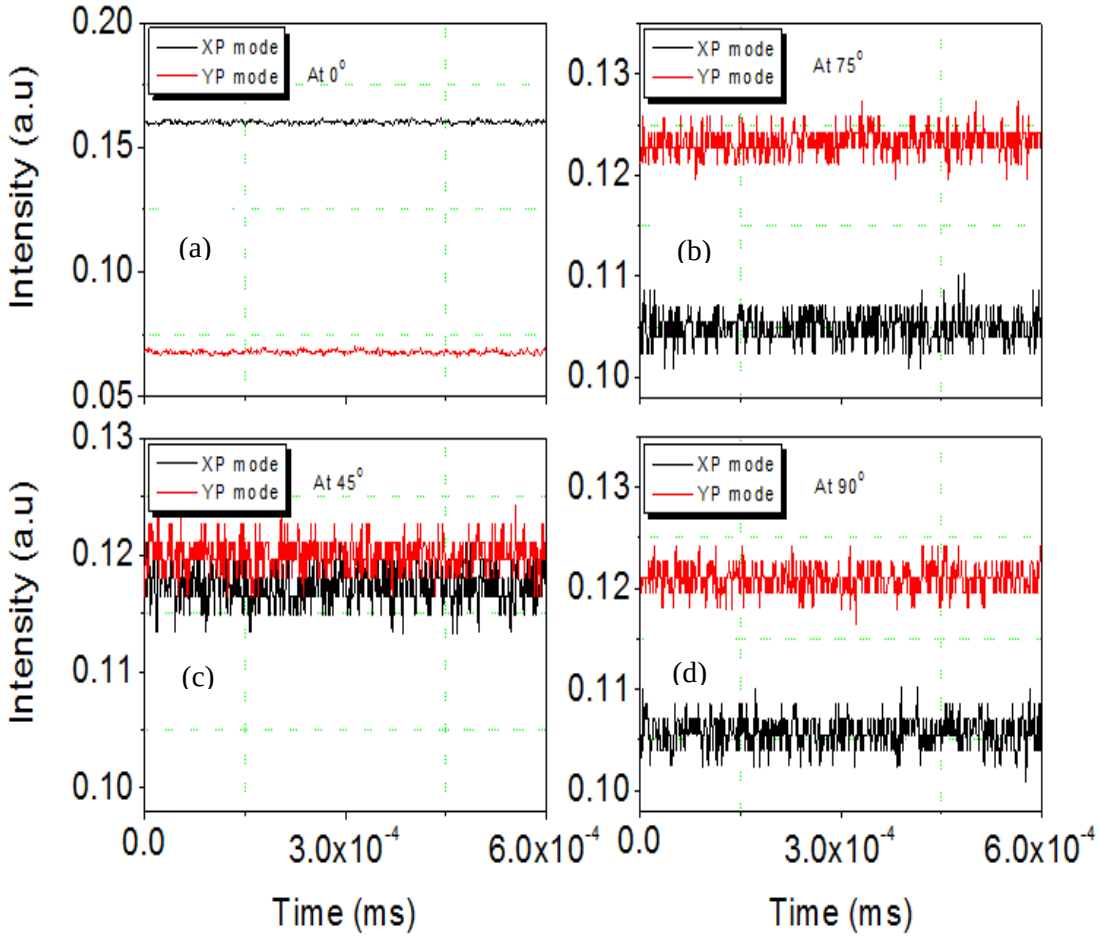

Figure 5-11: Intensity profile of the XP (black) and YP (red) polarization modes of VCSEL with a feedback strength of −5.5 dB, for θ_p of (a) 0°, (b) 45°, (c) 75° and (d) 90°.

For θ_p= 45°, the intensity of the XP and YP modes are almost the same. This is because the XP mode progressively loses light feedback with increasing θ_p, while the YP mode obtains more feedback [39]. As θ_p increase the XP (YP) mode intensity decrease (increase) as shown in Fig. 5-11(c and d). Furthermore, it can be seen from Fig. 5-10

that the RIN of the XP becomes higher than that of the YP mode for θ_p > 45° due to the PS effects. In addition, the RIN level of the two modes is relatively constant at these θ_p values. For the dominant polarization mode (i.e., XP) the RIN is a minimum at θ_p= 0°, while it is a minimum at 90° for the suppressed polarization mode (YP). Furthermore, for a higher OF level (-5.5 dB) RIN of the XP mode increases rapidly with θ_p, whereas for the YP mode the RIN is low for angles > 45°due to PS occurs between the XP and YP mode. In addition, when θ_p increase a number of spectral lines appear in spectrum profile, thus representing complex dynamics behaviour of the VCSEL induced by VPOF.

The frequency spectrum of the XP (black) and YP (red) mode of the VCSEL with a feedback strength of -5.5 dB, for θ_p of 0° (a) ,45° (b), 75°(c) and 90°(d) are displayed in Fig. 5-12. Fig. 5-12 a ($\bar{a}$,), b ($\bar{b}$), c ($\bar{c}$) and d ($\bar{d}$) represent the XP (YP) mode for θ_p of 0°,45°,75° and 90°, respectively. For the XP mode at θ_p= 0° there are no spectral peaks, see Fig. 5-12 (a). This indicates that the relaxation oscillations of the laser are damped due to the OF strength. For higher values of θ_p, where the OF level decreases, a number of spectral lines are observed, particularly for the YP mode, see Fig. 5-12 (b, c and d), which are in line with the data reported in [30].

Fig. 5-13 displays the power spectrums of the XP and YP modes corresponding to Fig. 5-12 for the low frequency range up to 50 MHz. Compared to Fig. 5-12 the noise level is higher by ≈ -1 dBm for both the XP and YP modes and for all values of the rotating phase angle. The increase in the relaxation oscillation peak amplitude by up to -3 dB indicates that the external OF affects the damping of the relaxation oscillations. With a strong OF level, the VCSEL output power becomes chaotic, which depends on the feedback level and the length of the external cavity [7]. A detailed study of the chaotic behaviour will be discussed in the next chapter.

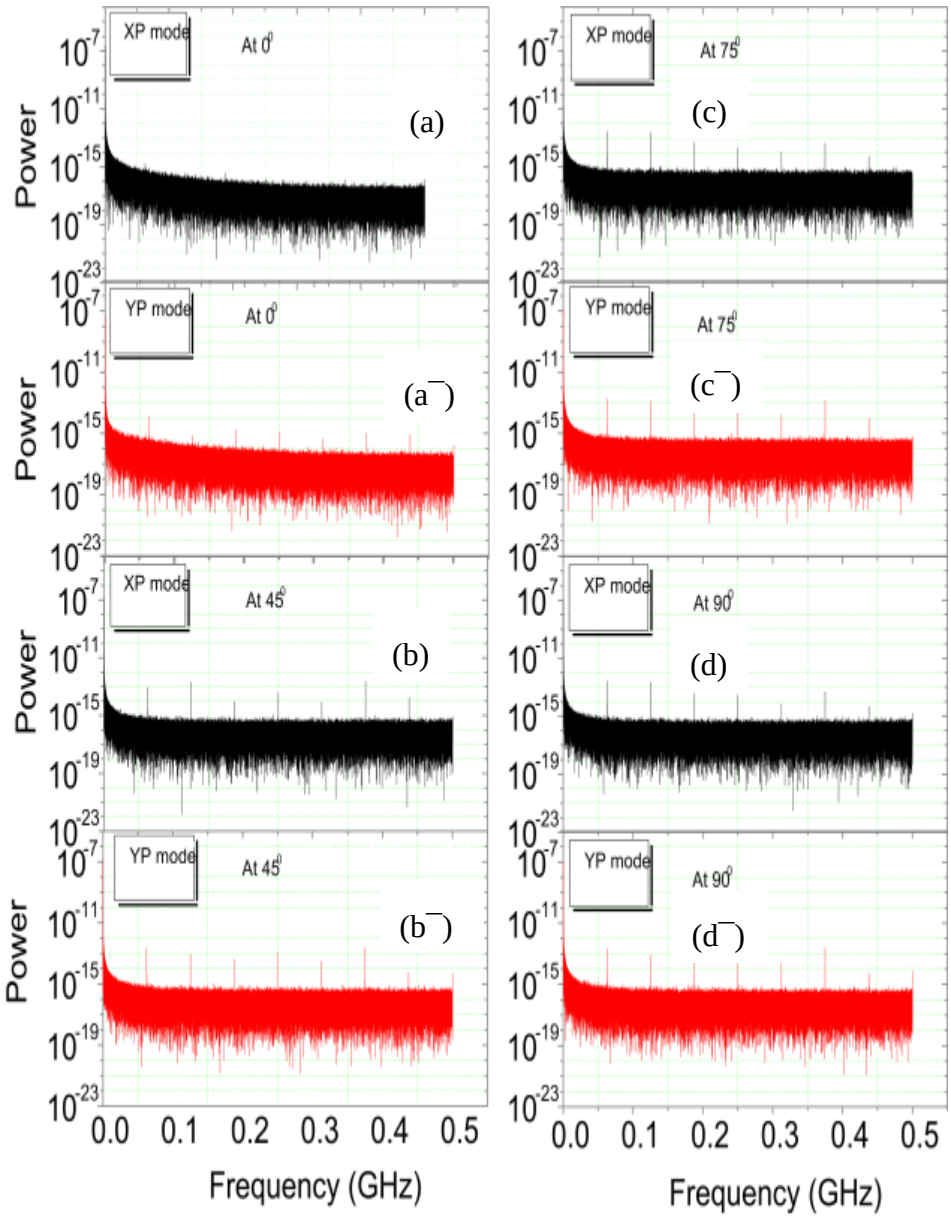

Figure 5-12: The output spectrum of the XP and YP polarization modes of VCSEL with a feedback strength of −5.5 dB, for XP mode at θ_p of (a) 0°,(b) 45°, (c) 75° and (d)90° and for YP mode at θ_p of (a¯) 0°,(b¯) 45°, (c¯) 75° and (d ¯) 90°

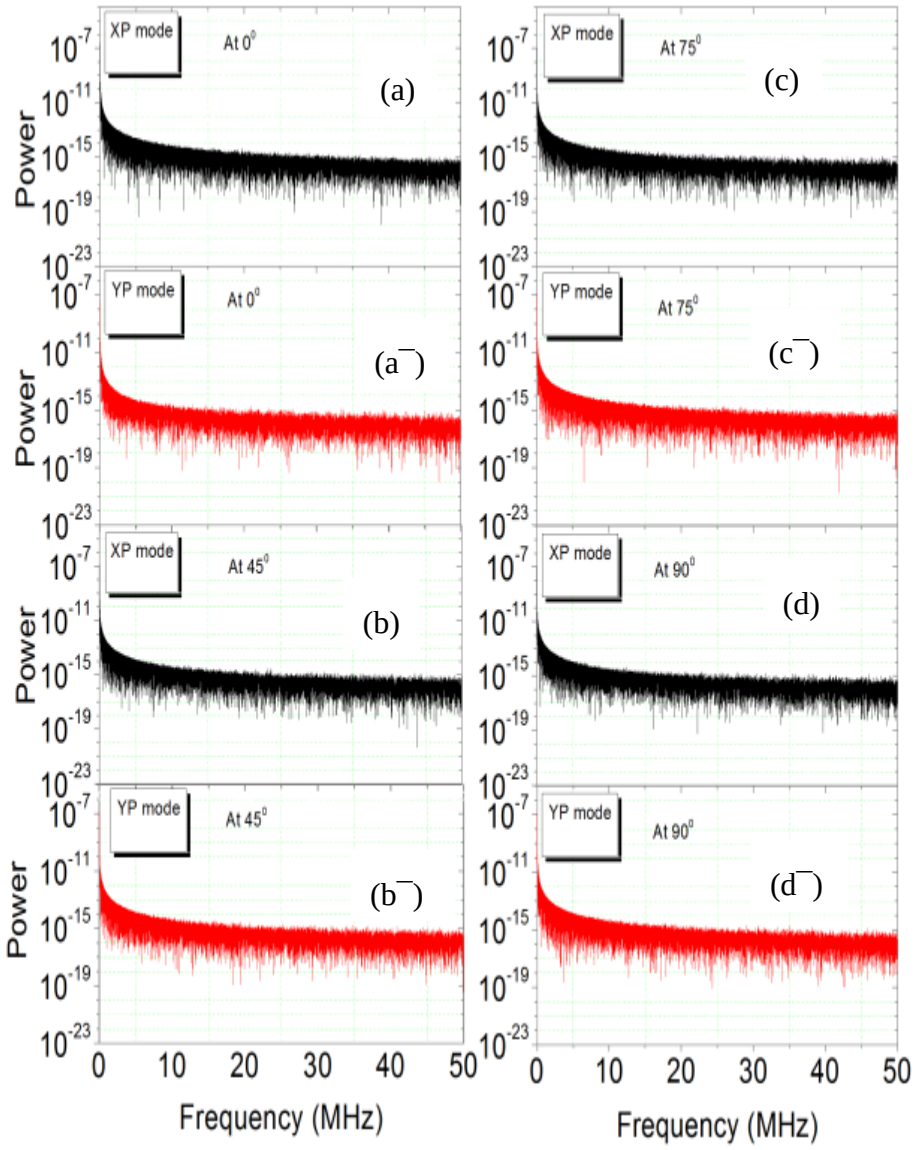

Figure 5-13: Display the Power in the frequency domain corresponding to Fig 5-11 for low frequency scale up to 50 MHz, for XP mode at θ_p of (a) 0°,(b) 45°, (c), 75° and (d) 90° and for YP mode at θ_p of (a¯) 0°,(b¯) 45°, (c¯), 75° and (d ¯)90°.

5.5 Relative Intensity Noise Characteristics Subject to Modulation Signal with VPOF

The influence of VPOF with the modulation signal on the RIN of a VCSEL was also experimentally investigated. The VCSEL has a different L-I curve characteristics (will explain later) than this used in previous section (5.3.1). A minimum RIN level of -156

dB/Hz with OF at the dominant mode is degraded to -139 dB/Hz under modulation signal. Preservation of the polarization OF with rotated θ_p is considered and its influences on the polarization-resolved RIN of the polarization modes of VCSEL is presented.

5.5.1 Experimental Setup

The experimental setup is showed in Fig. 5-14. A similar detail for the setup was provided in section 5.3.1 except that, we are used here an arbitrary vector signal

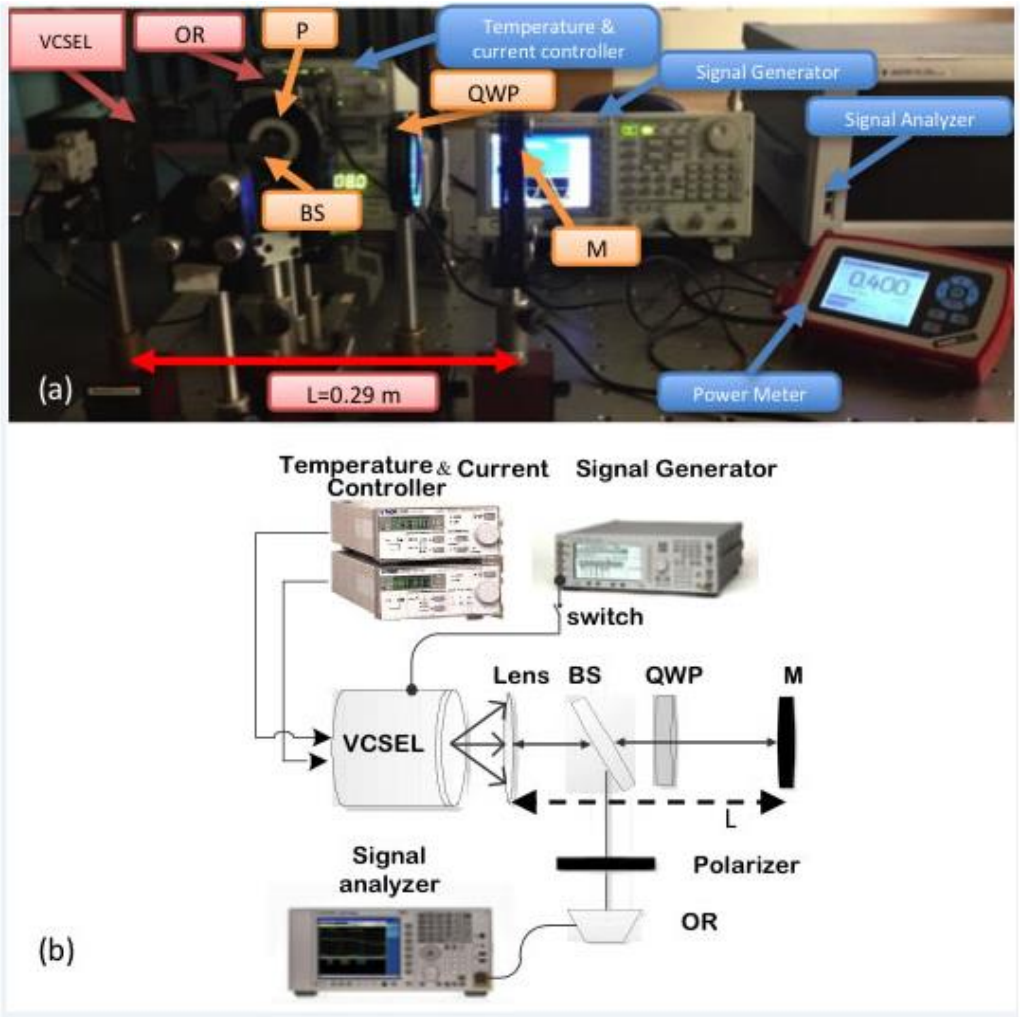

Figure 5-14: (a) Laboratory snapshot and (b) scheme of the experimental setup of RIN measurement of the VCSEL subjected to rotated OF and modulation signal. BS: non-polarizing beam splitter; M: feedback mirror; OR: optical receiver. QWP: quarter wave plate. P: polarizer.

generator (Tektronix, 2 GS/s, 240 MHz) to generate the modulation signal. The modulation signal is applied only if the switch is active, as depicted in the figure. Additionally, a linear polarizer (P) was used to select the polarization mode instead of the PBS and then only one OR (Newport, model No. 1601, 1 GHz) need in this setup. OF with XP and XP modes correspond to θ_p of 0° and 90°, respectively. The external cavity length from the VCSEL output to M was 29 cm. Finally, the electrical output power of the PD is stored by an electrical signal analyzer (Agilent MXA, N9020A 26.5 GHz) for further processing.

5.5.2 Results and Discussions

Similar details for the L-I curve of VCSEL were given in Chapter 4 (section 4.3.2). The VCSEL was biased under a fixed feedback level of −7 dB and I_b of 5.6 mA. The RIN is calculated using equation (5.1). Firstly, the polarization-resolved RIN of the VCSEL subject to OF with a rotated θ_p are shown in Fig. 5-15. For θ_p of 0° the XP mode (the dominant mode), display lower RIN compared to the YP mode. The RIN profile for the XP mode is around -156 dB/Hz over the entirely range of θ_p. This is due to the higher level of OF obtained by the XP mode because it is dominant mode. In the best case scenario, between $0 < \theta_p < 60°$ the RIN for the XP mode is 1-2 dB lower than the YP mode.

The RIN of the YP mode decreases reaching a minimum level below -155 dB/Hz and then increasing beyond $\theta_p > 45°$. This is because of progressively reduced level of OF with the XP mode when increasing θ_p, while the YP mode gaining higher level of OF [39]. At $\theta_p \geq 90°$ the RIN level difference between the XP and YP modes is about 5 dB/Hz.

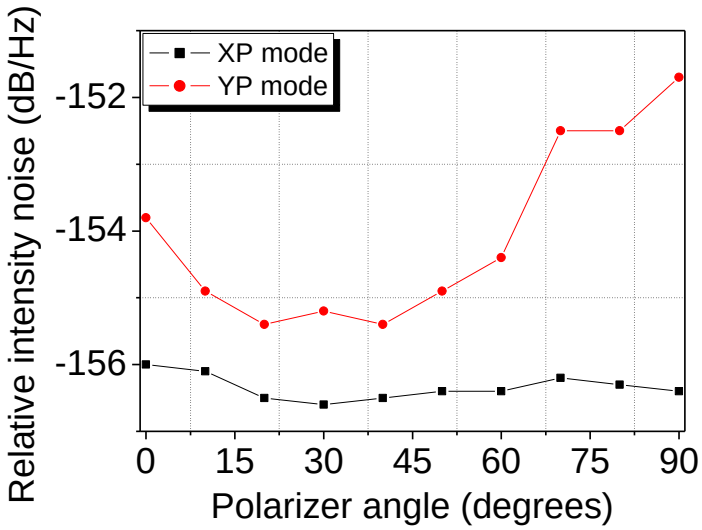

Figure 5-15: Polarization-resolved RIN of the VCSEL modes as a function of polarization angle subject to −7 dB OF level.

Similarly, Fig. 5-16 shows the measured RIN of the VCSEL modes against θ_p for the modulation frequency of 40.5 MHz and a modulation-depth of 68%. Note that for both modes the RIN levels are higher, by average RIN values of 16 and 20 dB for the XP and YP modes, respectively, compared to the case with no modulation as in Fig. 5-15, which can be attributed to modulation effects. Analogous to the previous case with no modulation, the RIN of the XP mode is lower than that of the YP mode over the whole range of θ_p by 5 dB/Hz. Moreover, Fig. 5-16 indicates that a rotating θ_p could significantly change the noise level of the YP mode compared with the XP mode of the VCSEL. In this case, the minimum RIN of -156 dB/Hz with OF at dominant mode was degraded to -139 dB/Hz under modulation signal.

In Fig. 5-17 the polarization modes output powers in the frequency domain are displayed for the case of free running operation, -7 dB of OF, and 10 MHz of modulation frequency with and without OF. The results indicated that the output power of the XP mode is higher by ~2 – 3 dBm than the YP mode for all cases depicted in Fig.

5-17. In this case, the output power of the two modes is higher with OF and modulation frequency. The higher output contributed to improve the RIN level for both modes, as shown in Fig. 5-16.

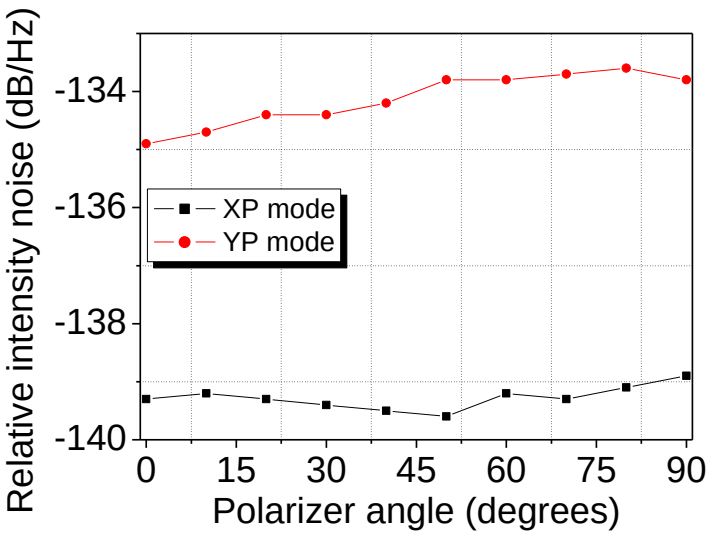

Figure 5-16: Polarization-resolved RIN of the VCSEL modes as a function of θ_p *subject to −7 dB OF level and 40.5 MHz modulation signal.*

A lower output power of around -77 dB for both XP and YP modes over a wide range of the frequency is achieved for the case with OF at 0^o and no modulation signal. Moreover, at low frequency range between 0 to ~12 MHz the harmonic frequencies for the case with the modulation frequency and OF lead to increased level of interference in both polarization modes. The power levels at the free running and at 10 MHz (without OF) cases are lower compared with the case of 10MHz with OF, for the frequency range of 12 MHz to 70 MHz for both XP and YP modes. The optical power increases with the case of applying modulation signal, which translates to the noise level increment in the output power of the VCSEL. For frequencies below ~ 12 MHz, the power level rapidly increased for all the cases, as shown at Fig. 5-17.

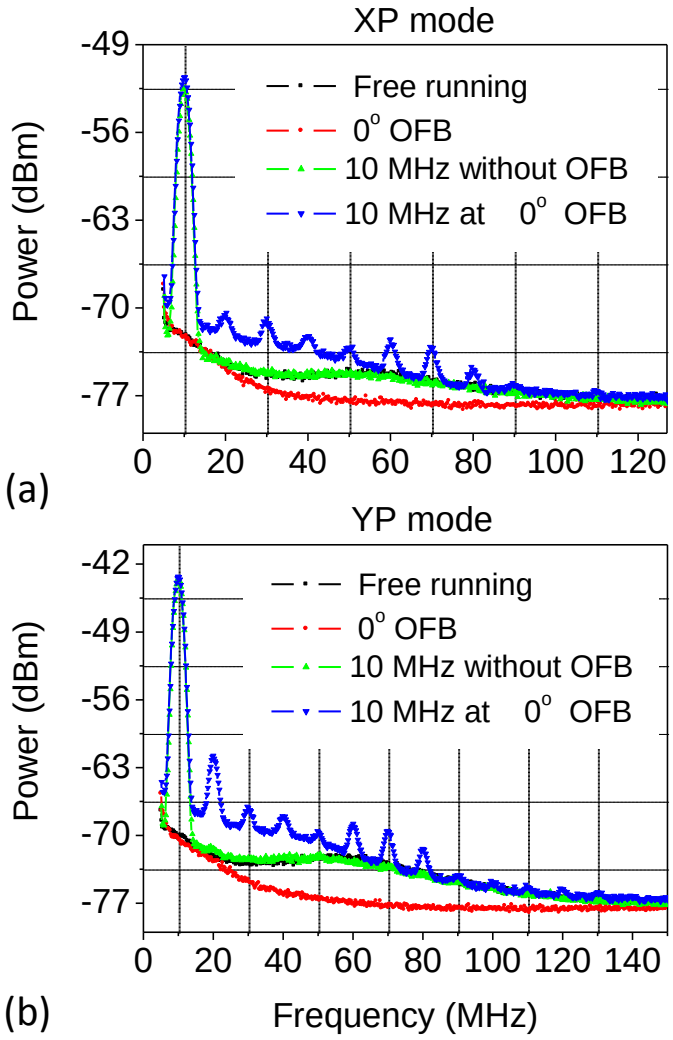

Figure 5-17: (colour lines), the output power of the XP mode (a) and YP mode (b) in frequency domain, at free running (Black), 0° OF (Red), 10 MHz signal modulation without OF (Green) and 0° OF with 10 MHz signal modulation (Blue).

However, the modulation signal in VCSEL results in an increment of RIN for both cases with and without OF. The modulation current gives energy to the modes oscillator and enhances the fluctuation [162]. Therefore, introducing the modulation signal in the VCSEL, results in the increased level of RIN with and without OF especially at the low frequency range of the spectrum.

5.6 Conclusions

In this chapter, the first experimental demonstration of the effects of selective-optical feedback on the nonlinear behaviour of the polarization properties of VCSEL was presented in Section 5.2. This investigation was carried out by observing the spectrum of the signal in the electrical domain. The results showed that the irregular dynamics of the polarization mode are drastically modified by using selective-optical feedback. It was demonstrated that the power peaks of the spectrum are strongly dependent on the type of the polarization that is being pumped back into the VCSEL. For 1 MHz modulation frequency at 3.6 mA of I_b , the HD decreased by 11dB compared to that of standalone VCSEL and the spectrum peaks (2^{nd} and 3^{rd}) were entirely suppressed.

For 240 MHz modulation frequency, the 2^{nd}, 3^{rd}, 4^{th} harmonics were completely suppressed and reached the noise floor when using the orthogonal optical feedback (OOF). The HD enhanced by ~2, ~11 and ~9 dB, for the 2^{nd}, 3^{rd} and 4^{th} harmonics, respectively when using the parallel (counterpart) polarization feedback (POF). In addition, it was shown that the HD is also influenced by variation of the operating temperature and bias current, which measured with 1 MHz, where in general the 2^{nd} (3^{rd}) harmonic increased (decreased) as the temperature and bias current increase. For instance at I_b of 3.6 mA , the 2^{nd} (3^{rd}) harmonic increased (decreased) by ~12 dB when the temperature increased from 0^o to 70^o, whilst the 2^{nd} (3^{rd}) harmonic increased (decreased) by ~10 dB when the I_b increased from 3 mA to 5.6 mA.

In Section 5.3, two VCSELs exhibit different properties under rotated θ_p of OF were used experimentally with /without modulation signal to describe the RIN characteristics. The results demonstrated that the VPOF can considerably affect the RIN properties of the VCSEL. For the first VCSEL, which had PS under VPOF, the RIN of the dominant

mode (XP) was a minimum at θ_p= 0^o and for the supressed mode (YP) it was a minimum at θ_p= 90^o. For the angles greater than 45° the RIN of the YP mode was lower than that of the XP mode due to the PS between the VCSEL modes. The relaxation oscillations were damped at higher feedback levels. At a higher θ_p a number of spectrum peaks were observed. The XP and YP modes have a similar RIN value at the PS position of this VCSEL. The noise level at lower frequencies from 0 to 50 MHz was greater than that of the higher frequencies by ~ 2- 3dBm, where the noise is distributed more consistently across the spectrum. In addition, the XP and YP modes experienced more feedback at $\theta_p$of 0° and 90°, respectively, which led to the one mode being dominant over the other at these angles of θ_p.

In Section 5.5 for the second investigation of the RIN with the second VCSEL, which has different characteristic under VPOF than this of the previous section, where no PS occurred with rotated θ_p. It was showed that a rotating θ_p of the OF does not affect the RIN characteristics of the dominant mode of the VCSEL. Whiles the RIN level of the YP mode progressively changed with increasing θ_p. However, the RIN level with modulation signal drastically changed for both XP and YP modes. In case of OF without modulation, the RIN (around -156 dB/Hz) of the XP mode was lower than this of the YP mode.

With OF and modulation signal, RIN levels of the XP and YP mode was higher than the case with no modulation by ~16 and ~20 dB, respectively. This behavior can be attributed to the power effect of the modulation signal. The difference in the RIN level of the XP mode with/without modulation is about 17 dB, while for the YP mode is 19 dB. Furthermore, the power spectra of the VCSEL showed OF with modulation signal could lead to further fluctuations in the power spectrum, which can significant degrade the noise level of the VCSEL.

Next chapter will provided chaotic dynamics of VCSEL with VPOF. In this chapter more attention has been given to chaos synchronization of the polarization modes of VCSEL.

Chapter 6

VCSEL Chaos and Synchronization Dynamics with Optical Feedback

6.1 Introduction

Chaotic systems with a number of unique features including noise-like shape with a broadband spectra, lower power implementations, and nonlinearity, have become appealing for modern secure communications applications. In such systems, a message is encoded into a noise like signal generated by laser source with chaotic behaviour [15, 79]. In the recent years, chaos synchronization has become a hot topic due to their potential applications in optical communication systems where security is paramount. Synchronization of chaos has attracted increasing attention especially in coupled VCSEL configurations based on polarization-rotated optical feedback and optical injection [10, 11, 169]. One of the important applications of a synchronized chaotic system is a mechanism used for encrypted communications. It is a very interesting step forward for controlling the chaotic dynamic in optical lasers through both synchronization phenomena and polarization-rotated optical feedback.

In VCSELs, detailed characteristics of chaos synchronization given in [13] showed that the anti-phase chaotic synchronization can be achieved between orthogonal polarization modes of the two mutually coupled VCSELs. The anti-phase correlation of a semiconductor laser is experimentally observed in [161] when the chaotic oscillation of the polarization modes is lower than the relaxation oscillation frequency. Enhance

chaotic signal has been achieved numerically based on two VCSELs as a master and slave laser subjected to optical feedback and optical injection, respectively. This proposed system reported in [10] based on two VCSELs shows high quality polarization resolved chaos signal between the slave and master signal. On the other hand, solitary VCSEL can exhibits strong anti-phase dynamics between own orthogonal polarization modes due to a nonlinear coupling of the orthogonal modes [170].

In this chapter in section 6.2 the impacts of the rotating polarization-preserved optical feedback on the chaotic synchronization dynamics of the VCSEL are investigated experimentally. A high level of preserve optical feedback is considered in this study, where the chaotic regime of VCSEL appears with high OF level [120, 171]. It is shown that high-quality anti-phase polarization-resolved chaos synchronization is achieved between the XP and YP modes at higher degree of θ_p. The quality of the chaotic synchronization increases with increase θ_p. The high correlation coefficient value of 0.99 obtained with a zero time delay has been reported theoretically in [42] but not confirmed experimentally yet. To the best of our knowledge, this is the first experimental report on how the anti-phase chaotic synchronization changes with the rotated polarization angle of the OF.

A numerical and analytical investigations in [172] has shown that basic Hopf bifurcations of the polarization modes of SL lead to sustained relaxation oscillation frequency of the laser. The bifurcation regimes always coexist close to square-wave switching and involve both relaxation oscillation and square-wave dynamics. Square wave switching has been theoretically reported in SL with polarization rotated OF in [172] and in VCSEL [102, 173]. In a theoretical study, square polarization dynamic has also been excited in VCSEL with perfect anti phase oscillations of the polarization modes, which greatly enhanced by small levels of polarization selective OF [174].

VCSEL itself can exhibit fast PS and polarization mode hopping under the influence of OF [151, 159, 175]. However, a free running laser diode can generate a low dimension chaotic oscillation and a small bandwidth without external perturbation [176].

Furthermore, the results show that different chaotic pattern can be achieved with the rotated-polarization OF as predicted in [35]. In SL diodes, the anti-phase correlation is experimentally observed when the chaotic oscillation is lower than the relaxation oscillation frequency of the polarization modes [161]. Solitary VCSELs can exhibits strong anti-phase dynamics between own orthogonal polarization modes [14], which could improve the quality of the chaotic synchronization of VCSEL.

In Section 6.5, a complex dynamics with high dimension chaotic mode hopping have been demonstrated with strong OF and a rotating polarization angle. Non-symmetrical switching and Irregular Square like dynamics are demonstrated with VPOF.

Simulation results, which are presented in section 6.6 shows that similar trends of the chaotic dynamics and polarization resolved mode hopping, can be observed with VPOF.

6.2 Chaos Synchronization in VCSEL Based on Rotate Polarization-Preserved Optical Feedback

VPOF lead to chaotic dynamics in the polarization modes of VCSEL, which could be exploited in optical communications for security reasons. In this investigation, the influence of the rotating polarization-preserved optical feedback (RPPOF) on the chaos synchronization of a VCSEL is investigated experimentally. The two VCSELs' polarization modes, XP and YP, are gradually rotated and re-injected back into the VCSEL. It is shown that high-quality anti-phase polarization-resolved chaos synchronization can be achieved at higher values of θ_p. The anti-phase dynamics

synchronization of the orthogonal polarization modes is evaluated using correlation coefficient (*C*) function. The maximum value of *C* obtained is about -0.99 with a zero time delay over a wide range of θ_p beyond 65°. A clear relationship is found between *C* and θ_p. VCSEL under VPOF can be a good candidate as a chaos synchronization source for secure communication systems.

6.2.1 Experimental Setup

To investigate the influences of RPPOF on the chaotic dynamics properties of the VCSEL, the following experimental set-up is employed as showed in Fig. 6-1. A commercial single mode 852 nm VCSEL is used with a linear optical L-I characteristic over a range of I_b .

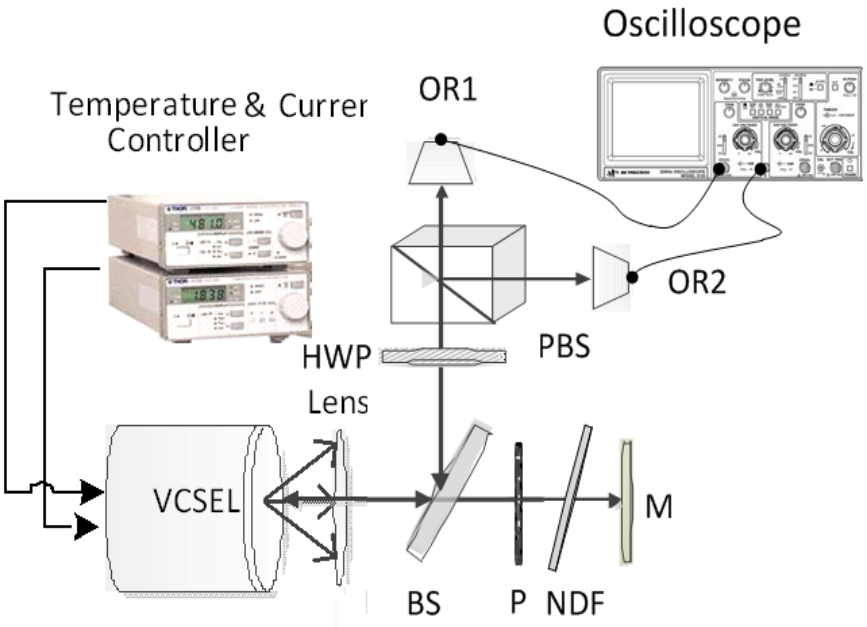

Figure 6-1: Experimental setup for chaotic dynamics measurements of the VCSEL, BS: beam splitter. HWP: half wave plate. M: mirror. NDF: neutral density filter. PBS: polarized beam splitter. P: linear polarizer. OR: optical receiver.

The VCSEL is driven by the laser diode driver module (Newport, 505B) and is temperature controlled using a thermoelectric temperature controller (TED 200C) to within 0.01° C. The external cavity is ~26 cm long, which corresponds to a feedback time of 1.7 ns. The solitary VCSEL lases' in the fundamental mode with two orthogonal polarization modes of XP and YP for the entire I_b range of 0-2 mA. The maximum measured output power of the VCSEL is 0.95 mW at I_b of 2 mA. The rest of the setup details are found in section 4.31 in Chapter 4.

6.2.2 Results and Discussions

The polarization-resolved L-I characteristics of free running VCSEL is shown in Fig. 6-2, at a room temperature of 20° C. It can be seen that the XP mode begins to oscillate at I_b of ~ 0.5 mA, which is the dominant mode.

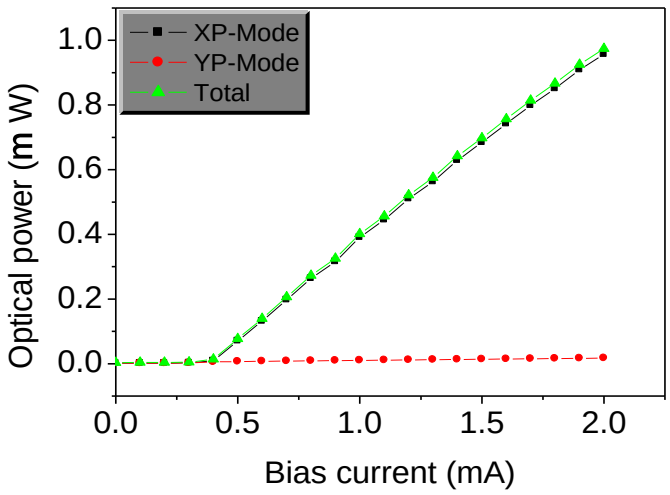

Figure 6-2: polarization-resolved L-I curve of the solitary VCSEL. Square black and dot red lines correspond to XP and YP modes, respectively. The triangle green line is referring to the total output power.

No PS is observed over I_b range. The power of the XP mode increase linearly and the YP mode is entirely suppressed. In the following discussions, we set I_b at 1.2 mA,

which is used in all the measurement campaign, where only the XP mode is oscillated. The standalone VCSEL's polarization modes, XP and YP, display quite different mode oscillation compared to the case when they subject to RPPOF. Fig. 6-3(a) shows the polarization-resolved time series of the XP mode (upper, black) and the YP mode (lower, red) of the standalone VCSEL at fixed I_b of 1.2 mA. The XP mode displays higher intensity levels compare with the YP mode.

6.2.3 Correlation Function

The correlation coefficient measurements can be used to evaluate the synchronization statues of the two systems. The correlation coefficient, $C_{x,y}$ for the XP and YP modes for evaluating the anti-phase chaotic synchronizations given by [177]:

$$C_{x,y} = \frac{<[I_x(t)-<I_x(t)>][I_y(t)-<I_y(t)>]>}{\sqrt{<[I_x(t)-<I_x(t)>]^2\ [I_y(t)-<I_y(t)>]^2>}} \quad (6.\ 1)$$

where $I_x(t)$ and $I_y(t)$ are the intensity outputs of the XP and YP modes, respectively; the terms < . > is mean value.

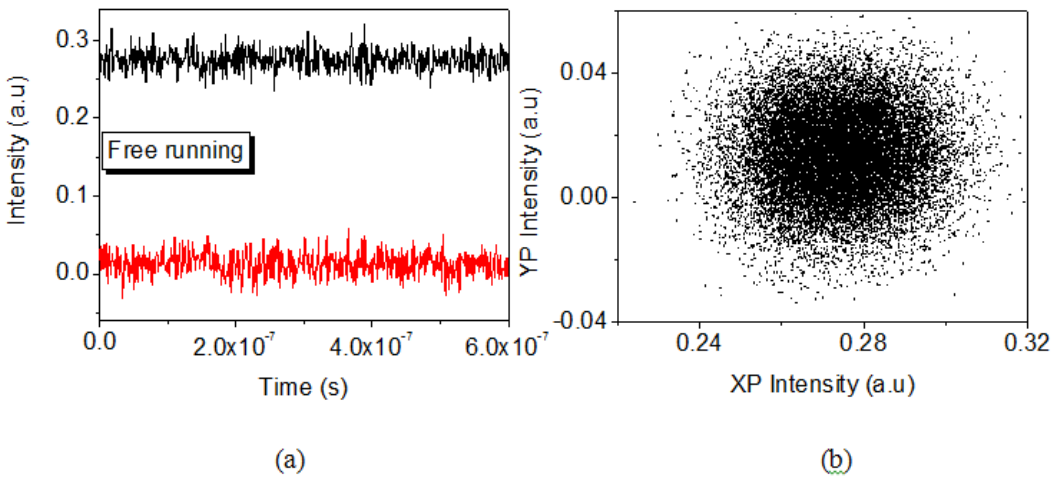

Figure 6-3: (a) Polarization-resolved time series of the VCSEL modes (XP (black) and YP (red)) at free running, (b) the corresponding correlation profile.

The corresponding correlation plot, which display in Fig. 6-3(b) confirmed that no chaotic synchronization is existed between the two polarizations modes.

6.2.4 Influence of RPPOF on Chaotic Dynamics of the Polarization Modes

After introducing the free running characteristics, the RPPOF effects on the chaotic dynamic of VCSEL are discussed. It should be noted that, when θ_p = 0° this corresponds to pure XP feedback and when θ_p= 90° this corresponds to pure YP feedback. The polarization-resolved intensities of the XP and YP modes as a function of polarizer angle are shown in Fig. 6-4 at a fixed level of OF (-7.4 dB).

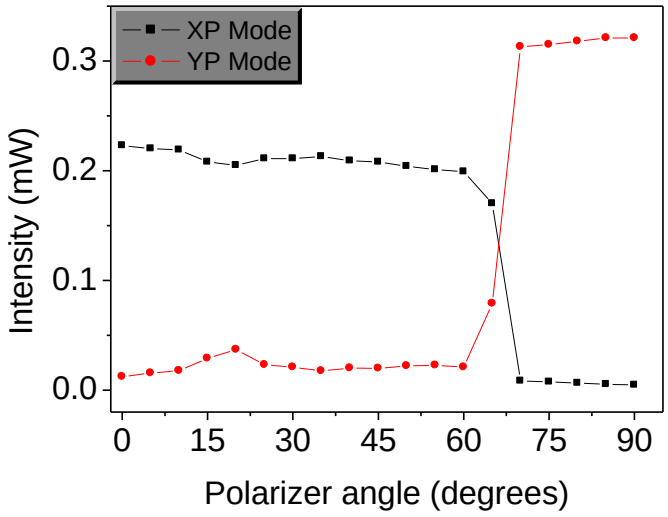

Figure 6-4: Polarization-resolved intensities as functions of θ_p under I_b of 1.2 mA and optical feedback level of -7.4 dB.

The XP mode is dominant and the YP mode is suppressed for a range of $\theta_p \leq$ ~65° with slight hump at 20°. At $\theta_p =$ ~65 the VCSEL show abrupt PS happen between the XP and YP mode. Once $\theta_p \geq$ ~70°, the XP mode is entirely suppressed with low output power of 0.004mW, while the YP mode becomes dominant with high output power of

0.32 mW. In this work, for a comprehensive of discussion of the polarization dynamics of VCSEL with VPOF, we covered a range of θ_p from 0° to 90°.

Next, Figure 6-5 shows the time series of the polarization modes and corresponding correlation plots under OF level of -7.4 dB. For a range of $\theta_p \leq 45°$, Fig. 5(a and b), it can be recognized that the XP mode exhibit high intensity signal compared with the YP mode and no synchronization between the oscillation modes is observed. As θ_p increase from 0° to 45°, the scatters points that appear in the figures distribute in one direction in the correlation plots, which is referring to the XP and YP modes initiate into the synchronization oscillation. However, the *C* at this range of θ_p is low of about 0.3, which is explained later in the next section. The XP and YP modes intensities are almost in a fixed level of the output power with no fluctuation are observed between them over the time series range see Fig 6-5(a).

However, as θ_p increases beyond ~45° the polarization dynamics show interesting results. High fluctuation and fast PS occur between the XP and YP modes. The corresponding correlation plots at θ_p of 67.5°,74° and 90° display a perfect anti-phase chaotic synchronization between the XP and YP modes. The maximum absolute value of *C* obtained beyond 65° is 0.99 with time shift of the anti- phase dynamics is zero. The laser modes dynamics could follow the instantaneous gain change between the two laser modes fluctuation nearby the PS point [178]. Dynamic fluctuations of VCSEL polarisation modes close to the PS point have been reported in literature from 1997 [104]. It can be attributed the anti-phase chaotic synchronization to the gain fluctuation close to the PS position between the orthogonal polarization modes of the VCSEL. Furthermore, mode competition could increase the anti-correlated oscillation of the VCSELs' modes [169]. On the other hand, when $\theta_p > 45°$ the XP mode loss the OF

while the YP mode experience more OF, which cause PS and then lead to the YP mode becomes a dominant [39].

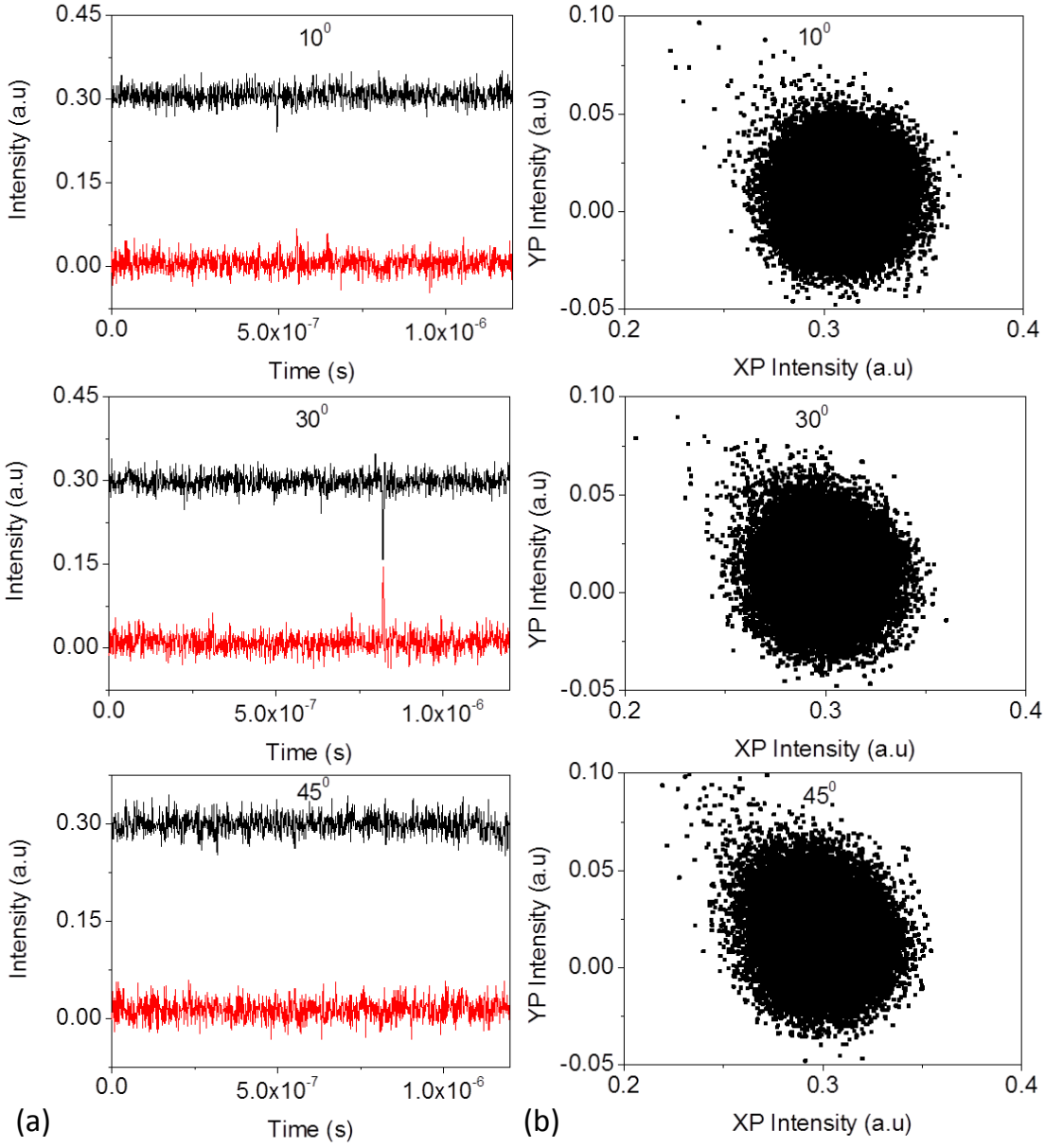

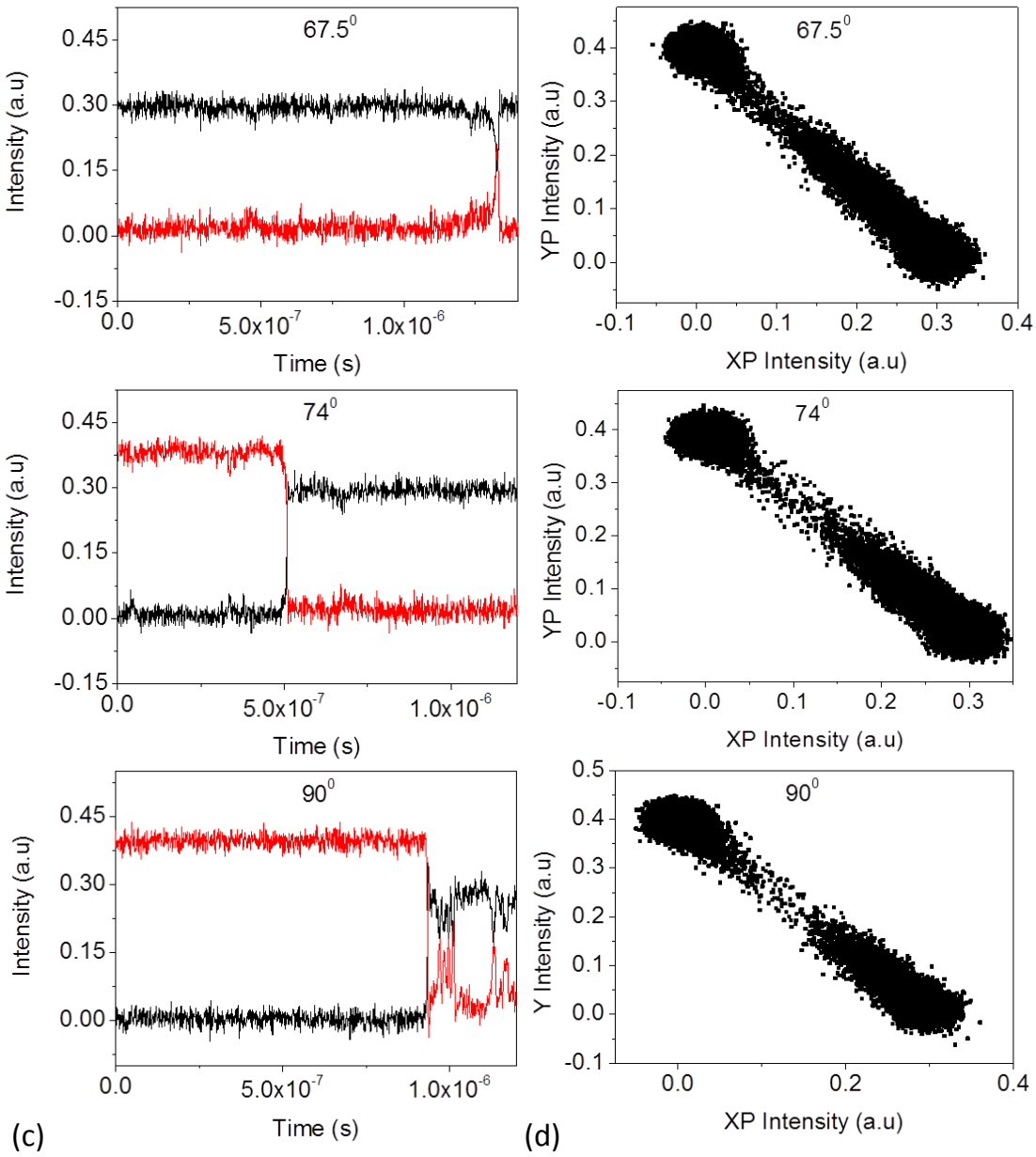

Figure 6-5: (a) and (c) Polarization-resolved time series of the polarization modes of the VCSEL , XP (black) and YP (red) at bias current of 1.2 mA and -7.4 dB feedback level,(a) for θ_p of 10°,30°,45°,(c) for θ_p 67.5°,74° and 90°, (b) and (d) corresponding correlation plots for (a) and (c) respectively.

The absolute values of $C_{x,y}$ between the two modes are presented in Fig. 6-6. It has been used of ~2×10^4 sample values to calculate each value of $C_{x,y}$ and evaluate the anti-phase correlation profile. Over the range of θ_p between 0° to ~ 60°, $C_{x,y}$ has relatively lower values and thus lower anti-phase synchronization between the XP and YP mode.

However, when θ_p increase beyond 60° $C_{x,y}$ value display a higher value of 0.99 over a wide range of θ_p .These results of $C_{x,y}$ at higher angles of θ_p clearly show high quality anti-phase chaotic synchronization between the orthogonal polarizations modes of the VCSEL.

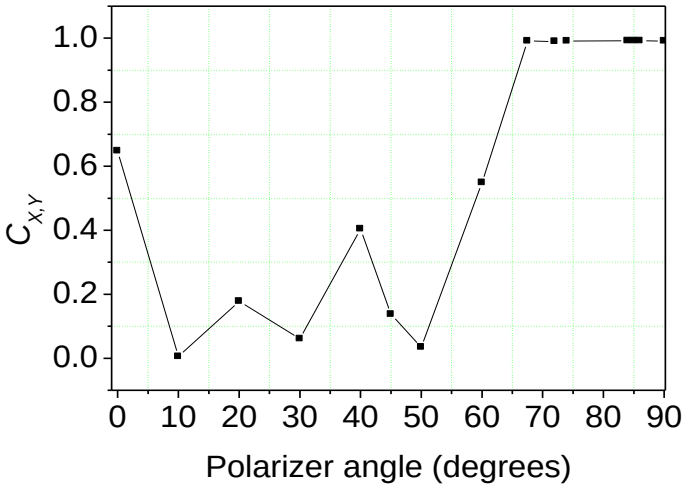

Figure 6-6: The absolute value of the correlation coefficient ($C_{x,y}$) of the two polarization modes (XP) and (YP) as a function of polarizer angle.

6.3 Influence of Optical Feedback Level on the Chaotic Synchronization

In the last section, characteristics of chaos synchronization of VCSEL subjected to RPPOF are described. For more investigation purpose, chaos synchronization dynamics of the VCSEL subjected to variable level of OF are provided in this section. First, Fig. 6-7 displays the polarization-resolved intensities of XP and YP mode as a function of OF levels, from low feedback level of about -27 dB to high feedback level of about -7.4 dB. For the OF range from -27 dB to -8 dB, as shown in Fig. 6-7, the XP mode is the dominant mode with almost constant intensity level, while the YP mode is entirely suppressed. When the OF level increases beyond ~ -8 dB the VCSEL polarization

modes exhibit abrupt PS, where the YP became the dominant mode with high intensity level, while the XP mode completely suppressed with a low intensity level.

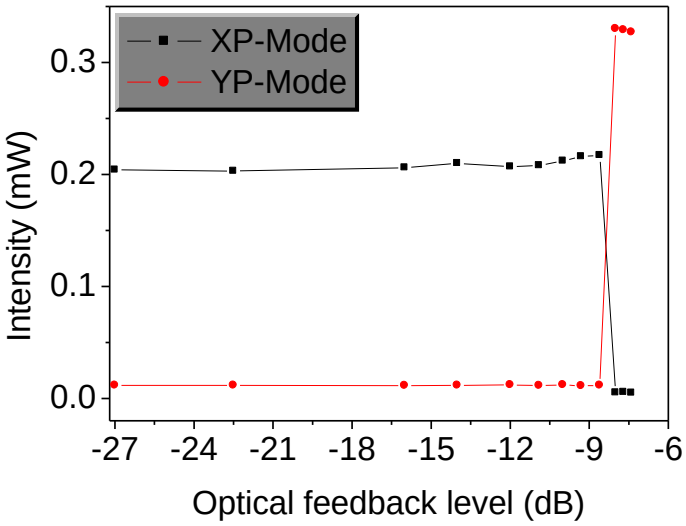

Figure 6-7: Polarization-resolved intensities as functions of optical feedback level under I_b of 1.2 mA

Next we observe the temporal waveform of the XP and YP modes with varying the OF levels from -27 dB to -7.4 dB. Fig. 6-8 gives the time trace of the XP and YP modes intensities subjected to -27 dB, -10.9 dB, -8 dB and -7.4 dB as we can see from column (a), while column (b) displays the corresponding correlation profiles. At a low feedback level of -27 dB, the XP and YP modes intensities are almost constants with high and low output power emissions, respectively. It can be clearly seen from correlation plot of -27 dB that the XP and YP modes are not in synchronization dynamic.

As the OF level increase the PS occurs and strong fluctuation is observed between the two polarization modes. The wider scattering points that appear in the correlation plots of -10.9 dB and -8 dB are indicated to the orthogonal polarization modes start to synchronized dynamics.

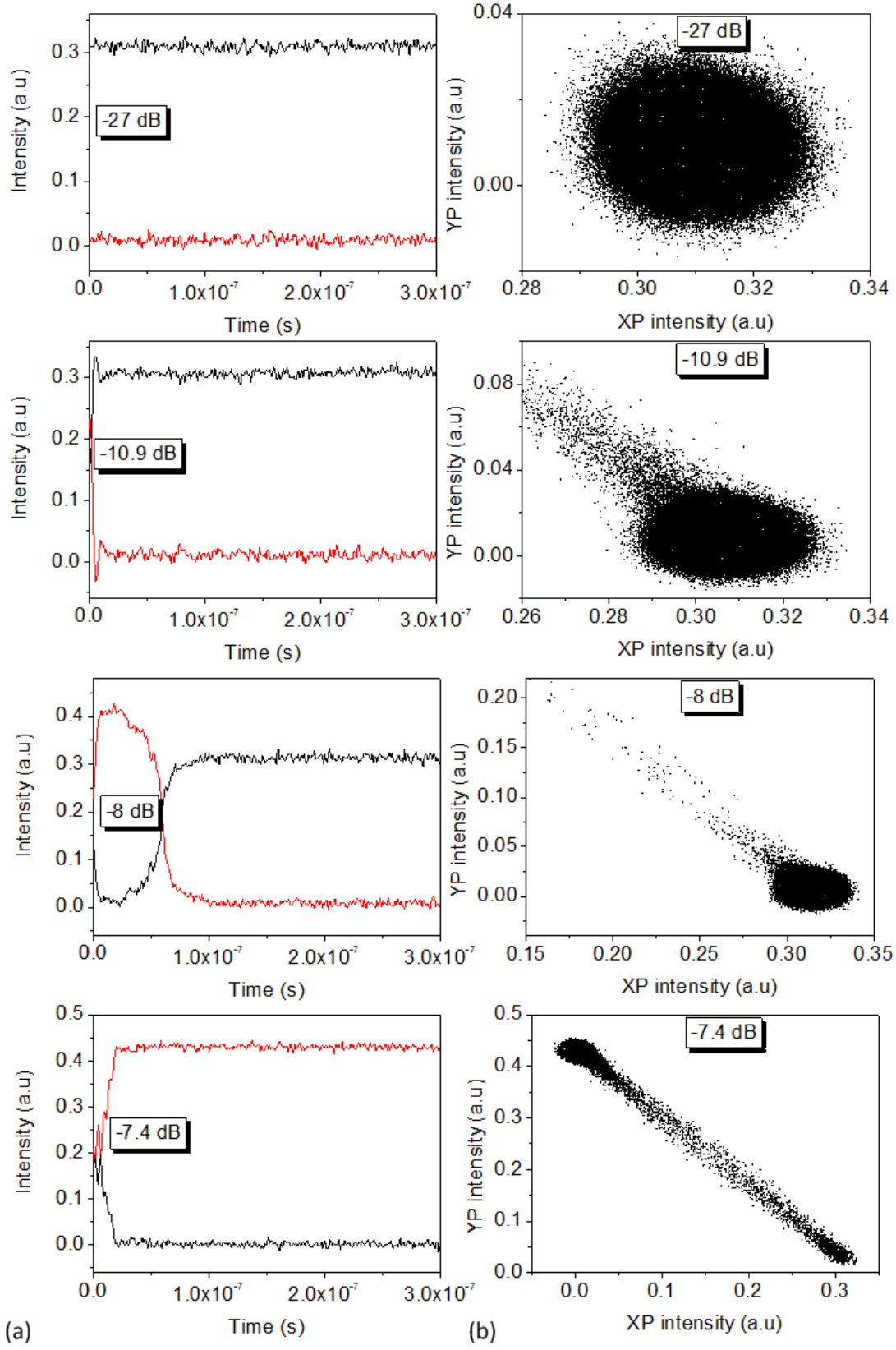

Figure 6-8: (a), Polarization-resolved time series of the VCSEL modes, XP (black) and YP (red), at bias current of 1.2 mA for OF level of -27,-10.9,-8 and -7.4 dB , (b) the corresponding correlation plots for (a).

A perfect synchronization is achieved at strong OF at the level of -7.4 dB, see the corresponding correlation plot.

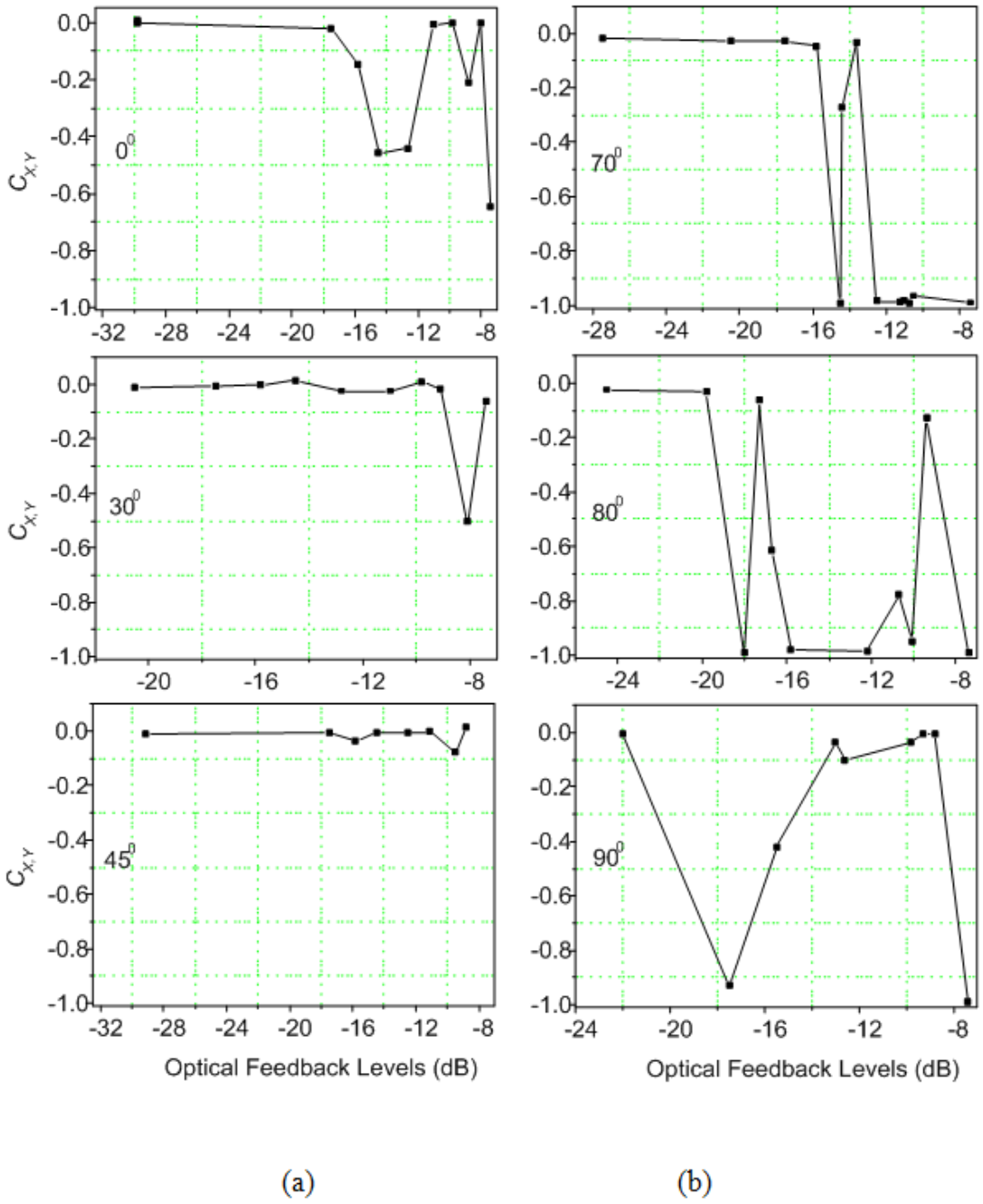

Figure 6-9: The correlation coefficient ($C_{x,y}$) plots of the two polarization mode (XP) and (YP) mode as function of optical feedback level, (a) for θ_p of 0°, 30°and 45°, (b) for θ_p of 70°, 80° and 90°.

The quality of the ant-phase synchronization of the VCSEL with variable levels of the OF are evaluated by calculating $C_{x,y}$. First, Fig. 6-9 displays the $C_{x,y}$ values as a function of the OF levels from -30 dB to -7.4 dB, for a range of θ_p. For the angles of 0°, 30° and 45°, a lower values of $C_{x,y}$ have achieved, while the maximum values are obtained beyond 45° with almost high OF levels. Fig. 6-9(b) show the $C_{x,y}$ measurements at θ_p of 70°, 80° and 90° from low to high levels of OF. At θ_p = 70° the $C_{x,y}$ values is almost zero until -14.5 dB, after that a maximum value of -0.99 is achieved over a wide range of the feedback levels. As θ_p increase the probability of achieving high quality of ant-phase chaotic synchronization increases and can be obtained at lower values of the feedback level.

Since the frequency detuning and phase difference of the external cavity of the OF affect the synchronization dynamics of the XP and YP modes [179], low quality of the synchronization is displayed at higher angles of θ_p and higher levels of OF. The results reveal that the chaotic synchronization have improved with close to the PS positions of the VCSELs' modes where the high quality of the anti-phase chaotic synchronization is achieved nearby the PS [180].

6.4 Selective-Optical Feedback Effects on the Chaos Synchronization

Next, the influence of the rotating parallel-polarization optical feedback (Parallel-POF) is considered for this investigation. VCSEL with similar characteristic of that used in pervious section (section 6.2) is used her to study the chaotic synchronization properties of parallel polarization OF with rotating θ_p. It has shown that the high-quality anti-phase polarization-resolved chaos synchronization is achieved in VCSEL at a strong

level of OF with rotating θ_p. The quality of the chaotic synchronization increases as θ_p increase.

6.4.1 Experimental Setup

To investigate the effect of the rotated parallel-POF on the chaotic dynamics of the VCSEL, we employ the following experimental set-up as depicted in Fig. 6-10. Similar VCSEL characteristics were provided in section (6.2.2) have been used in the experiment. Here, two polarization beam splitters (PBS1 and PBS2) are used to implement the parallel-POF and direct the orthogonal polarizations modes to the two identical optical receivers (OR), respectively. The external cavity is ~27 cm long, which corresponds to a feedback time of 1.8 ns. The rests of details are described in section (6.2.1) in this chapter.

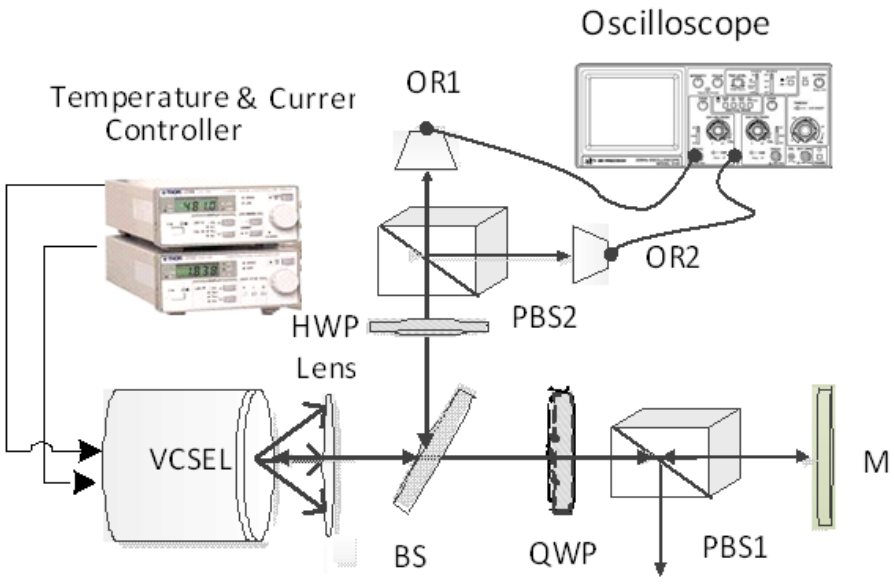

Figure 6-10: Experimental setup of selective-optical feedback for chaotic dynamics measurements of the VCSEL.

6.4.2 Anti-Phase Chaos Synchronization

Fig. 6-11 show the polarization-resolved time series of the XP mode (upper, black) and the YP mode (lower, red) of the VCSEL at I_b of 1.5 mA with an OF level of -7 dB, which is used in all the measurement campaign. θ_p is set at different values using QWP to rotate the OF signal. The OF level is defined as a ratio of the reflected power, measured at BS to the total optical power of the VCSEL measured directly after the objective lens in Fig. 6-10. The intensity of the XP and YP modes of the free running VCSEL is shown in Fig. 6-11(a), where the XP mode displays higher intensity levels compare with the YP mode. No anti-phase chaotic synchronization is observed, as confirmed in Fig. 6-12(a) between the two polarizations modes with no OF. The dynamics of the two modes at free running are much smoother compared to that of OF.

However, when the VCSEL subjected to parallel-POF the results reveal high quality anti-phase chaotic oscillation synchronization over a wide range of θ_p from 0^o to 90^o. Fig. 6-11(b, c, d) show the temporal waveform of the XP and YP at 0^o, 45^o and 90^o. At θ_p of 90^o the time trace of the XP has been shifted up by 0.1 (a.u) for clarity. As θ_p increase the XP and YP modes display strong fluctuation and show close similarity to each other. However, the XP intensity decreases as θ_p increase while the YP intensity increase. This is because for θ_p of 40^o to 90^o the XP and YP modes experience reduced and increased OF, respectively [39].

Furthermore, under parallel-POF the quality of the anti-phase chaotic synchronization increases as θ_p increases, particularly beyond 30^o. The corresponding correlation profile of the two chaotic oscillations of the XP and YP modes are presented in Fig. 6-12. Fig. 6-12(a) shows the correlation plot of the VCSEL at the free running operation, clearly displaying that there is no anti-phase dynamics synchronization between the

orthogonal modes. However, a high anti-phase chaotic synchronisation can be achieved when applied Parallel-POF as depicted in the correlation plots in Fig. 6-12(b, c, d), with high-degree achievement when θ_p = 90^o, see Table 6-1.

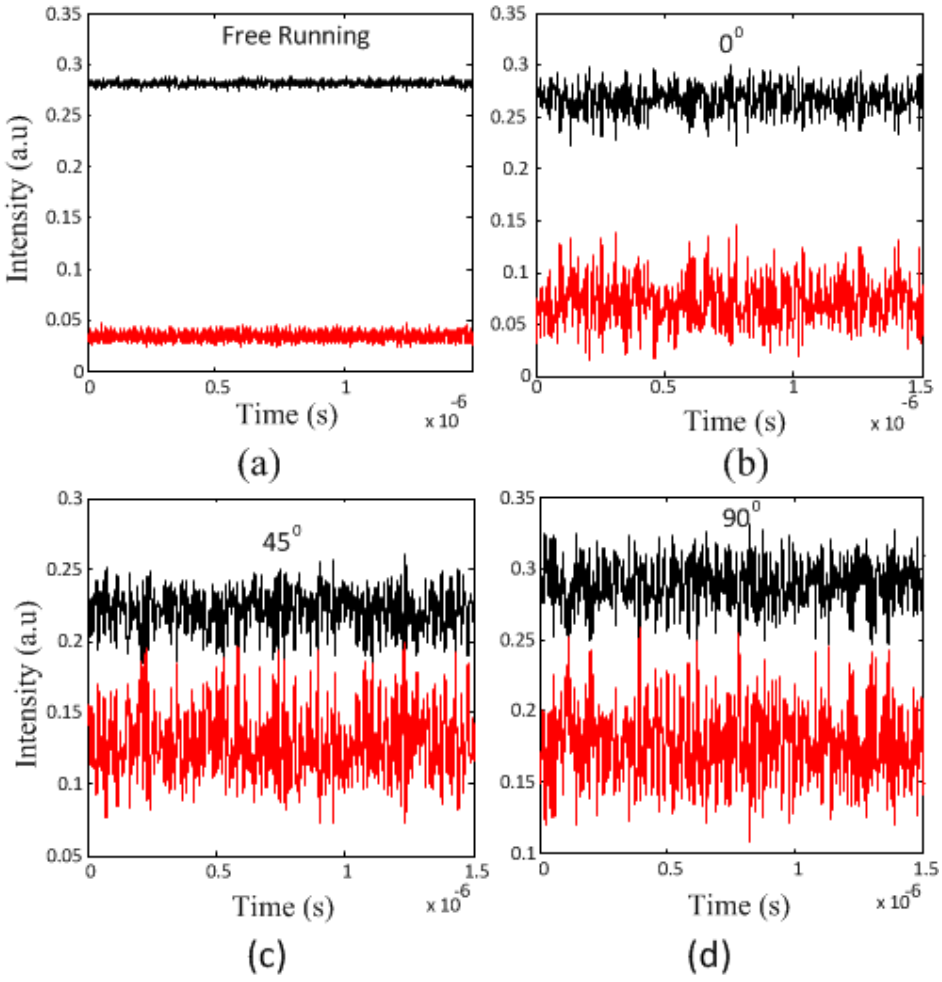

Figure 6-11: Polarization-resolved time series of the VCSEL modes (XP (red) and YP (black)) at a bias current of 1.5 mA, -7 dB of feedback level at (a) free running, (b) 0^o, (c) 45^o and (d) 90^o of θ_p.

The absolute values of $C_{x,y}$ between the two modes are presented in Table 6-1. Note that $C_{x,y}$ decreases at lower values of θ_p (i.e. 0 ^{o} to 30^o) and then increases for θ_p > 30^o with the maximum value of 0.982 observed at θ_p of 90^o. We have used 4×10^6 sample values to calculate $C_{x,y}$ and evaluate the anti-phase correlation profile.

Table 6-1*: Relationship between polarization angle and correlation coefficient*

θ_p (degrees)	0^o	10^o	20^o	30^o	40^o	45^o
$C_{x,y}$ *(Absolute values)*	0.966	0.959	0.955	0.963	0.971	0.975
θ_p (degrees)	50^o	60^o	70^o	80^o	90^o	
$C_{x,y}$ *(Absolute values)*	0.977	0.978	0.980	0.981	0.982	

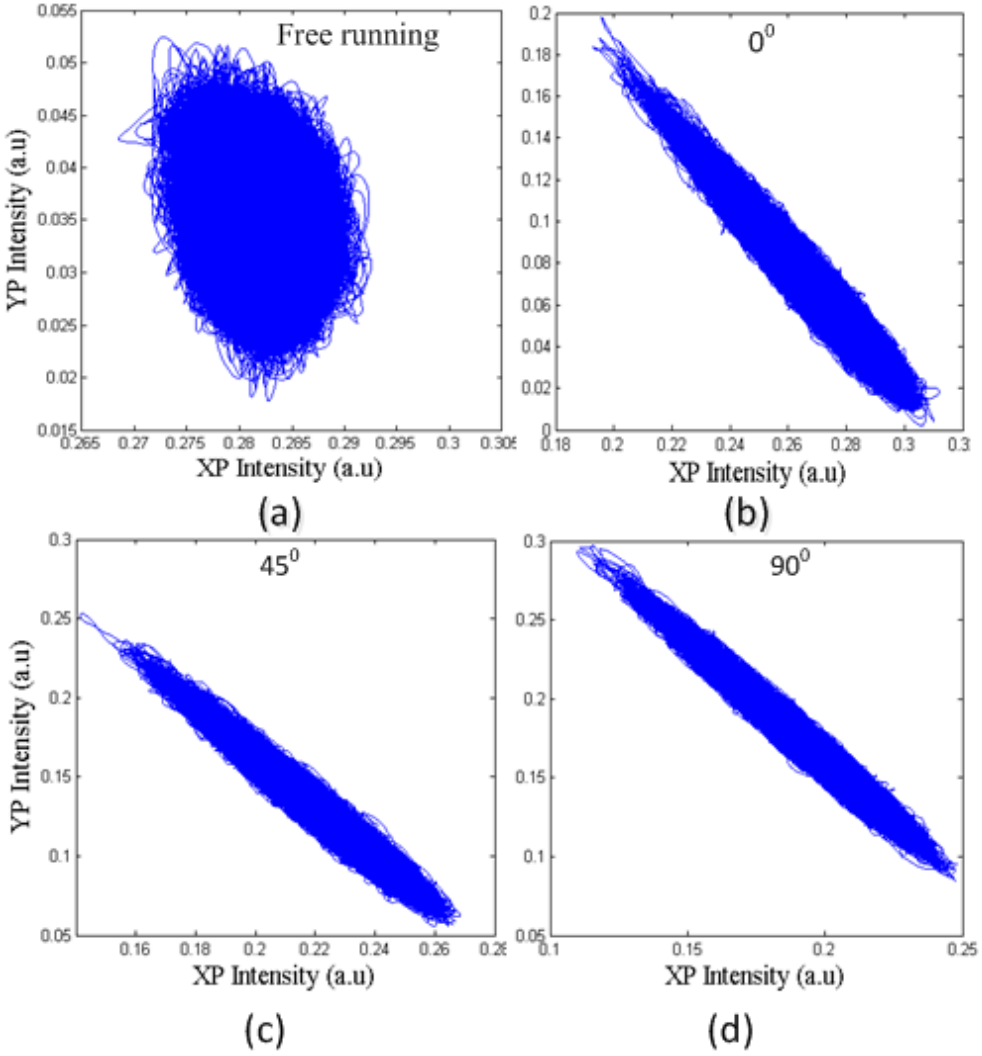

Figure 6-12: Corresponding correlation plots between the XP and YP modes for the same θ_p in Fig. 6-11.

6.5 Complex Polarization Dynamics of VCSEL under Rotated Polarization Optical Feedback

Further investigation for the chaotic dynamics of the orthogonal polarization modes of VCSEL with VPOF are described in this section. The VCSEL subjected to VPOF with feedback level of -7.4 dB at a fixed I_b of 1.2 mA. Fig. 6-13 presents measured dynamics of the polarization-resolved output power in VCSEL, where the polarization angle plays a role as rotating the polarization state to re-inject to the laser.

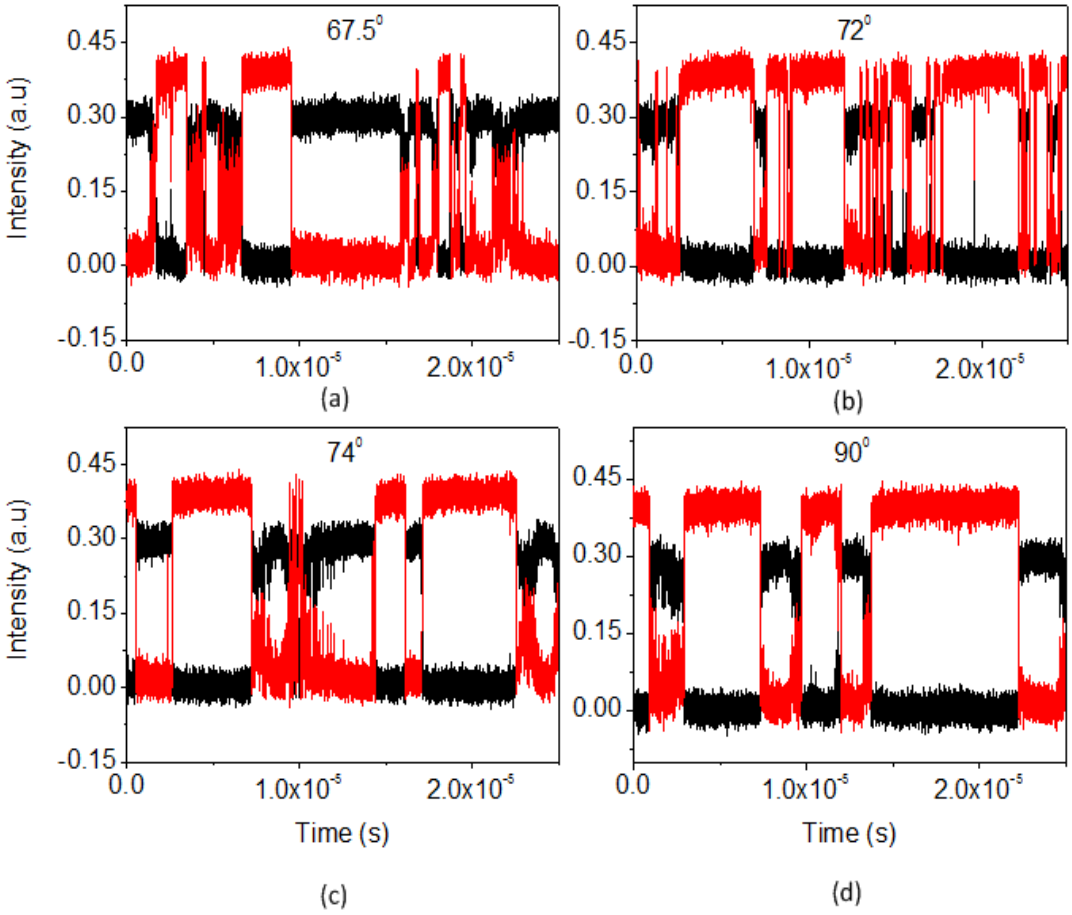

Figure 6-13: Polarization-resolved time series of the VCSEL modes (XP (black) and YP (red)) with rotated polarization angle of optical feedback. VCSEL driven by constant injection current of 1.2 mA and subjected to fix optical feedback of -7.4 dB, the device can exhibit chaotic mode hopping between two polarized modes.

Similarity mode hopping is observed between the two polarizations modes combined with high chaotic dimension oscillation. The results displayed in Fig. 6-13(a, b, c, d) are for the XP and YP polarization modes, in black and red line respectively, with a range of θ_p of 67.5^o, 72^o, 74^o and 90^o. Obviously can be seen that the mode hopping coexist between the polarization modes over a wide range of θ_p beyond 45^o. The modes instability appears due to gain competition between co-existing polarization modes [181]. Furthermore, the results show that the VPOF can provide a rich dynamics and patterns compared with the conventional OF as reported in literature [35].Similar mode hopping have been found at fee running VCSEL, however with low dimension chaotic oscillation [170].

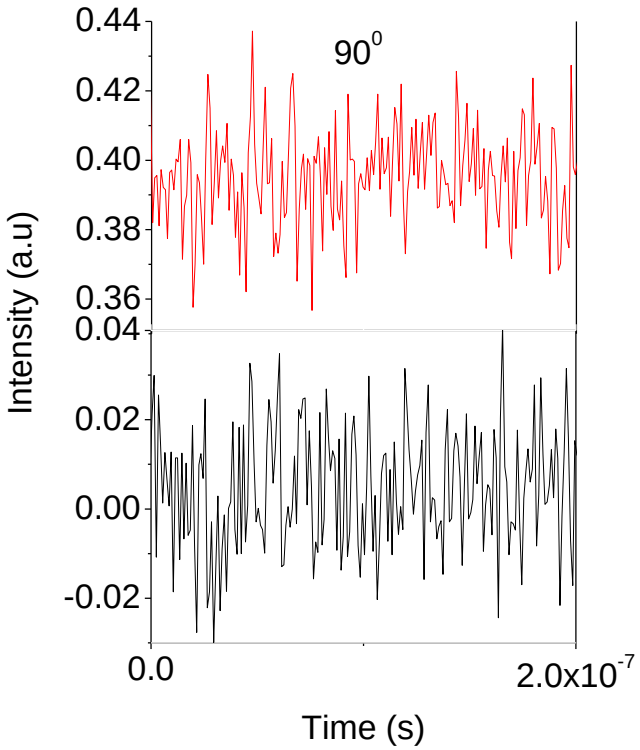

Figure 6-14: Polarization-resolved output power–time trace showing chaotic polarization dynamics at constant injection currents of 1.2 mA and optical feedback of -7.4 dB over a time series scale of 2 micro second.

The oscillation in the orthogonally polarisations modes are in anti-phase dynamic. In Fig. 6-14 the polarization-resolved output power are presented with zooming the time trace to 2 micro second to show the chaotic polarization oscillation at θ_p = 90^o. At this short time trace the YP mode is the dominant mode with high output power as display in the figure. From zero to 2 micro second, the time trace show that the XP and YP modes are in chaotic oscillation.

The underlying physics of the orthogonally polarization modes fluctuation is a nonlinear coupling mechanisms between the two polarization modes due to the effects of the external polarization feedback [181, 182].

6.6 Simulation Results for VCSEL under Optical Feedback

Set equations (2.18 to 2.28) that were implemented in Chapter 2 section 2.12.4 are modelled in a Simulink model to obtain polarization properties of VCSEL under VPOF. The Lang-Kobayashi model have been considered to analyse VCSEL properties [33], which shows highly accurate analysis for SLs with OF [39, 183]. The Simulink model is used to confirm the experiment results presented in section 6.4.1. The delay time τ of the OF is equivalent to the light round trip of the external cavity, which is set to 1.8 ns. The parameters used in the Simulink model in all experiments are identical, and provided in Table 4-1 except for the followings: feedback coefficient k, time delay τ, polarization angle θ_p, injection current I, wavelength λ and the angular frequency ω. These are the actual parameters value of the experiment setup.

6.6.1 Simulation Results and Discussion

Many theoretical parameters such as gain G, feedback strength k, θ_p and delay time τ can play a role in the obtained results of the Simulink. First, the numerical results show the XP and YP modes gain and the carrier density profile with OF (k =1.60×10^{11} ns^{-1}) and I_b of 1.5 mA, see Fig. 6-15. Fig.6-15(a) shows the carrier density of VCSEL in the time domain with strong OF. It is obvious from this figure that the laser reaches the threshold point at about 1.2 ns, where the gain and the internal loss are equal.

In Fig.6-15(b), the XP and YP gains, which increase with the time until the threshold point where VCSEL start lasing and then becoming almost constant. The lasing threshold is determined by the difference between the gain and internal loss of the laser [184, 185]. The gain trends of the two modes are following the carrier density or the gain is a function of the carrier density [186, 187]. From equation (2.7), the threshold gain is depending on the parameters of the laser cavity such as L the cavity length and R the mirror reflectivity. Clearly can be seen that the theoretical gain of XP mode is higher than that of the YP mode. This indicates that XP is being lasing at a higher intensity level than that of the YP mode. The gain of polarization modes is a linear dependence on the carrier density below the threshold following which it is saturated [186].

Next, the polarization resolved waveforms of both XP and YP modes are presented in Fig.6-16 for a short time period of 17 ns. The simulation was run over a time period that was several orders of magnitude longer than the delay time of the OF(i.e., at 1.8 ns) to clearly display the oscillatory behaviour of the XP and YP modes in this region. For the convenience of discussion the intensities of the XP and YP modes are normalized to the first component on each plot for the all simulation measurements.

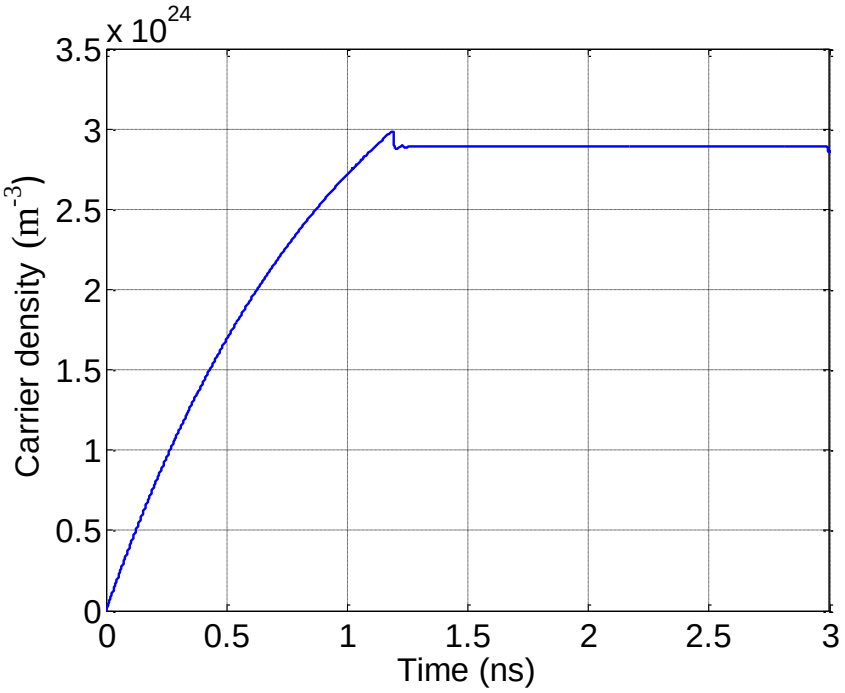

(a)

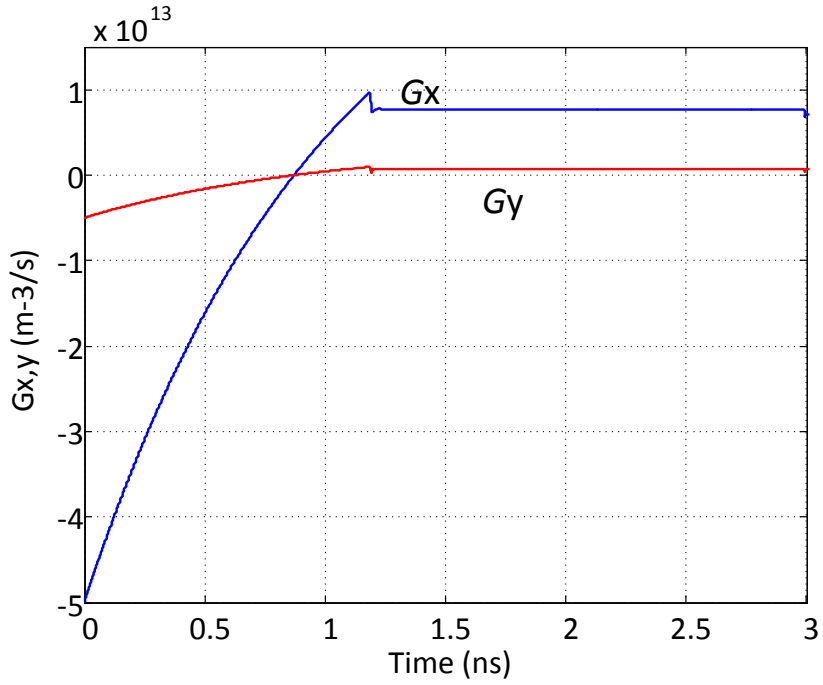

(b)

Figure 6-15: Numerical results of VCSEL under optical feedback to evolution the carrier density and gain; (a) the carrier density profile, (b) gain of the XP mode (blue) and gain of the YP (red).

It is observed that the two polarization modes oscillation with a delay time τ = 1.8 ns, which is because of the feedback delay associated with the external cavity length. The intensity of XP mode is higher than the intensity of YP mode because of the XP mode is the dominant mode as show from Fig. 6-16.

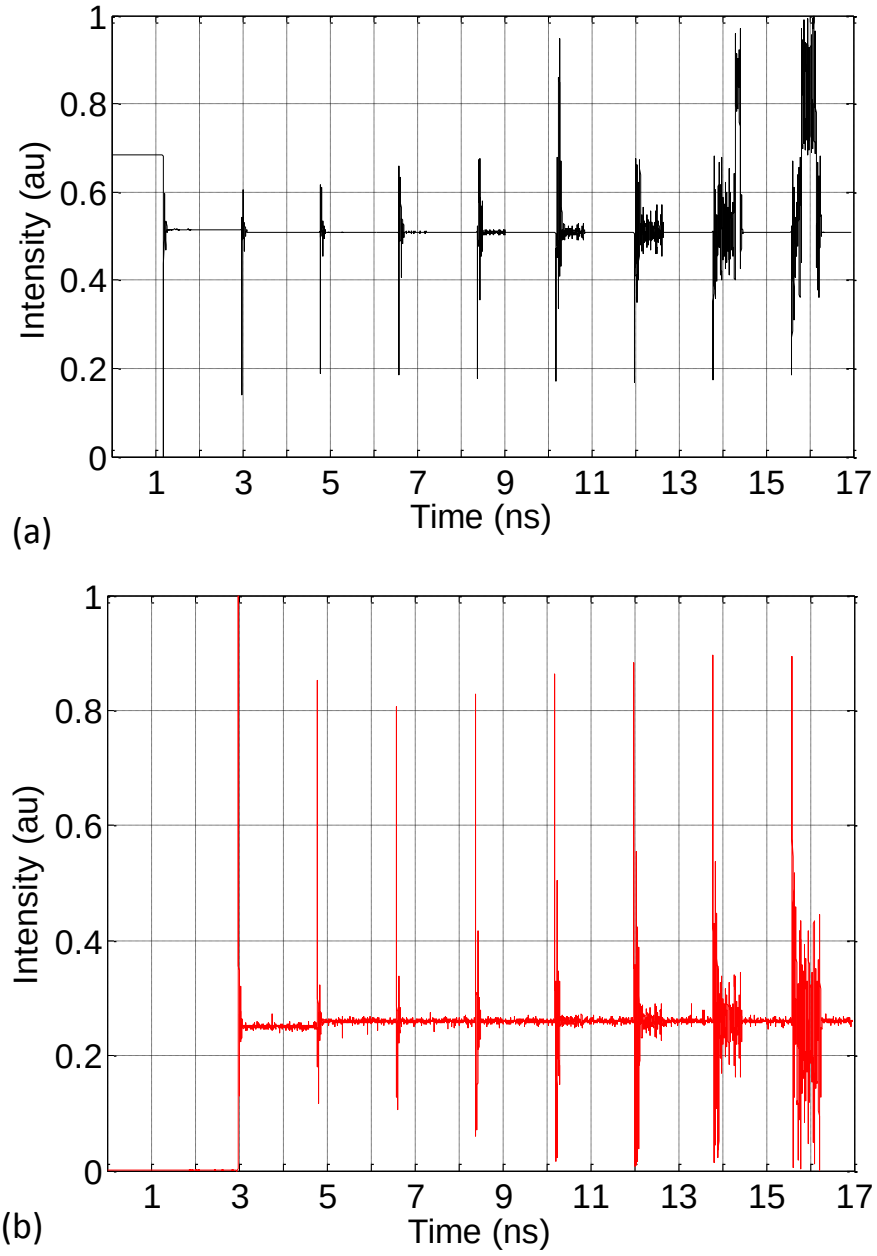

Figure 6-16: Tim series of the XP and YP modes for 1 ns,(a) intensity of the XP mode, (b) intensity of the YP mode.

In Fig. 6-17, for a weak OF where the feedback coefficient k = 1.188×10^{10} ns^{-1}, which is about -30 dB, the results show poor chaotic dynamics synchronization between the orthogonal polarization modes, XP and YP modes. Fig. 6-17(a) and (b) display the intensity of the XP and YP modes, respectively in the time domain. The intensity of both modes is almost steady and no chaotic synchronization is observed, as the trajectory attractor and the correlation plots show in Figs. 6-17(c) and (d), respectively. The feedback coefficient strength plays a role and significantly changes the dynamics of the polarization modes as the next results demonstrate. At higher values of k the output power of the VCSEL becomes chaotic and agrees with the experiment finding that was presented in section 6.5 when a strong OF at 90^{o} of θ_p was applied.

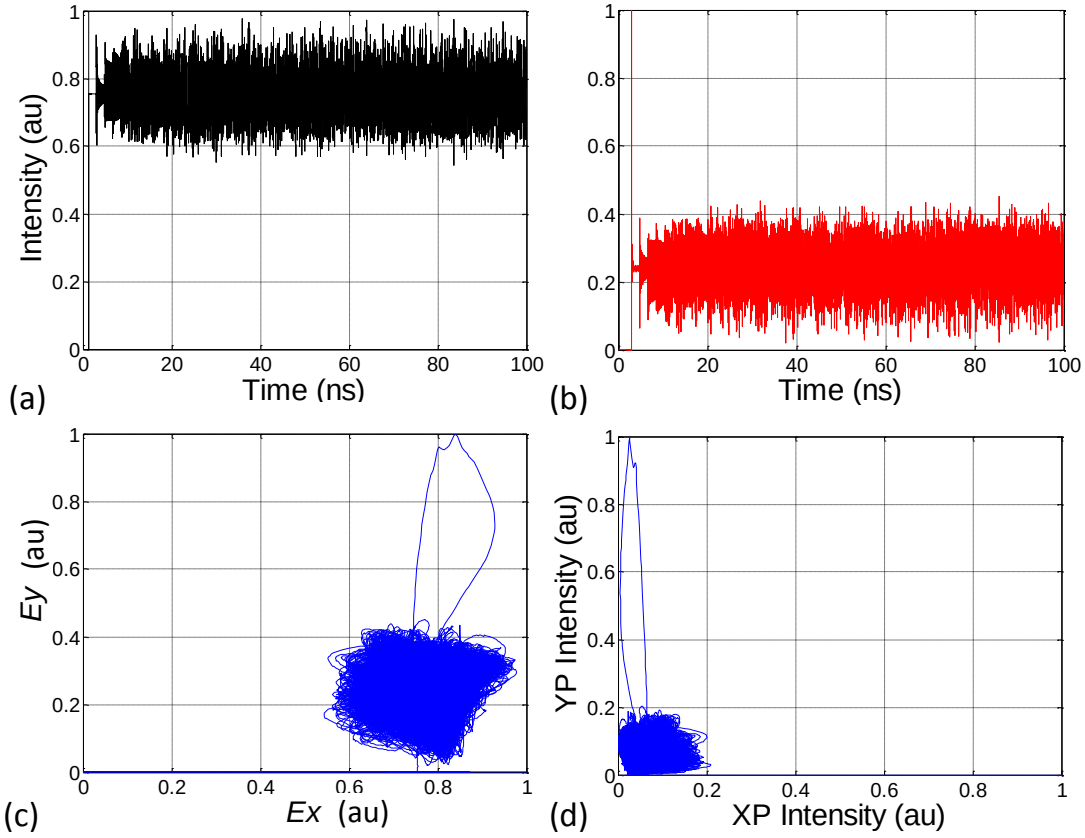

Figure 6-17: (a) and (b) the polarization intensity for the XP and YP modes, respectively with the feedback coefficient k of 1.18×10^{10} at θ_p=90, (c) and (d) the trajectory attractor and correlation plot of the polarization modes, respectively.

For k =1.60×10^{11} ns^{-1}, which is equivalent to -7.4 dB similar to the that used in the experiment in section 6-5 of this chapter, the chaotic dynamics are clearly observed, which is in line with the experiment observations. Fig 6-18 demonstrated the chaotic dynamics in both modes oscillation of the XP and YP with a strong OF level at θ_p= 90^o. Obviously VCSEL lases in random jumps between the XP and YP modes as observed in the experiment. Figs. 6-18 (a) and (b) show the polarization resolved intensity of the XP and YP modes, respectively. The polarization OF induces polarization mode hopping in the output modes intensities of the VCSEL.

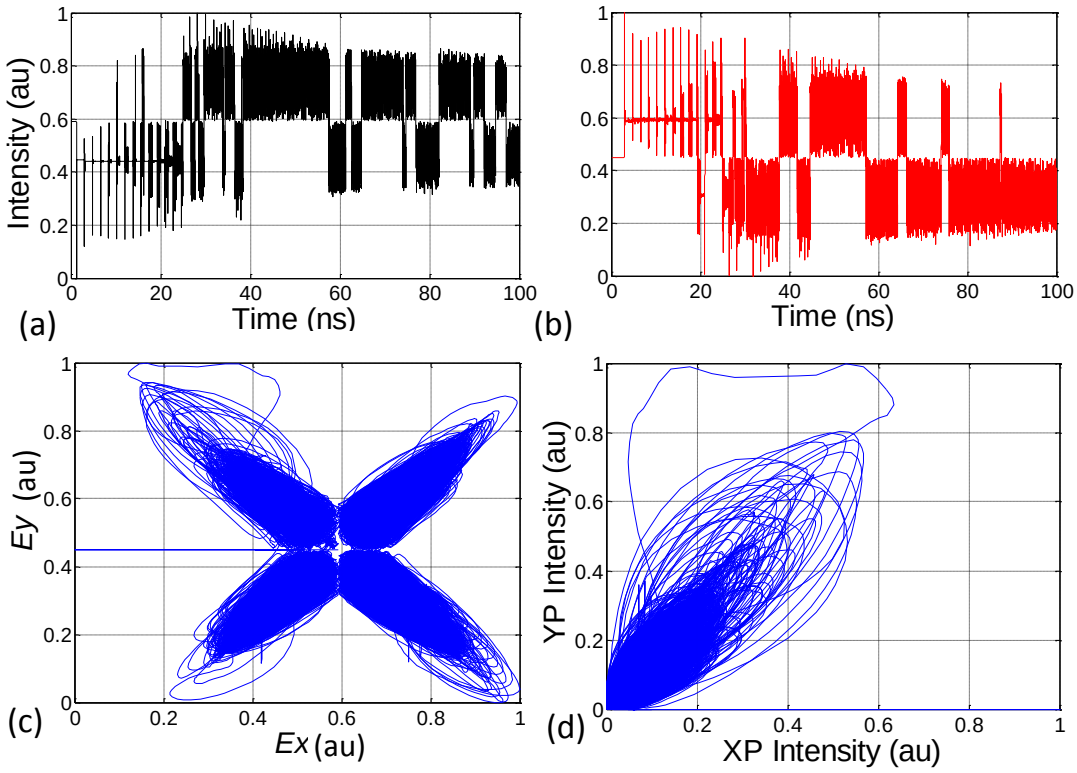

Figure 6-18: (a) and (b) the polarization mode hopping intensity for the XP and YP modes, respectively with optical feedback of 1.60×10^{11} at θ_p=90^o, (c) and (d) the trajectory attractor and correlation plot of the polarization modes, respectively.

The trajectory attractor in Fig. 6-18 (c) and the correlation plot in Fig. 6-18(d) show that the polarization modes are in a good synchronization dynamic. Fig 6-18(d) shows the in-phase synchronization dynamics, which is the inverse of the experiment results,

because of in the numerical model the absolute values were used to display the results. The polarization modes chaotic dynamics of VCSEL are highly dependent on the OF level and variable angle of θ_p as demonstrated in sections 6.2, 6.3 and 6.4. Figs. 6-19(a) and (b) display the polarization intensity modes of the XP and YP modes respectively, with the trajectory attractor in Fig. 6-19(c) and the correlation plot in Fig. 6-19(d). For a strong value of k of 1.60×10^{11} ns^{-1} at θ_p= 0^o the VCSEL emit only the XP mode with very fast oscillation while the YP mode is entirely suppressed.

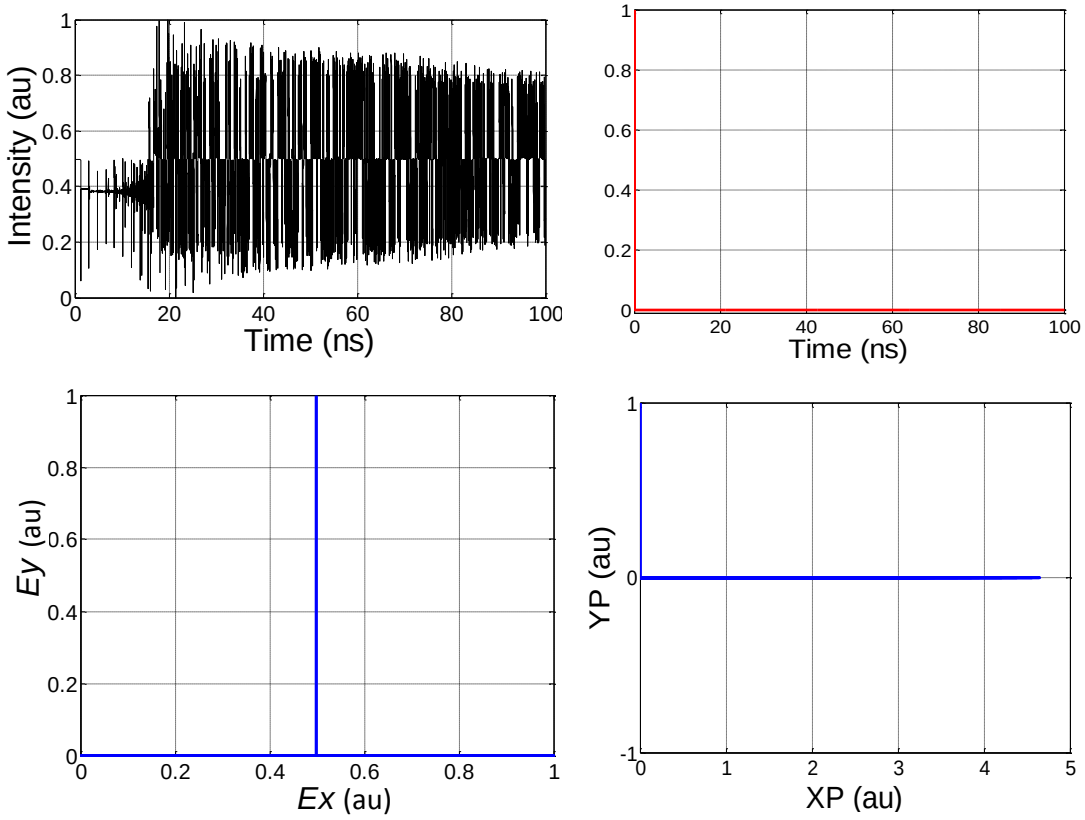

Figure 6-19: (a) and (b) the polarization intensity of the XP and YP modes respectively with a feedback coefficient of 1.60×10^{11} at $\theta_p=0^o$, (c) and (d) the trajectory attractor and correlation plot of the polarization modes, respectively.

This is because of the YP mode gets zero feedback at zero angle of θ_p. The results obtained from the Simulink model are consistent with the experimental results of the chaos synchronization of VCSEL with VPOF that were presented in this chapter. In the Simulink model, chaotic dynamics appear with the XP mode oscillation at a higher level

of OF equivalent to the experiment feedback level of -7.4 dB. However, the YP mode oscillation is completely supressed and therefore no correlation dynamic appear between the XP and YP modes as show in Fig 6-19(d). These behaviours are depending on the rotating of θ_p, where a good correlation between the two modes is obtained at a higher value of θ_p (i.e., 90^o) similar to the experiment finding.

6.6.2 Simulink Blocks Diagrams

The main block diagram of the Simulink model of the laser diode is shown in Fig. 6-20. The model permits to study the VCSEL properties with the OF for a range of θ_p. The model is described by the rate equations (2.18) - (2.23), which describe the carrier density, photon density and optical phase of the laser with OF effect. No noise is considered in the simulation model, and all the parameters adopted are given in Table 4-1. In the simulation model the parameters of the feedback strength and θ_p from the main block, K_d and THETA as shown in the main block diagram can be changed externally. Each block contains dynamics of the VSCEL, which describes each elements of the rate equations, namely *Ex*(t), *Phi_x*(t), *N*(t), *Ey*(t), *Gx*(t), *Phi_y*(t) and *Gy*(t) as described by Equations (2.18) - (2.23).

More precisely, the following blocks diagrams in Figs. 6.21 to 6.27 describing every elements of the rate equations in order to analyze the system dynamics along the propagation direction of the polarization modes using the Simulink model. The Simulink blocks enable to construct the equations describing the polarization properties of VCSEL. Figs. 6.21 and 6.24 show the dynamic model of the electric field of the XP and YP modes, respectively. The temporal electric field for the XP and YP modes in the laser cavity are showed in Figs. 6-16(a,c), 6-17(a,c), 6-18(a,c) and 6-19(a,c).

The carrier density distribution and analysis of the dynamic system inside the VCSEL cavity in the time domains is shown in Fig. 6.15(a). The block diagram in Fig. 6.23

depicts the carrier density calculation based on Equation 2.22. The Simulink blocks parameters are interconnected mathematically to represent the whole systems dynamics. The gain effect of the both polarization modes, which is inserted in the main Simulink program (yellow blocks for the XP and YP modes), is determined from Equation 2.3 combined with Equations 2.18 and 2.19.

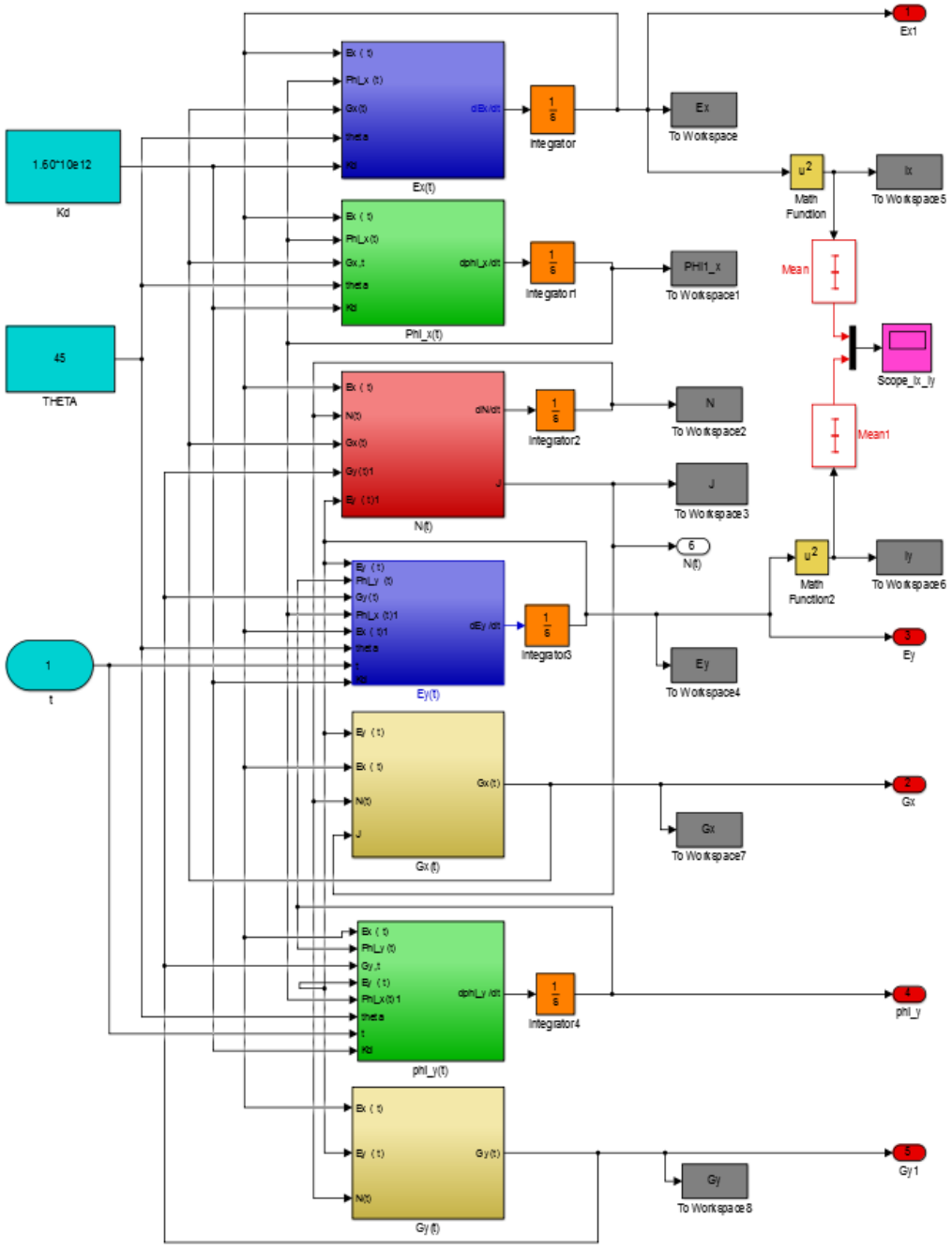

Figure 6-20: The main Simulink block diagram of the VCSEL with the optical feedback.

The procedure of calculating the gain quantities of the polarization modes of the VCSEL are shows in Simulink blocks in Figs 6-25 and 6-27 for the XP and YP modes, respectively and the gain profile is displayed in Fig. 6-15.

The phase effect for both XP and YP modes are simulated using Equations 2.20 and 2.21 and the schematic blocks diagrams in Figs 6.22 and 6.26, respectively. The model is realized using Simulink together with MATLAB, which are connected by Workspace blocks as shown in the main diagram in order to obtain and plot the measured data in a chart form for each parameter.

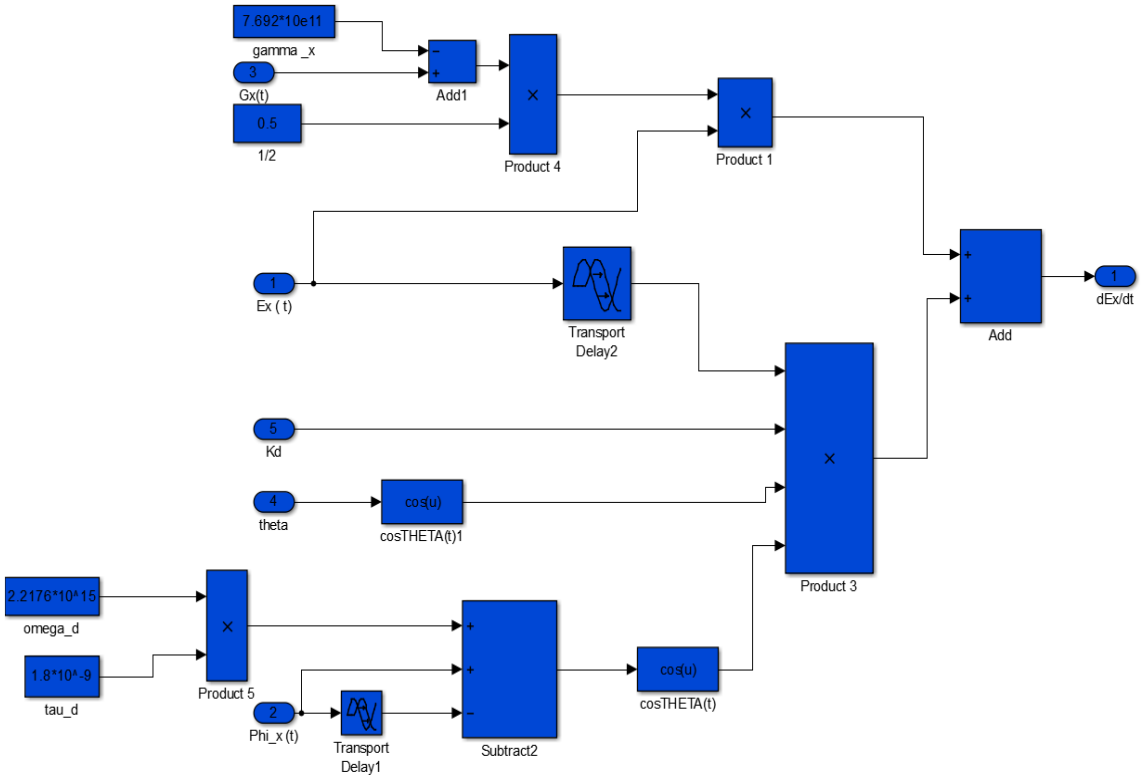

Figure 6-21: Simulink block diagram to determine the electric field of the XP mode.

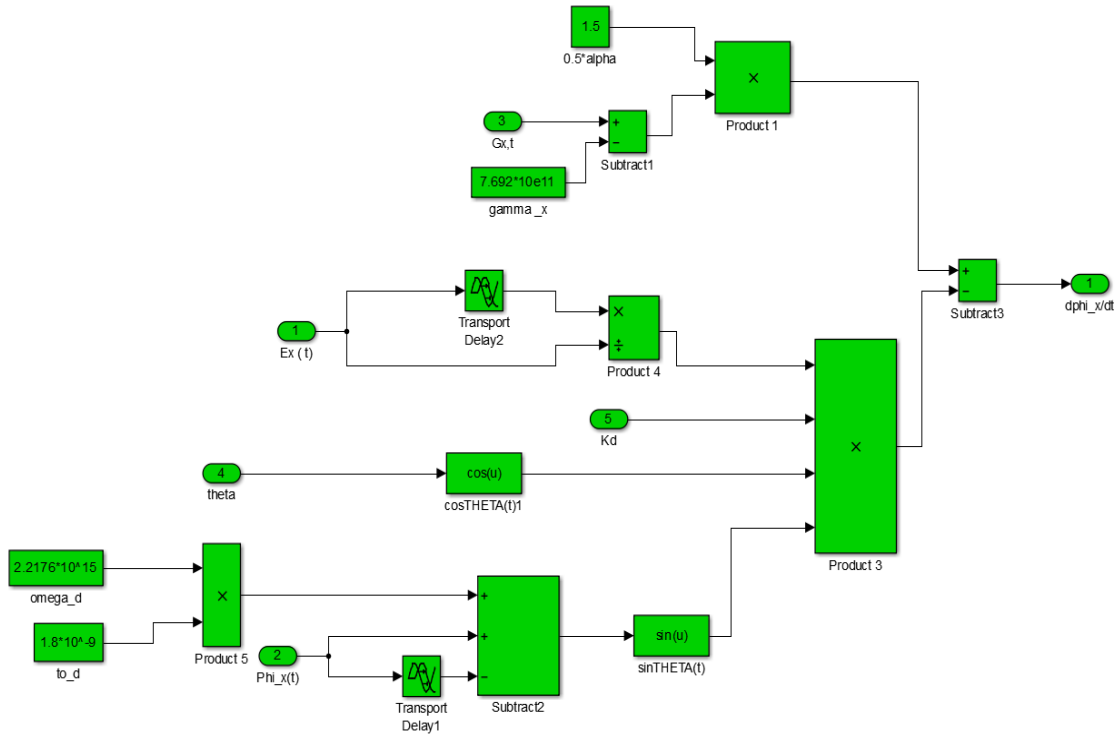

Figure 6-22: Simulink block diagram to determine the phase of the XP mode.

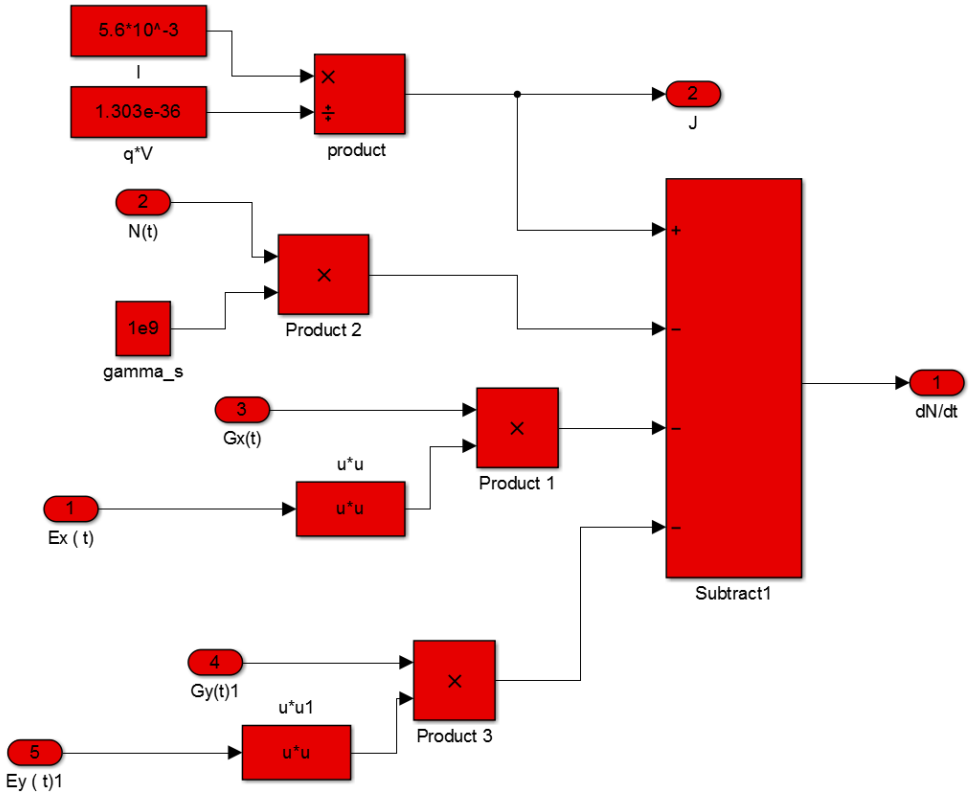

Figure 6-23: Simulink block diagram to determine the carrier density.

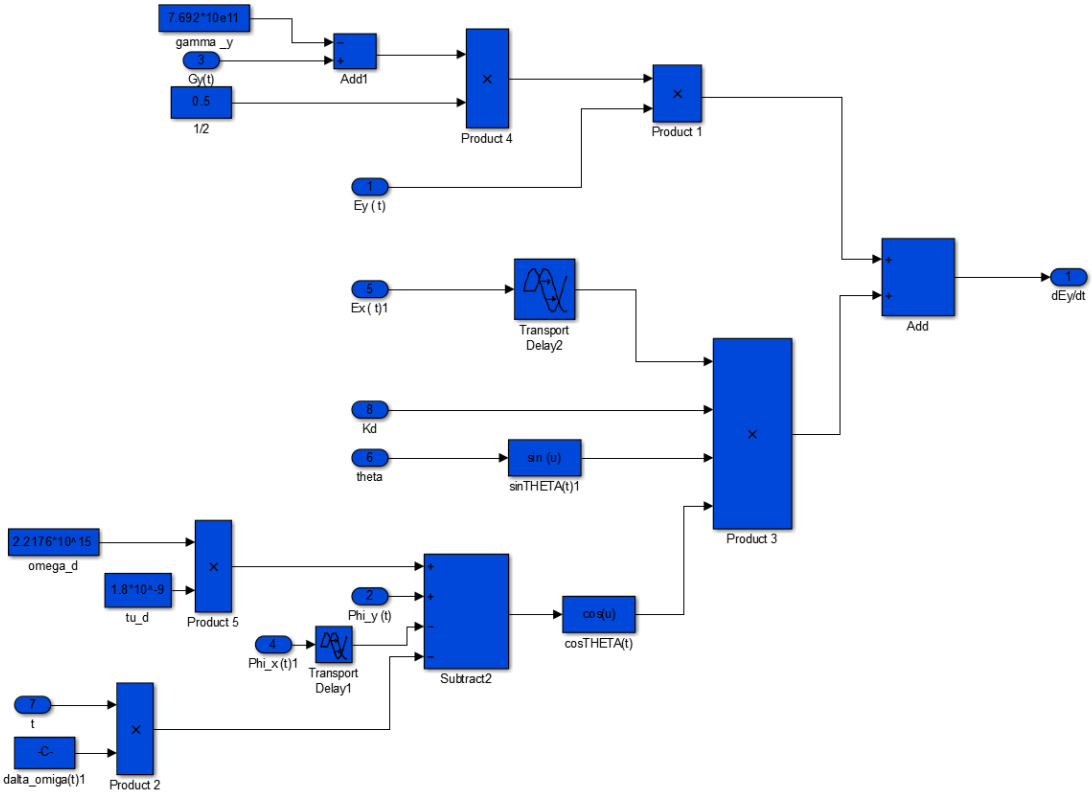

Figure 6-24: Simulink block diagram to determine the electric field of the YP mode.

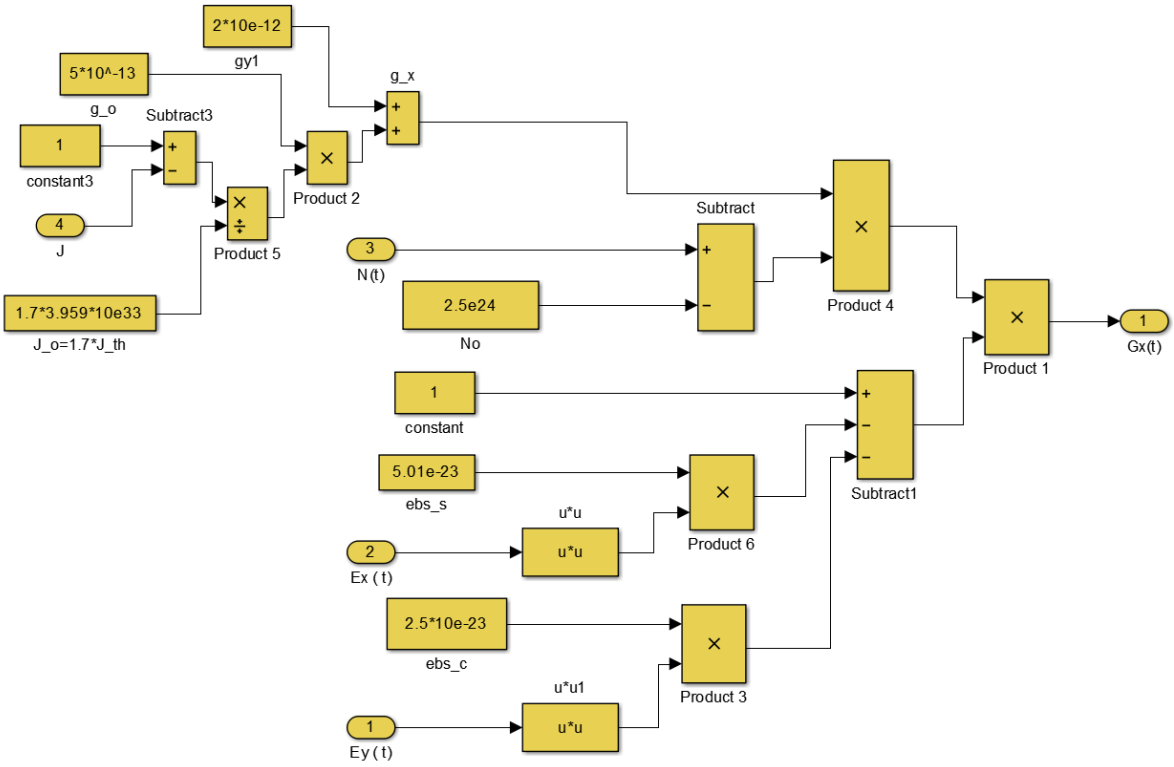

Figure 6-25: Simulink block diagram to determine the gain of the XP mode.

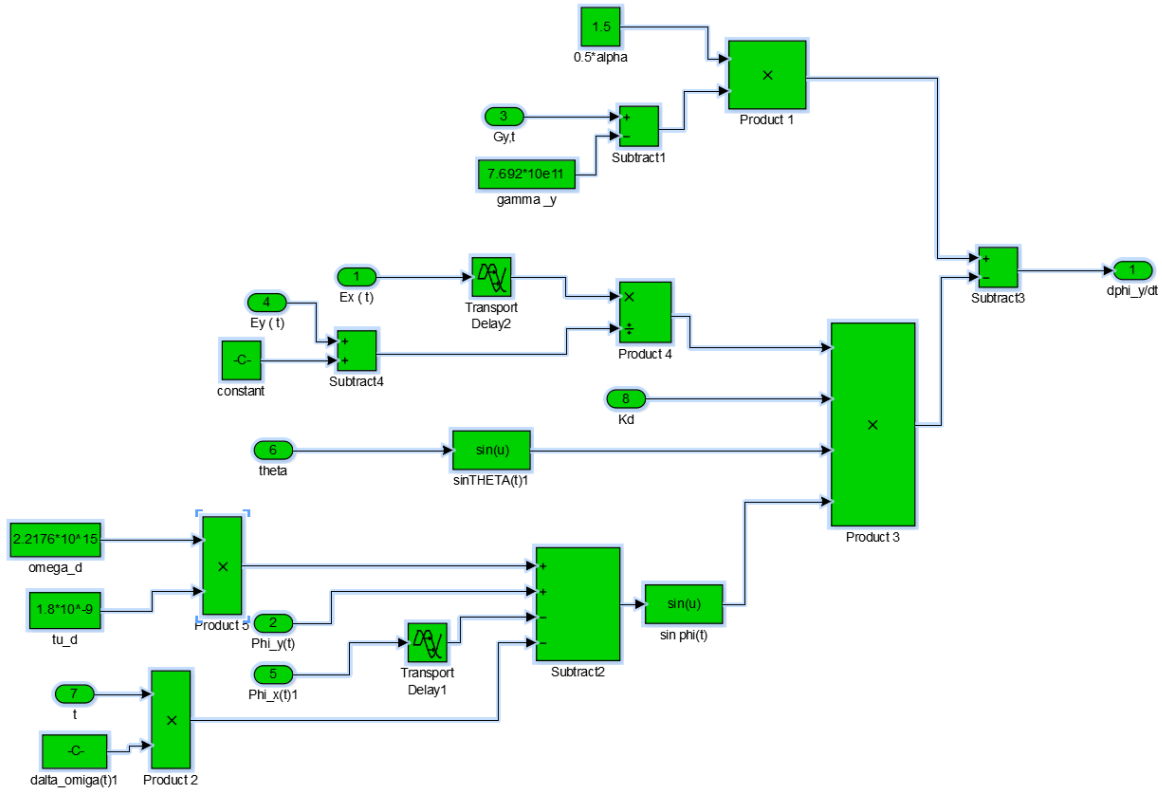

Figure 6-26: Simulink block diagram to determine the phase of the YP mode.

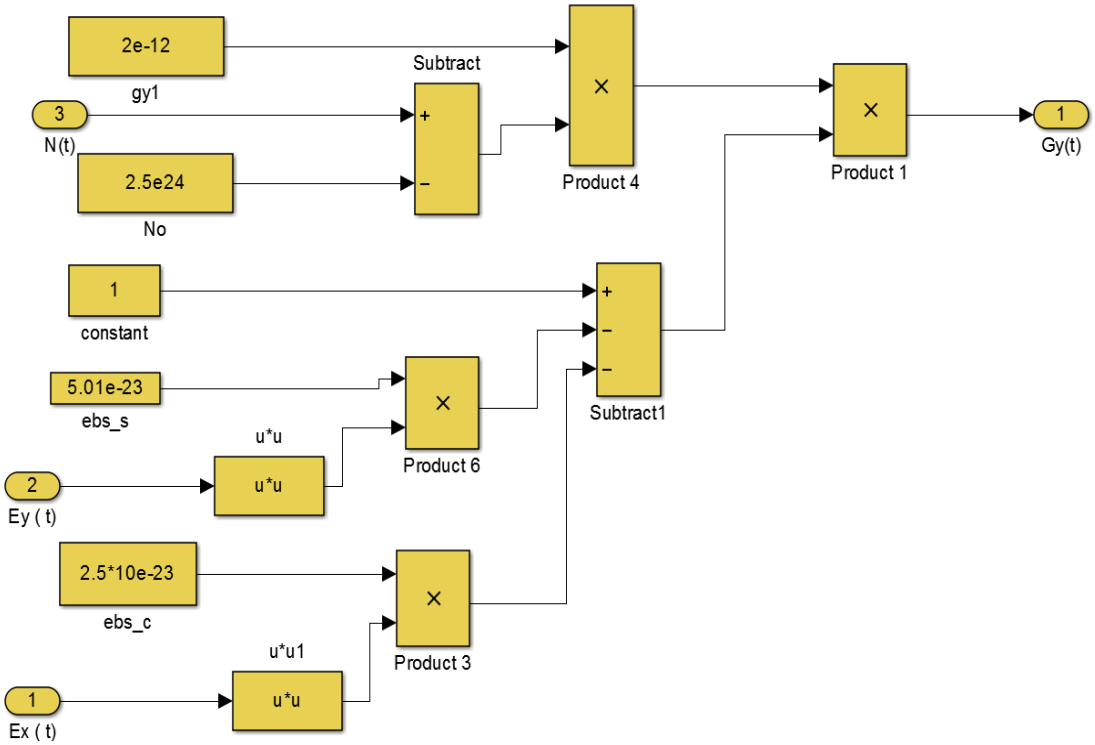

Figure 6-27: Simulink block diagram to determine the gain of the YP mode.

6.7 Conclusions

The possibility of high-quality anti-phase chaotic synchronization between the two polarization modes of VCSEL under rotated-polarization preserved OF (RPPOF) have been experimentally demonstrated when varying the OF level. The time series of the XP and YP modes showed a good anti-phase chaotic oscillation for different values of θ_p. The anti-phase chaotic synchronization gradually increased with θ_p. With rotating θ_p the VCSEL showed abrupt PS at 65^o, which led to suppressed the dominant mode (XP) with 0.004 mW output power and the YP mode was dominant with high output power of 0.32 mW. A perfect anti-phase synchronization dynamic was possible with a wide range of $\theta_p > 65^o$. A perfect chaotic synchronization dynamic with higher values of correlation coefficient $C_{x,y}$ of -0.99 was observed at $\theta_p = 90^o$ under high level of OF (-7.4 dB). Furthermore, with increased θ_p the probability of achieving high quality of ant-phase chaotic synchronization was increased and it was obtained at lower value of the feedback level.

The chaotic synchronization dynamics of VCSEL under selective OF with rotating θ_p were also experimentally demonstrated. With parallel-POF and under a high level of OF (-7 dB), the time series of the XP and YP modes showed a good anti-phase chaotic oscillation for different θ_p. When θ_p increased from 0^o to 30^o $C_{x,y}$ was slightly reduced, while it increased for θ_p in the range of 30^o - 90^o reaching the highest value of 0.982 at $\theta_p = 90^o$ with a zero time delay between the polarization modes. For both investigations, RPPOF and Parallel-POF, a perfect anti-phase synchronization was obtained over a wide range of the OF levels and θ_p beyond 65^o and 45^o, respectively. The strong anti-phase dynamics in VCSEL could be increase the anti-phase synchronization of the chaos. A clear relationship is found between $C_{x,y}$ and θ_p, where

the $C_{x,y}$ values increased with increased θ_p. The OF and θ_p play a significant role in the chaos synchronization of VCSEL. As a result, VCSEL with VPOF can be used as a chaotic light source for the synchronization of communication systems.

Furthermore, a complex dynamics between the XP and YP modes were existed with high feedback levels of -7.4 dB and VPOF. Fast PS and mode hopping were observed between the polarizations modes. This can be found over a wide range of θ_p beyond 45 ^{o}, which attributed to the mode competition inside the cavity of the VCSEL.

The Simulink model was established to investigate the polarization dynamics of VCSEL. The time period of the Simulink was several orders longer than 1.8 ns, which is the magnitude of the feedback delay, to clearly display the oscillatory behaviour of the XP and YP in this region. The trajectory attractor and correlation function were employed to verify the experiment results of chaotic and synchronization dynamics. Similar finding of the experimental measurements were demonstrated numerically, where the chaotic dynamics of the XP and YP modes were observed with VPOF under high OF level. The chaotic dynamic synchronization and polarization mode hopping also clearly observed between the VCSEL polarization modes with VPOF at the same OF level of the experiment (-7.4 dB). The numerical measurements were in good agreement with the experimental finding to describe the polarization dynamics of VCSEL under VPOF.

Chapter 7

Conclusions and Future Work

7.1 Conclusions

This thesis focused on the polarization properties of VCSEL subject to optical feedback (OF) mechanism for FSO communications. Considerable emphasis has been given to the influence of variable polarization optical feedback (VPOF) of the external cavity semiconductor laser on the polarization modes properties of VCSEL. The experimental and theoretical works devoted to study and expand understanding of the flowing aspects; L-I characteristics, PS, RIN and hysteresis loop of the polarization modes. Further investigations were carried out focusing on the following aspects of the polarization modes properties; PS properties, RIN, nonlinearity behaviours and chaotic dynamics with the modulation signal and VPOF effects. On the other hand, with the view of practical deployment of VCSEL in FSO, chaotic dynamics Synchronization of polarization modes of VCSEL received more attention in this work. In this thesis, it was shown that variable polarization angle (θ_p) of OF, which used as an experimentally adjustable parameter, leads to control the polarization modes properties and created a complex dynamics in VCSEL.

In Chapter 3, it was illustrated that the threshold current I_{th} of VCSEL can be reduced by 11.5% under the orthogonal polarization OF. VPOF significantly affected the bi-stability properties of the polarization modes, where the OF level greater than -8 dB induced hysteresis cycles beyond θ_p of 45^o. The hysteresis width reduced from 11.6^o and 11.7^o for the XP and YP modes to 10.4^o and 10.2^o, respectively when the OF level increased from -8.3 dB to -6.4 dB. Furthermore, the results showed that the orthogonal

polarization OF imposed the laser to emit in a certain polarization mode and increased the polarization selectivity of the VCSEL. While the parallel polarization OF enhanced the corresponding polarization mode of the VCSEL.

In Chapter 4, PS proprieties of two different VCSELs devices were theoretically and experimentally investigated. It was found that the PS occurred at higher values of θ_p ($> 45^o$) and the laser favoured emitting of the suppressed polarization mode. Moreover, PS was observed between the VCSEL polarization modes for a fixed I_b of 3.2, 5.2 and 5.8 mA and strong feedback level with VPOF. While with the modulation signal and OF, the PS point shifted to higher θ_p values compared with no modulation signal. Interestingly, it was shown that both the frequency modulation f_m (200 MHz) and modulation depth M_d (78.66%) limited the effect of the OF on the PS properties of VCSEL. The PS position dropped back to lower values of $\theta_p$when the I_b increased from 3.2 mA to 5.2 mA.

In Chapter 5, a novel OF method based on T-shaped polarization OF was proposed to suppress the nonlinear behaviours of the polarization modes of VCSEL with the modulation signal. The irregular dynamics of the polarization modes with the modulation signal f_m of 240 and 100 MHz were drastically modified using orthogonal OF (OOF). For the OOF, the HD decreased by 23, 20 and 12 dB for the 2^{nd}, 3^{rd} and 4^{th} harmonics, respectively and the spectrum peaks of the polarization modes were completely suppressed to the noise floor. However, when using the counterpart (parallel) polarization feedback (POF) the HD and the spectrum peaks of the 2^{nd}, 3^{rd} and 4^{th} harmonics enhanced by 2,11 and 9 dB, respectively . In addition, it was shown that HD is also influenced by variation of the operating temperature and I_b.The RIN characteristics were also depending on the polarization instability of VCSEL, where the relaxation oscillations were damped at higher feedback levels. Furthermore, the RIN

levels were higher for the XP and YP mode with the OF and modulation signal by 17 dB and 19 dB, respectively than the case with no modulation signal.

In Chapter 6 of this work, obtained high-quality anti-phase chaos synchronization, which was coincided with zero time delay an optimal operating condition was identified in order to, of the polarization modes. The anti-phase chaotic synchronization gradually increased with θ_p. A high level of the anti-phase synchronization dynamic was possible with a wide range of the OF levels more than - 18 dB for the angle of $\theta_p > 65^o$.

As far as we know this is the first experimental work reported with high quality of the anti-phase chaotic synchronization with $C_{x,y}$ of -0.99 and zero time delay between two signals oscillations of the VCSEL polarizations modes. Finally, Numerical model using Simulink was developed for the polarization resolved of VCSEL with VPOF using Lang-Kobayashi model of the external cavity semiconductor lasers. The numerical results have essentially verified the experiments findings of the PS position with the VPOF and the chaotic synchronization of the polarization modes of VCSEL at 90^o of θ_p under strong OF.

7.1 Future Work

This thesis reveals interesting lines of research for future work. The central interest are the nonlinearity improvement of the laser with OF and chaos generation using VCSEL with high quality synchronization dynamics.

The nonlinearity investigations were limited to 240 MHz frequency modulation due to experiment limitation. This work can be expanded to several GHz of the frequency modulation.

One further line of the research was hysteresis properties of VCSEL under VPOF. This investigation can be extended to use the following parameters; time delay and sweep rate of the polarization angle of OF to study their impacts on the hysteresis width.

Finally, chaos synchronization investigations of the VCSELs' polarization modes can be extended to include factors such as frequency detuning, optical phase effects, and coupling factor.

In this work, only the transmitter side of the communication system was investigated. VCSEL as an optical transmitter was investigated in the experimental work and the theoretical model. VPOF technique can be applied in the Simulink model for both transmitter (VCSEL1) and receiver sides (VCSEL2) to achieved chaotic synchronization signals for secure FSO systems.

References

[1] W. Popoola, "Subcarrier intensity modulated free-space optical communication systems," Northumbria University, 2009.

[2] S. G. Wilson, M. Brandt-Pearce, C. Qianling, and J. H. Leveque, III, "Free-Space Optical MIMO Transmission With Q-ary PPM," *Communications, IEEE Transactions on,* vol. 53, pp. 1402-1412, 2005.

[3] N. Cvijetic, S. G. Wilson, and M. Brandt-Pearce, "Performance bounds for free-space optical MIMO systems with APD receivers in atmospheric turbulence," *Selected Areas in Communications, IEEE Journal on,* vol. 26, pp. 3-12, 2008.

[4] R. S. G. a. L. A. Coldren, "Sub-milliamp threshold vertical cavity laser diodes," *Appl.Phys. Lett.,* vol. 16, pp. 1605-1607, 1991 1991.

[5] J. A. Tatum, A. Clark, J. K. Guenter, R. A. Hawthorne III, and R. H. Johnson, "Commercialization of Honeywell's VCSEL technology," in *Symposium on Integrated Optoelectronics*, International Society for Optics and Photonics, 2000, pp. 2-13.

[6] A. Mutig, *High speed VCSELs for optical interconnects*: Springer Science & Business Media, 2011.

[7] R. Yi, Y. Weijian, C. Chase, M. C. Y. Huang, D. D. P. Worland, S. Khaleghi, *et al.*, "Long-Wavelength VCSEL Using High-Contrast Grating," *Selected Topics in Quantum Electronics, IEEE Journal of,* vol. 19, pp. 1701311-1701311, 2013.

[8] A. Valle and L. Pesquera, "Theoretical calculation of relative intensity noise of multimode vertical-cavity surface-emitting lasers," *Quantum Electronics, IEEE Journal of,* vol. 40, pp. 597-606, 2004.

[9] S. Y. Xiang, W. Pan, B. Luo, L. S. Yan, X. H. Zou, N. Jiang, *et al.*, "Synchronization of unpredictability-enhanced chaos in VCSELs with variable-polarization optical feedback," *Quantum Electronics, IEEE Journal of,* vol. 47, pp. 1354-1361, 2011.

[10] J.-J. Chen, Z.-M. Wu, X. Tang, T. Deng, L. Fan, Z.-Q. Zhong, *et al.*, "Generation of polarization-resolved wideband unpredictability-enhanced chaotic signals based on vertical-cavity surface-emitting lasers subject to chaotic optical injection," *Optics express,* vol. 23, pp. 7173-7183, 2015.

[11] J. Liu, Z.-M. Wu, and G.-Q. Xia, "Dual-channel chaos synchronization and communication based on unidirectionally coupled VCSELs with polarization-rotated optical feedback and polarization-rotated optical injection," *Optics express,* vol. 17, pp. 12619-12626, 2009.

[12] Y. Hong, P. Spencer, and K. Shore, "Wideband Chaos with Time-Delay Concealment in Vertical-Cavity Surface-Emitting Lasers with Optical Feedback and Injection," *Quantum Electronics, IEEE Journal of* vol. 4, pp. 236-242, Apr 2014.

[13] M. Ozaki, H. Someya, T. Mihara, A. Uchida, S. Yoshimori, K. Panajotov, *et al.*, "Leader-laggard relationship of chaos synchronization in mutually coupled vertical-cavity surface-emitting lasers with time delay," *Physical Review E,* vol. 79, p. 026210, 2009.

[14] A. Uchida, H. Someya, M. Ozaki, K. Tanaka, S. Yoshimori, K. Panajotov, *et al.*, "Synchronization of chaos in mutually coupled vertical-cavity surface-emitting lasers with time delay," in *IEEE/LEOS Winter Topicals Meeting Series, 2009*, 2009, pp. 126-127.

[15] M. Sciamanna and K. Shore, "Physics and applications of laser diode chaos," *Nature Photonics,* vol. 9, pp. 151-162, 2015.

[16] Y. Hong, "Experimental study of time-delay signature of chaos in mutually coupled vertical-cavity surface-emitting lasers subject to polarization optical injection," *Optics express,* vol. 21, pp. 17894-17903, 2013.

[17] K. Iga, "Surface-emitting laser-its birth and generation of new optoelectronics field," *Selected Topics in Quantum Electronics, IEEE Journal of,* vol. 6, pp. 1201-1215, 2000.

[18] S. Yu, "Theoretical analysis of polarization bistability in vertical cavity surface emitting semiconductor lasers," *Lightwave Technology, Journal of,* vol. 15, pp. 1032-1041, 1997.

[19] J. Y. Law and G. P. Agrawal, "Effects of optical feedback on static and dynamic characteristics of vertical-cavity surface-emitting lasers," *Selected Topics in Quantum Electronics, IEEE Journal of,* vol. 3, pp. 353-358, 1997.

[20] M. Sciamanna and K. Panajotov, "Route to polarization switching induced by optical injection in vertical-cavity surface-emitting lasers," *Physical Review A,* vol. 73, p. 023811, 2006.

[21] A. Uchida, *Optical communication with chaotic lasers: applications of nonlinear dynamics and synchronization*. Saitama,Japan: John Wiley & Sons, 2012.

[22] Z. Qin and S. Azouigui, *Analysis of coherence-collapse regime of semiconductor lasers under external optical feedback by perturbation method*. France: InTech, 2012.

[23] E. Kapon, *Semiconductor lasers I: fundamentals*. San Diego, USA: Academic Press, 1999.

[24] J. Ohtsubo, *Semiconductor lasers: stability, instability and chaos* vol. 111: Taylor & Francis, 2006.

[25] T. Heil, I. Fischer, W. Elsäßer, and A. Gavrielides, "Dynamics of semiconductor lasers subject to delayed optical feedback: The short cavity regime," *Physical review letters,* vol. 87, p. 243901, 2001.

[26] M. C. Soriano, T. Berkvens, G. Van der Sande, G. Verschaffelt, J. Danckaert, and I. Fischer, "Interplay of current noise and delayed optical feedback on the dynamics of semiconductor lasers," *Quantum Electronics, IEEE Journal of,* vol. 47, pp. 368-374, 2011.

[27] Y. Chung and Y. Lee, "Spectral characteristics of vertical-cavity surface-emitting lasers with external optical feedback," *Photonics Technology Letters, IEEE,* vol. 3, pp. 597-599, 1991.

[28] P. Spencer, C. R. Mirasso, and K. A. Shore, "Effect of strong optical feedback on vertical-cavity surface-emitting lasers," *Photonics Technology Letters, IEEE,* vol. 10, pp. 191-193, 1998.

[29] S. Jiang, Z. Pan, M. Dagenais, R. A. Morgan, and K. Kojima, "Influence of external optical feedback on threshold and spectral characteristics of vertical-cavity surface-emitting lasers," *Photonics Technology Letters, IEEE,* vol. 6, pp. 34-36, 1994.

[30] K. I. Kallimani and M. J. O'Mahony, "Relative intensity noise for laser diodes with arbitrary amounts of optical feedback," *Quantum Electronics, IEEE Journal of,* vol. 34, pp. 1438-1446, 1998.

[31] J. Wang and K. Petermann, "Small signal analysis for dispersive optical fiber communication systems," *Lightwave Technology, Journal of,* vol. 10, pp. 96-100, 1992.

[32] L. A. Coldren, S. W. Corzine, and M. L. Mashanovitch, *Diode lasers and photonic integrated circuits* vol. 218: Wiley. com, 2012.

[33] H. Keang-Po, J. D. Walker, and J. M. Kahn, "External optical feedback effects on intensity noise of vertical-cavity surface-emitting lasers," *Photonics Technology Letters, IEEE,* vol. 5, pp. 892-895, 1993.

[34] H. K. Hisham, A. F. Abas, G. A. Mahdiraji, M. A. Mahdi, and A. M. Noor, "Relative intensity noise reduction by optimizing fiber grating Fabry–Perot laser parameters," *Quantum Electronics, IEEE Journal of,* vol. 48, pp. 375-383, 2012.

[35] T. Heil, A. Uchida, P. Davis, and T. Aida, "TE-TM dynamics in a semiconductor laser subject to polarization-rotated optical feedback," *Physical Review A,* vol. 68, p. 033811, 2003.

[36] G. Dudzik and J. Rzepka, "Polarization axis fluctuations in a single mode VCSEL laser at 780nm," *Photonics Letters of Poland,* vol. 5, pp. pp. 94-96, 2013.

[37] J. Albert, K. P. Panajotov, G. Verschaffelt, B. Nagler, H. Thienpont, I. P. Veretennicoff, *et al.*, "Polarization switching dynamics in single-mode VCSELs," in *Symposium on Integrated Optics*, 2001, pp. 34-43.

[38] M. Sondermann, M. Weinkath, and T. Ackemann, "Polarization switching to the gain disfavored mode in vertical-cavity surface-emitting lasers," *Quantum Electronics, IEEE Journal of,* vol. 40, pp. 97-104, 2004.

[39] S. Xiang, W. Pan, L. Yan, B. Luo, N. Jiang, and L. Yang, "Polarization properties of vertical-cavity surface-emitting lasers subject to feedback with variably rotated polarization angle," *Applied optics,* vol. 48, pp. 5176-5183, 2009.

[40] S. Xiang, W. Pan, L. Yan, B. Luo, X. Zou, N. Jiang, *et al.*, "Variable-polarization optical feedback induced hysteresis of the polarization switching in vertical-cavity surface-emitting lasers," *JOSA B,* vol. 27, pp. 2512-2517, 2010.

[41] S. Y. Xiang, W. Pan, B. Luo, L. S. Yan, X. H. Zou, and N. Q. Li, "Influence of Variable-Polarization Optical Feedback on Polarization Switching Properties of Mutually Coupled VCSELs," *Selected Topics in Quantum Electronics, IEEE Journal of,* vol. 19, pp. 1700108-1700108, 2013.

[42] Y. O. Takeuchi, Junji; Shogenji, Rui, "Chaotic dynamics in semiconductor lasers subjected to polarization-rotated optical feedback," *Applied Physics Letters,* vol. 93, pp. 181105-181105, 2008-11-04 2008.

[43] K. Panajotov, M. Sciamanna, I. Gatare, M. Arteaga, and H. Thienpont, "Nonlinear dynamics of vertical-cavity surface-emitting lasers," *Advances in Optical Technologies,* vol. 2011, pp. 1-16, 2011.

[44] J. Kaiser, C. Degen, and W. Elsässer, "Polarization-switching influence on the intensity noise of vertical-cavity surface-emitting lasers," *JOSA B,* vol. 19, pp. 672-677, 2002.

[45] H. Nihei and A. Okamoto, "Photonic crystal systems for high-speed optical memory device on an atomic scale," in *Optical Engineering for Sensing and Nanotechnology (ICOSN'01)*, 2001, pp. 470-473.

[46] H. Kawaguchi, "Polarization-bistable vertical-cavity surface-emitting lasers: application for optical bit memory," *Opto-Electronics Review,* vol. 17, pp. 265-274, 2009.

[47] S. Benedetto, R. Gaudino, and P. Poggiolini, "Direct detection of optical digital transmission based on polarization shift keying modulation," *Selected Areas in Communications, IEEE Journal on,* vol. 13, pp. 531-542, 1995.

[48] J. Grosinger, *Investigation of polarization modulation in optical free space communications through the atmosphere*. Technischen UniversitÄat Wien FakultÄat fÄur Elektrotechnik und Informationstechnik: na, 2008.

[49] T. Yang, "A survey of chaotic secure communication systems," *International Journal of Computational Cognition,* vol. 2, pp. 81-130, 2004.

[50] G. Ribordy, J. Brendel, J.-D. Gautier, N. Gisin, and H. Zbinden, "Long-distance entanglement-based quantum key distribution," *Physical Review A,* vol. 63, p. 012309, 2000.

[51] I. J. Cox, J. Kilian, F. T. Leighton, and T. Shamoon, "Secure spread spectrum watermarking for multimedia," *Image Processing, IEEE Transactions on,* vol. 6, pp. 1673-1687, 1997.

[52] H. Yanhua, J. Rui, P. S. Spencer, and K. A. Shore, "Investigation of polarization bistability in vertical-cavity surface-emitting lasers subjected to optical feedback," *Quantum Electronics, IEEE Journal of,* vol. 41, pp. 619-624, 2005.

[53] D. Parekh, "Optical Injection Locking of Vertical Cavity Surface-Emitting Lasers: Digital and Analog Applications," 2012.

[54] A. Valle and L. Pesquera, "Relative intensity noise of multitransverse-mode vertical-cavity surface-emitting lasers," *Photonics Technology Letters, IEEE,* vol. 13, pp. 272-274, 2001.

[55] K.-P. Ho, J. D. Walker, and J. M. Kahn, "External optical feedback effects on intensity noise of vertical-cavity surface-emitting lasers," *Photonics Technology Letters, IEEE,* vol. 5, pp. 892-895, 1993.

[56] Y. Hong, J. Paul, P. S. Spencer, and K. A. Shore, "The effects of polarization-resolved optical feedback on the relative intensity noise and polarization stability of vertical-cavity surface-emitting lasers," *Journal of Lightwave Technology,* vol. 24, pp. 3210-3216, 2006.

[57] S. Nazhan, Z. Ghassemlooy, K. Busawon, and J. Perez, "Hysteresis properties induced by variable polarization angle in the polarization switching of VCSELs," in *Communication Systems, Networks & Digital Signal Processing (CSNDSP), 2014 9th International Symposium on*, 2014, pp. 325-329.

[58] S. Nazhan, Z. Ghassemlooy, K. Busawon, and A. Gholami, "Investigation of polarization switching of VCSEL subject to intensity modulated and optical feedback," *Optics & Laser Technology,* vol. 75, pp. 240-245, 2015.

[59] S. Nazhan, Z. Ghassemlooy, K. Busawon, and A. Gholami, "Suppressing the Nonlinearity of Free Running VCSEL Using Selective-Optical Feedback," *Photonics Technology Letters, IEEE,* vol. 28, pp. 185-188, 2016.

[60] S. Nazhan, Z. Ghassemlooy, and K. Busawon, "Harmonic distortion dependent on optical feedback, temperature and injection current in a vertical cavity surface emitting laser," *Journal of Physics D: Applied Physics,* vol. 49, p. 145107, 2016.

[61] S. N. Ahmed, Z. Ghassemlooy, K. Busawon, and S. Zvanovec, "Relative intensity noise of vertical-cavity surface-emitting lasers subject to variable polarization-optical feedback," in *Optical Wireless Communications (IWOW), 2014 3rd International Workshop in*, 2014, pp. 21-24.

[62] S. Nazhan, Z. Ghassemlooy, K. Busawon, and J. Perez, "Polarization RIN of VCSEL subject to modulation signal with variable polarization angle of optical feedback," in *Optical Wireless Communications (IWOW), 2015 4th International Workshop on*, 2015, pp. 65-68.

[63] S. Nazhan, Z. Ghassemlooy, and K. Busawon, "Chaos synchronization in vertical-cavity surface-emitting laser based on rotated polarization-preserved optical feedback," *Chaos: An Interdisciplinary Journal of Nonlinear Science,* vol. 26, p. 013109, 2016.

[64] S. Nazhan, Z. Ghassemlooy, K. Busawon, and A. Gholami, "Variable-polarization optical feedback induced high-quality polarization-resolved chaos synchronization in VCSEL," in *Science and Information Conference (SAI), 2015*, 2015, pp. 1052-1055.

[65] A. K. Majumdar, *Advanced Free Space Optics (FSO): A Systems Approach* vol. 186: Springer, 2014.

[66] W. Jin-Yuan, W. Jun-Bo, C. Ming, T. Yang, and Z. Ying, "Outage Analysis for Relay-Aided Free-Space Optical Communications Over Turbulence Channels With Nonzero Boresight Pointing Errors," *Photonics Journal, IEEE,* vol. 6, pp. 1-15, 2014.

[67] A. M. Khalid, G. Cossu, R. Corsini, P. Choudhury, and E. Ciaramella, "1-Gb/s Transmission Over a Phosphorescent White LED by Using Rate-Adaptive Discrete Multitone Modulation," *Photonics Journal, IEEE,* vol. 4, pp. 1465-1473, 2012.

[68] H. Soda, K.-i. Iga, C. Kitahara, and Y. Suematsu, "GaInAsP/InP surface emitting injection lasers," *Japanese Journal of Applied Physics,* vol. 18, pp. 2329-2330, 1979.

[69] S. Bloom, E. Korevaar, J. Schuster, and H. Willebrand, "Understanding the performance of free-space optics [Invited]," *Journal of optical Networking,* vol. 2, pp. 178-200, 2003.

[70] R. Paudel, H. Le Minh, Z. Ghassemlooy, M. Iaz, and S. Rajbhandari, "High speed train communications systems using free space optics," *IET,* 2010.

[71] D. Huffaker, J. Shin, and D. Deppe, "Low threshold half-wave vertical-cavity lasers," *Electronics Letters,* vol. 30, pp. 1946-1947, 1994.

[72] F. H. Peters, M. L. Majewski, M. G. Peters, J. W. Scott, B. Thibeault, D. B. Young, *et al.*, "Vertical-cavity surface-emitting laser technology," in *OE/LASE'93: Optics, Electro-Optics, & Laser Applications in Science& Engineering*, 1993, pp. 122-127.

[73] A. Hayat, A. Bacou, A. Rissons, and J.-C. Mollier, *Optical Injection-Locking of VCSELs*. France: INTECH Open Access Publisher, 2010.

[74] J. Ohtsubo, "Chaos synchronization and chaotic signal masking in semiconductor lasers with optical feedback," *Quantum Electronics, IEEE Journal of,* vol. 38, pp. 1141-1154, 2002.

[75] Y. Hong, M. W. Lee, J. Paul, P. S. Spencer, and K. A. Shore, "GHz bandwidth message transmission using chaotic vertical-cavity surface-emitting lasers," *Journal of Lightwave Technology,* vol. 27, pp. 5099-5105, 2009.

[76] S. Y. Xiang, W. Pan, B. Luo, L. S. Yan, X. H. Zou, N. Jiang, *et al.*, "Message encoding/decoding using unpredictability-enhanced chaotic VCSELs," *Photonics Technology Letters, IEEE,* vol. 24, pp. 1267-1269, 2012.

[77] M. W. Lee, Y. Hong, and K. A. Shore, "Experimental demonstration of VCSEL-based chaotic optical communications," *Photonics Technology Letters, IEEE,* vol. 16, pp. 2392-2394, 2004.

[78] L. M. Pecora and T. L. Carroll, "Synchronization in chaotic systems," *Physical review letters,* vol. 64, pp. 821-824, 1990.

[79] N. Jiang, W. Pan, L. Yan, B. Luo, X. Zou, S. Xiang, *et al.*, "Multiaccess optical chaos communication using mutually coupled semiconductor lasers subjected to identical external injections," *Photonics Technology Letters, IEEE,* vol. 22, pp. 676-678, 2010.

[80] N. Shibasaki, A. Uchida, S. Yoshimori, and P. Davis, "Characteristics of chaos synchronization in semiconductor lasers subject to polarization-rotated optical feedback," *Quantum Electronics, IEEE Journal of,* vol. 42, pp. 342-350, 2006.

[81] D. W. Sukow, K. L. Blackburn, A. R. Spain, K. J. Babcock, J. V. Bennett, and A. Gavrielides, "Experimental synchronization of chaos in diode lasers with polarization-rotated feedback and injection," *Optics letters,* vol. 29, pp. 2393-2395, 2004.

[82] P. Spencer, C. R. Mirasso, P. Colet, and K. A. Shore, "Modeling of optical synchronization of chaotic external-cavity VCSELs," *Quantum Electronics, IEEE Journal of,* vol. 34, pp. 1673-1679, 1998.

[83] A. Scire, J. Mulet, C. R. Mirasso, J. Danckaert, and M. San Miguel, "Polarization message encoding through vectorial chaos synchronization in vertical-cavity surface-emitting lasers," *Physical review letters,* vol. 90, p. 113901, 2003.

[84] G.-Q. X. Z.-L. ZHANG, X.-D. LIN, Z.-M. WU*, "Comparison of closed-loop and open-loop in incoherent optical feedback chaos synchronization system," *OPTOELECTRONICS AND ADVANCED MATERIALS,* vol. 3, p. 5, 2009.

[85] S. Y. Xiang, W. Pan, L. S. Yan, B. Luo, X. H. Zou, N. Jiang, *et al.*, "Quantifying chaotic unpredictability of vertical-cavity surface-emitting lasers with polarized optical feedback via permutation entropy," *Selected Topics in Quantum Electronics, IEEE Journal of,* vol. 17, pp. 1212-1219, 2011.

[86] S. Takougang Kingni, J. Hervé Talla Mbé, and P. Woafo, "Semiconductor lasers driven by self-sustained chaotic electronic oscillators and applications to optical chaos cryptography," *Chaos: An Interdisciplinary Journal of Nonlinear Science,* vol. 22, pp. 033108-033108-8, 2012.

[87] Y. Hong, M. W. Lee, P. S. Spencer, and K. A. Shore, "Synchronization of chaos in unidirectionally coupled vertical-cavity surface-emitting semiconductor lasers," *Optics letters,* vol. 29, pp. 1215-1217, 2004.

[88] S. Priyadarshi, Y. Hong, I. Pierce, and K. A. Shore, "Experimental Investigations of Time-Delay Signature Concealment in Chaotic External Cavity VCSELs Subject to Variable Optical Polarization-Angle of Feedback," 2013.

[89] S. F. Yu, *Analysis and design of vertical cavity surface emitting lasers* vol. 7: John Wiley & Sons, 2003.

[90] I. Kenichi, "Vertical-cavity surface-emitting laser: its conception and evolution," *Jpn. J. Appl. Phys,* vol. 47, pp. 1-10, 2008.

[91] M. Ahmed, A. Bakry, M. S. Alghamdi, H. Dalir, and F. Koyama, "Enhancing the modulation bandwidth of VCSELs to the millimeter-waveband using strong transverse slow-light feedback," *Optics Express,* vol. 23, pp. 15365-15371, 2015.

[92] A. Boletti, P. Boffi, P. Martelli, M. Ferrario, and M. Martinelli, "Performance analysis of communication links based on VCSEL and silicon photonics technology for high-capacity data-intensive scenario," *Optics express,* vol. 23, pp. 1806-1815, 2015.

[93] Y. Hong, P. S. Spencer, and K. A. Shore, "Suppression of polarization switching in vertical-cavity surface-emitting lasers by use of optical feedback," *Optics letters,* vol. 29, pp. 2151-2153, 2004.

[94] K. D. Choquette, R. Schneider, K. L. Lear, and R. E. Leibenguth, "Gain-dependent polarization properties of vertical-cavity lasers," *Selected Topics in Quantum Electronics, IEEE Journal of,* vol. 1, pp. 661-666, 1995.

[95] J. M. Ostermann and R. Michalzik, "Polarization control of VCSELs," in *VCSELs*, ed: Springer, 2013, pp. 147-179.

[96] M. Wu, L. Buckman, G. Li, K. Lau, and C. Chang-Hasnain, "Polarization Induced Enhancement of Relative Intensity Noise and Modulation Distortion of Vertical Cavity Surface Emitting Lasers," in *Guided-Wave Optoelectronics*, ed: Springer, 1995, pp. 59-65.

[97] J.-W. Shi, C.-C. Chen, Y.-S. Wu, S.-H. Guol, C. Kuo, and Y.-J. Yang, "High-power and high-speed Zn-diffusion single fundamental-mode vertical-cavity surface-emitting lasers at 850-nm wavelength," *Photonics Technology Letters, IEEE,* vol. 20, pp. 1121-1123, 2008.

[98] J. Martin-Regalado, F. Prati, M. San Miguel, and N. Abraham, "Polarization properties of vertical-cavity surface-emitting lasers," *Quantum Electronics, IEEE Journal of,* vol. 33, pp. 765-783, 1997.

[99] K. Panajotov, B. Ryvkin, J. Danckaert, M. Peeters, H. Thienpont, and I. Veretennicoff, "Polarization switching in VCSEL's due to thermal lensing," *Photonics Technology Letters, IEEE,* vol. 10, pp. 6-8, 1998.

[100] J. Paul, C. Masoller, Y. Hong, P. S. Spencer, and K. Alan Shore, "Impact of orthogonal optical feedback on the polarization switching of vertical-cavity surface-emitting lasers," *JOSA B,* vol. 24, pp. 1987-1994, 2007.

[101] Z. G. Pan, S. Jiang, M. Dagenais, R. A. Morgan, K. Kojima, M. T. Asom, *et al.*, "Optical injection induced polarization bistability in vertical-cavity surface-emitting lasers," *Applied Physics Letters,* vol. 63, pp. 2999-3001, 1993.

[102] C. Masoller and N. Abraham, "Polarization dynamics in vertical-cavity surface-emitting lasers with optical feedback through a quarter-wave plate," *Applied Physics Letters,* vol. 74, pp. 1078-1080, 1999.

[103] X. F. Li, W. Pan, B. Luo, D. Ma, and G. Deng, "Static and dynamic characteristics of VCSELs with polarisation-selective optical feedback," *Optoelectronics, IEE Proceedings -,* vol. 153, pp. 67-74, 2006.

[104] D. V. Kuksenkov and H. Temkin, "Polarization related properties of vertical-cavity surface-emitting lasers," *Selected Topics in Quantum Electronics, IEEE Journal of,* vol. 3, pp. 390-395, 1997.

[105] A. Chavez-Pirson, H. Ando, H. Saito, and H. Kanbe, "Polarization properties of a vertical cavity surface emitting laser using a fractional layer superlattice gain medium," *Applied Physics Letters,* vol. 62, pp. 3082-3084, 1993.

[106] X. Li, W. Pan, B. Luo, D. Ma, and G. Deng, "Static and dynamic characteristics of VCSELs with polarisation-selective optical feedback," *IEE Proceedings-Optoelectronics,* vol. 153, pp. 67-74, 2006.

[107] M. Arteaga, M. Valencia, H. Thienpont, K. Panajotov, H. Unold, J. Ostermann, *et al.*, "Study of polarization properties of VCSELs subject to optical feedback from an extremely short external cavity," in *Lasers and Electro-Optics Europe, 2005. CLEO/Europe. 2005 Conference on*, 2005, p. 148.

[108] E. A. Viktorov and P. Mandel, "Low frequency fluctuations in a multimode semiconductor laser with optical feedback," *Physical review letters,* vol. 85, p. 3157, 2000.

[109] J. Martin-Regalado, S. Balle, and M. San Miguel, "Polarization and transverse-mode dynamics of gain-guided vertical-cavity surface-emitting lasers," *Optics letters,* vol. 22, pp. 460-462, 1997.

[110] S. Xiang, W. Pan, L. Yan, B. Luo, N. Jiang, K. Wen, *et al.*, "Polarization degree of vertical-cavity surface-emitting lasers subject to optical feedback with controllable polarization," *JOSA B,* vol. 27, pp. 476-483, 2010.

[111] J. Martin-Regalado, J. Chilla, J. Rocca, and P. Brusenbach, "Polarization switching in vertical-cavity surface emitting lasers observed at constant active region temperature," *Applied Physics Letters,* vol. 70, pp. 3350-3352, 1997.

[112] B. Ryvkin, K. Panajotov, E. Avrutin, I. Veretennicoff, and H. Thienpont, "Optical-injection-induced polarization switching in polarization-bistable vertical-cavity surface-emitting lasers," *Journal of applied physics,* vol. 96, pp. 6002-6007, 2004.

[113] M. A. Arteaga, H. J. Unold, J. M. Ostermann, R. Michalzik, H. Thienpont, and K. Panajotov, "Investigation of polarization properties of VCSELs subject to optical feedback from an extremely short external cavity-Part I: Theoretical analysis," *Quantum Electronics, IEEE Journal of,* vol. 42, pp. 89-101, 2006.

[114] H. G. Schuster and K. Lüdge, *Nonlinear laser dynamics: from quantum dots to cryptography*: John Wiley & Sons, 2012.

[115] R. W. Tkach and A. R. Chraplyvy, "Regimes of feedback effects in 1.5-µm distributed feedback lasers," *Lightwave Technology, Journal of,* vol. 4, pp. 1655-1661, 1986.

[116] K. Kikuchi and T. Okoshi, "Simple formula giving spectrum-narrowing ratio of semiconductor-laser output obtained by optical feedback," *Electronics Letters,* vol. 18, pp. 10-12, 1982.

[117] R. Tkach and A. Chraplyvy, "Linewidth broadening and mode splitting due to weak feedback in single-frequency 1.5 μm lasers," *Electronics Letters,* vol. 21, pp. 1081-1083, 1985.

[118] D. Lenstra, B. Verbeek, and A. Den Boef, "Coherence collapse in single-mode semiconductor lasers due to optical feedback," *Quantum Electronics, IEEE Journal of,* vol. 21, pp. 674-679, 1985.

[119] S.-Y. Lin, Y.-C. Su, Y.-C. Li, H.-L. Wang, G.-C. Lin, S.-M. Chen, *et al.*, "10-Gbit/s direct modulation of a TO-56-can packed 600-μm long laser diode with 2% front-facet reflectance," *Optics express,* vol. 21, pp. 25197-25209, 2013.

[120] J. Y. Law and G. P. Agrawal, "Feedback-induced chaos and intensity-noise enhancement in vertical-cavity surface-emitting lasers," *JOSA B,* vol. 15, pp. 562-569, 1998.

[121] N. Oliver, M. C. Soriano, D. W. Sukow, and I. Fischer, "Dynamics of a semiconductor laser with polarization-rotated feedback and its utilization for random bit generation," *Optics letters,* vol. 36, pp. 4632-4634, 2011.

[122] S. Ura, S. Shoda, K. Nishio, and Y. Awatsuji, "In-line rotation sensor based on VCSEL behavior under polarization-rotating optical feedback," *Optics express,* vol. 19, pp. 23683-23688, 2011.

[123] J.-M. Liu, *Photonic devices*: Cambridge University Press, 2005.

[124] H. Kawaguchi, "Bistable laser diodes and their applications: state of the art," *Selected Topics in Quantum Electronics, IEEE Journal of,* vol. 3, pp. 1254-1270, 1997.

[125] R. Hui, A. Paradisi, S. Benedetto, and I. Montrosset, "Dynamics of optically switched bistable laser diodes in the injection-locked state," *Optics letters,* vol. 18, pp. 1733-1735, 1993.

[126] G. Assanto, Z. Wang, D. Hagan, and E. VanStryland, "All-optical modulation via nonlinear cascading in type II second-harmonic generation," *Applied Physics Letters,* vol. 67, pp. 2120-2122, 1995.

[127] D. A. Mazurenko, R. Kerst, J. Dijkhuis, A. Akimov, V. Golubev, D. Kurdyukov, *et al.*, "Ultrafast optical switching in three-dimensional photonic crystals," *Physical review letters,* vol. 91, p. 213903, 2003.

[128] F. Zhou, Y. Liu, Z.-Y. Li, and Y. Xia, "Analytical model for optical bistability in nonlinear metal nano-antennae involving Kerr materials," *Opt. Express,* vol. 18, pp. 13337-13344, 2010.

[129] C. Masoller, M. Torre, and P. Mandel, "Influence of the injection current sweep rate on the polarization switching of vertical-cavity surface-emitting lasers," *Journal of applied physics,* vol. 99, pp. 026108-026108-3, 2006.

[130] S. De, V. Pal, A. El Amili, G. Pillet, G. Baili, M. Alouini, *et al.*, "Intensity noise correlations in a two-frequency VECSEL," *Optics express,* vol. 21, pp. 2538-2550, 2013.

[131] J. Y. Law, "Static, dynamic, and noise characteristics of vertical-cavity surface-emitting lasers," University of Rochester, 1997.

[132] A. Quirce, A. Valle, C. Giménez, and L. Pesquera, "Experimental study of relative intensity noise of multimode vertical-cavity surface-emitting lasers," in *SPIE Photonics Europe*, 2010, pp. 772024-772024-11.

[133] T. T. Lee, P. G. Lim, J. S. Harris Jr, K. V. Shenoy, and S. J. Smith, "Low-frequency noise characterization of near-IR VCSELs for functional brain imaging," in *Biomedical Optics (BiOS) 2008*, 2008, pp. 68422T-68422T-8.

[134] S. Yu, "Nonlinear dynamics of vertical-cavity surface-emitting lasers," *Quantum Electronics, IEEE Journal of,* vol. 35, pp. 332-341, 1999.

[135] C. H. Cox III, E. I. Ackerman, G. Betts, and J. L. Prince, "Limits on the performance of RF-over-fiber links and their impact on device design," *Microwave Theory and Techniques, IEEE Transactions on,* vol. 54, pp. 906-920, 2006.

[136] H.-F. Liu and W. F. Ngai, "Nonlinear dynamics of a directly modulated 1.55 μm InGaAsP distributed feedback semiconductor laser," *Quantum Electronics, IEEE Journal of,* vol. 29, pp. 1668-1675, 1993.

[137] S. Yu, W. Wong, P. Shum, and E. H. Li, "Theoretical analysis of modulation response and second-order harmonic distortion in vertical-cavity surface-emitting lasers," *Quantum Electronics, IEEE Journal of,* vol. 32, pp. 2139-2147, 1996.

[138] A. Valle, M. Sciamanna, and K. Panajotov, "Irregular pulsating polarization dynamics in gain-switched vertical-cavity surface-emitting lasers," *IEEE Journal of Quantum Electronics,* vol. 44, pp. 136-143, 2008.

[139] G. Shtengel, H. Temkin, P. Brusenbach, T. Uchida, M. Kim, C. Parsons, *et al.*, "High-speed vertical-cavity surface emitting laser," *Photonics Technology Letters, IEEE,* vol. 5, pp. 1359-1362, 1993.

[140] G. S. Gordon, M. J. Crisp, R. V. Penty, and I. H. White, "High-order distortion in directly modulated semiconductor lasers in high-loss analog optical links with large RF dynamic range," *Lightwave Technology, Journal of,* vol. 29, pp. 3577-3586, 2011.

[141] B. Kuntsevich, A. Pisarchik, and V. Kononenko, "Nonlinear dynamics of a directly modulated semiconductor laser with cavity detuning," *Optical and quantum electronics,* vol. 37, pp. 675-693, 2005.

[142] M. Giudici, S. Balle, T. Ackemann, S. Barland, and J. R. Tredicce, "Polarization dynamics in vertical-cavity surface-emitting lasers with optical feedback: experiment and model," *JOSA B,* vol. 16, pp. 2114-2123, 1999.

[143] J. W. Shi, W. C. Weng, F. M. Kuo, Y.-J. Yang, S. Pinches, M. Geen, *et al.*, "High-Performance Zn-Diffusion 850-nm Vertical-Cavity Surface-Emitting Lasers With Strained InAlGaAs Multiple Quantum Wells," *Photonics Journal, IEEE,* vol. 2, pp. 960-966, 2010.

[144] J.-W. Shi, Z.-R. Wei, K.-L. Chi, J.-W. Jiang, J.-M. Wun, I. Lu, *et al.*, "Single-Mode, High-Speed, and High-Power Vertical-Cavity Surface-Emitting Lasers at

850 nm for Short to Medium Reach (2 km) Optical Interconnects," *Journal of Lightwave Technology,* vol. 31, pp. 4037-4044, 2013.

[145] P. Westbergh, R. Safaisini, E. Haglund, J. S. Gustavsson, A. Larsson, M. Geen, *et al.*, "High-Speed Oxide Confined 850-nm VCSELs Operating Error-Free at 40 Gb/s up to 85 ºC," *Photonics Technology Letters, IEEE,* vol. 25, pp. 768-771, 2013.

[146] A. Gholami, D. Molin, and P. Sillard, "Physical modeling of 10 GbE optical communication systems," *Lightwave Technology, Journal of,* vol. 29, pp. 115-123, 2011.

[147] X.-F. Wang, G.-Q. Xia, and Z.-M. Wu, "Theoretical investigations on the polarization performances of current-modulated VCSELs subject to weak optical feedback," *JOSA B,* vol. 26, pp. 160-168, 2009.

[148] Y. Hong, J. Paul, P. S. Spencer, and K. A. Shore, "Influence of low-frequency modulation on polarization switching of VCSELs subject to optical feedback," *IEEE Journal of Quantum Electronics,* vol. 44, p. 30, 2008.

[149] L. A. Coldren and S. W. Corzine, "Diode lasers and photonic integrated circuits," *Optical Engineering,* vol. 36, pp. 616-617, 1997.

[150] S. Li, "UWB Radio-over-Fiber System Using Direct Modulated VCSEL," 2007.

[151] M. Sciamanna, K. P. Panajotov, P. Megret, H. Thienpont, M. Blondel, and I. P. Veretennicoff, "Optical feedback induces polarization mode-hopping in vertical-cavity surface-emitting lasers," in *Photonics Fabrication Europe*, 2003, pp. 103-111.

[152] H. Yasaka, Y. Yoshikuni, and H. Kawaguchi, "FM noise and spectral linewidth reduction by incoherent optical negative feedback," *Quantum Electronics, IEEE Journal of,* vol. 27, pp. 193-204, 1991.

[153] K. Otsuka and J.-L. Chern, "High-speed picosecond pulse generation in semiconductor lasers with incoherent optical feedback," *Optics letters,* vol. 16, pp. 1759-1761, 1991.

[154] X. Li, W. Pan, B. Luo, D. Ma, N. Li, and Y. Wang, "Suppressing nonlinear dynamics induced by external optical feedback in vertical-cavity surface-emitting lasers," *Optics & Laser Technology,* vol. 37, pp. 438-443, 2005.

[155] M. F. Salvide, M. S. Torre, I. D. Henning, M. J. Adams, and A. Hurtado, "Dynamics of Normal and Reverse Polarization Switching in 1550-nm VCSELs Under Single and Double Optical Injection," *Selected Topics in Quantum Electronics, IEEE Journal of,* vol. 21, pp. 1-9, 2015.

[156] C. Masoller and M. Torre, "Influence of optical feedback on the polarization switching of vertical-cavity surface-emitting lasers," *Quantum Electronics, IEEE Journal of,* vol. 41, pp. 483-489, 2005.

[157] M. F. Salvide, C. Masoller, and M. S. Torre, "Polarization Switching and Hysteresis in Vertical-Cavity Surface-Emitting Lasers Subject to Orthogonal Optical Injection," *Quantum Electronics, IEEE Journal of,* vol. 50, pp. 848-853, 2014.

[158] A. Valle, I. Gatare, K. Panajotov, and M. Sciamanna, "Transverse mode switching and locking in vertical-cavity surface-emitting lasers subject to orthogonal optical injection," *Quantum Electronics, IEEE Journal of,* vol. 43, pp. 322-333, 2007.

[159] T. Liu, T. Katayama, and H. Kawaguchi, "High-Frequency Self-Modulation in Short-External-Cavity VCSEL With Concave Mirror," *Photonics Technology Letters, IEEE,* vol. 27, pp. 280-283, 2015.

[160] M. P. Tan, "Modulation approaches of vertical-cavity surface-emitting lasers with mode control," University of Illinois at Urbana-Champaign, 2013.

[161] Y. Takeuchi, R. Shogenji, and J. Ohtsubo, "Chaos dynamics in semiconductor lasers with polarization-rotated optical feedback," *Optical review,* vol. 17, pp. 144-151, 2010.

[162] H. Lin, A. Khurram, M. D. Black-Ingersoll, and A. Valle, "Polarization and modal dynamics of multimode vertical-cavity surface-emitting lasers subject to optical feedback and current modulation," *Optics Communications,* vol. 350, pp. 178-188, 2015.

[163] M. Virte, K. Panajotov, and M. Sciamanna, "Mode competition induced by optical feedback in two-color quantum dot lasers," *Quantum Electronics, IEEE Journal of,* vol. 49, pp. 578-585, 2013.

[164] K. Panajotov, M. Virte, M. Sciamanna, M. Tlidi, and H. Thienpont, "Nonlinear dynamics of Vertical-Cavity Surface-Emitting Lasers: deterministic chaos, random number generation and chaotic cavity solitons," *18th INTERNATIONAL SCHOOL ON CONDENSED MATTER PHYSICS,* vol. 22, p. 34, 2014.

[165] C. Masoller, M. S. Torre, and K. A. Shore, "Polarization dynamics of current-modulated vertical-cavity surface-emitting lasers," *Quantum Electronics, IEEE Journal of,* vol. 43, pp. 1074-1082, 2007.

[166] G. Morthier and P. Vankwikelberge, *Handbook of distributed feedback laser diodes*: Artech House, 2013.

[167] A. Valle, J. Sarma, and K. Shore, "Spatial holeburning effects on the dynamics of vertical cavity surface-emitting laser diodes," *Quantum Electronics, IEEE Journal of,* vol. 31, pp. 1423-1431, 1995.

[168] Y. K. Chembo, S. K. Mandre, I. Fischer, W. Elsässer, and P. Colet, "Controlling the emission properties of multimode vertical-cavity surface-emitting lasers via polarization-and frequency-selective feedback," *Physical Review A,* vol. 79, p. 013817, 2009.

[169] N. Fujiwara, Y. Takiguchi, and J. Ohtsubo, "Observation of the synchronization of chaos in mutually injected vertical-cavity surface-emitting semiconductor lasers," *Optics letters,* vol. 28, pp. 1677-1679, 2003.

[170] M. Virte, K. Panajotov, H. Thienpont, and M. Sciamanna, "Deterministic polarization chaos from a laser diode," *Nat Photon,* vol. 7, pp. 60-65, 2013.

[171] H. Yanhua, C. Xianfeng, P. S. Spencer, and K. A. Shore, "Enhanced Flat Broadband Optical Chaos Using Low-Cost VCSEL and Fiber Ring Resonator," *Quantum Electronics, IEEE Journal of,* vol. 51, pp. 1-6, 2015.

[172] G. Friart, L. Weicker, J. Danckaert, and T. Erneux, "Relaxation and square-wave oscillations in a semiconductor laser with polarization rotated optical feedback," *Optics express,* vol. 22, pp. 6905-6918, 2014.

[173] M. Marconi, J. Javaloyes, S. Barland, S. Balle, and M. Giudici, "Polarization dynamics of VCSELs in external cavities," in *SPIE Photonics Europe*, 2014, pp. 913412-913412-10.

[174] J. Javaloyes, M. Marconi, and M. Giudici, "Phases dynamics in VCSELs with delayed optical feedback and cross re-injection," *arXiv preprint arXiv:1405.7493*, 2014.

[175] L. Olejniczak, K. Panajotov, H. Thienpont, M. Sciamanna, A. Mutig, F. Hopfer, *et al.*, "Polarization switching and polarization mode hopping in quantum dot vertical-cavity surface-emitting lasers," *Optics express*, vol. 19, pp. 2476-2484, 2011.

[176] M. Virte, E. Mercier, H. Thienpont, K. Panajotov, and M. Sciamanna, "Physical random bit generation from chaotic solitary laser diode," *Optics express*, vol. 22, pp. 17271-17280, 2014.

[177] I. Gatare, M. Sciamanna, A. Locquet, and K. Panajotov, "Influence of polarization mode competition on the synchronization of two unidirectionally coupled vertical-cavity surface-emitting lasers," *Optics letters*, vol. 32, pp. 1629-1631, 2007.

[178] R. Michalzik, *VCSELs : Fundamentals, Technology and Applications of Vertical-Cavity Surface-Emitting Lasers*. Berlin, Heidelberg: Springer Berlin Heidelberg, 2013.

[179] P. Spencer and C. R. Mirasso, "Analysis of optical chaos synchronization in frequency-detuned external-cavity VCSELs," *Quantum Electronics, IEEE Journal of*, vol. 35, pp. 803-809, 1999.

[180] K. Panajotov, M. Sciamanna, H. Thienpont, and A. Uchida, "Impact of light polarization on chaos synchronization of mutually coupled VCSELs," *Optics letters*, vol. 33, pp. 3031-3033, 2008.

[181] S. Bandyopadhyay, Y. Hong, P. Spencer, and K. Shore, "Experimental observation of anti-phase polarisation dynamics in VCSELS," *Optics communications*, vol. 202, pp. 145-154, 2002.

[182] M. Virte, K. Panajotov, H. Thienpont, and M. Sciamanna, "Deterministic polarization chaos from a laser diode," *Nature Photonics*, vol. 7, pp. 60-65, 2013.

[183] A. Aragoneses, T. Sorrentino, S. Perrone, D. J. Gauthier, M. Torrent, and C. Masoller, "Experimental and numerical study of the symbolic dynamics of a modulated external-cavity semiconductor laser," *Optics express*, vol. 22, pp. 4705-4713, 2014.

[184] K. Iga and H. E. Li, *Vertical-cavity surface-emitting laser devices*: Springer, 2003.

[185] B. Ryvkin, K. Panajotov, A. Georgievski, J. Danckaert, M. Peeters, G. Verschaffelt, *et al.*, "Effect of photon-energy-dependent loss and gain mechanisms on polarization switching in vertical-cavity surface-emitting lasers," *JOSA B*, vol. 16, pp. 2106-2113, 1999.

[186] B. Zhao, T. Chen, and A. Yariv, "The gain and carrier density in semiconductor lasers under steady-state and transient conditions," *Quantum Electronics, IEEE Journal of*, vol. 28, pp. 1479-1486, 1992.

[187] Z. Jing and N. Tansu, "Optical Gain and Laser Characteristics of InGaN Quantum Wells on Ternary InGaN Substrates," *Photonics Journal, IEEE*, vol. 5, pp. 2600111-2600111, 2013.